
MARINE FUNGI AS SOURCE OF PROTEIN BIOSURFACTANTS

Paola Cicatiello

Dottorato in Biotecnologiche – XXIX ciclo

Università di Napoli Federico II



Dottorato in Scienze Biotecnologiche – XXIX ciclo

Università di Napoli Federico II



MARINE FUNGI AS SOURCE OF PROTEIN BIOSURFACTANTS

Paola Cicatiello

Dottoranda: Paola Cicatiello

Relatore: Prof.ssa Paola Giardina

Coordinatore: Prof. Giovanni Sannia

*Ai ricordi
Per non dimenticare
A te amico mio
A te B.*

*Learn from yesterday,
live for today,
hope for tomorrow.
The important thing is not
to stop questioning*

Albert Einstein

INDEX

RIASSUNTO	1
SUMMARY	6
CHAPTER 1	8
1. INTRODUCTION	9
1.1. Investigation of marine environment for interesting products	9
1.1.1. Marine fungi as source of novel industrial molecules	9
1.1.2. Biosurfactant molecules: the hydrophobins	11
1.2. Hydrophobins	11
1.2.1. General features	11
1.2.2. Biological roles	13
1.2.3. Applications	14
1.3. Class I hydrophobin from <i>Pleurotus ostreatus</i> : Vmh2	15
1.4. Work description	17
1.5. References	18
CHAPTER 2	24
2. ISOLATION AND CHARACTERIZATION OF NEW HYDROPHOBINS FROM MARINE FUNGI	25
2.1. Marine fungi as source of new hydrophobins	26
2.2. Amyloid aggregation and surface interactions of two Class I hydrophobins from marine fungi, a comparative study	33
CHAPTER 3	54
3. APPLICATIONS OF THE CLASS I HYDROPHOBIN VMH2	55
3.1. Vmh2 layer used in MALDI-IMS (Matrix Assisted Laser Desorption/Ionization Imaging Mass Spectrometry)	56
3.2. A proteomic approach for the rapid, multi-informative and reliable identification of blood	60
3.3. Rapid and ultrasensitive detection of active thrombin based on the Vmh2 hydrophobin fused to a Green Fluorescent Protein	72
CHAPTER 4	84
4. USE OF HYDROPHOBIN COATINGS FOR ANTI-BIOFILM ACTIVITY	85
4.1. Hydrophobin coated surface prevents <i>Staphylococcus epidermidis</i> biofilm formation	86
5. CONCLUSIONS	104
Communications, Publications	105
Appendix	107

RIASSUNTO

A. INTRODUZIONE

A1. Le idrofobine

Le idrofobine sono una famiglia di piccole proteine di origine fungina che possiedono la caratteristica di auto-assemblare spontaneamente alle interfacce idrofiliche-idrofobiche. Le idrofobine svolgono un ruolo chiave nella crescita e nello sviluppo dei funghi filamentosi. Queste proteine possono assemblare sia all'interfaccia aria-acqua, in modo da ridurre la tensione superficiale del mezzo di crescita permettendo a strutture fungine come le ife di fuoriuscire, sia possono assemblare sulle pareti delle ife o delle spore in modo da favorirne la crescita o la dispersione aerea. Tradizionalmente sono state divise in idrofobine di classe I e II. Quelle di classe I sono prodotte sia da funghi Basidiomiceti che Ascomiceti, invece quelle di classe II sono state isolate solo da Ascomiceti. Tutte possiedono un motivo conservato di otto cisteine implicate nella formazione di quattro ponti disolfurici. Gli spazi inter-cisteina in quelle di classe I sono meno conservati rispetto a quelle di classe II. La differenza sostanziale tra le due classi risiede nella stabilità dei film anfifilici che formano. Le idrofobine di classe I formano film più stabili e resistenti ai lavaggi con solventi e detergenti come ad esempio l'etanolo al 60% e il sodio dodecil solfato (SDS) al 2% e hanno delle strutture simili a fibrille amiloidi dissociabili solo in presenza di acidi forti come l'acido formico o l'acido trifluoroacetico (TFA), mentre i film formati da quelle di classe II sono poco stabili e mancano di strutture amiloidi. Quindi le idrofobine di classe II sono più solubili e meno tendenti all'aggregazione, utilizzabili per scopi diversi rispetto a quelle di classe I.

I settori industriali più interessati all'uso di queste proteine possono essere quello alimentare e cosmetico, per stabilizzare prodotti aereati o emulsioni, quello medico-farmaceutico per drug delivery, per ricoprire dispositivi, come cateteri e vene artificiali riducendo il legame di batteri patogeni. Inoltre possono essere utilizzate per la creazione di biosensori essendo in grado di funzionalizzare differenti superfici capaci di immobilizzare proteine nella loro forma attiva.

Le strutture formate dalle idrofobine di classe I definite "rodlet", simili a fibrille di tipo amiloide, sono interessanti nel campo delle nano biotecnologie in quanto conservano le caratteristiche dei peptidi amilogenici, quali la possibilità di funzionalizzare superfici in modo semplice, la robustezza e la stabilità del "layer" formato, ma non sono implicate in malattie neurodegenerative. La formazione di fibrille è legata ad un cambio conformazionale della proteina verso la struttura cross- β , cambio che può essere indotto in diverse condizioni, quali aumento della concentrazione proteica, della temperatura, presenza di sali o detergenti. Lo studio di queste condizioni è essenziale per l'utilizzo di queste proteine nei settori industriali.

Affinché il loro utilizzo possa essere diffuso in alcuni dei loro campi di applicazione è necessaria un'elevata produzione su larga scala. Nel caso dell'idrofobina di classe II, HFBI è stato costruito un ceppo di *Trichoderma reesei* iperproduttore, ottenendo una resa di proteina di 600mg per litro di coltura. L'idrofobina di classe I H*Protein A è stata prodotta come proteina ricombinante di fusione dalla multinazionale BASF su impianto pilota per la produzione su scala di chilogrammi. L'estrazione di nuove idrofobine con interessanti proprietà potrebbe aiutare ad ampliare le conoscenze fino ad ora acquisite su queste proteine. In particolare, l'indagine di ambienti inesplorati potrebbe essere un'ottima risorsa per scoprire nuove biomolecole.

L'ambiente marino è una ricca fonte di biodiversità ancora poco esplorata ospitando piante, animali, invertebrati, e micro-organismi come batteri, funghi, cianobatteri e

micro-alghe. Gli habitat marini sono caratterizzati da parametri, quali salinità, luce, pressione, temperatura e nutrienti, che influenzano le evoluzioni dei micro-organismi che li popolano, rendendo l'ecosistema marino complesso e dinamico. I micro-organismi che si adattano a questi unici e differenti habitat possono produrre una varietà di nuovi composti dal grande potenziale industriale. A tal proposito una delle sfide di questo nuovo millennio è quella di trovare nuovi metodi di campionatura, coltivazione e screening di micro-organismi marini, promettenti produttori di interessanti molecole.

Nel laboratorio dove ho svolto il mio progetto di ricerca da anni si studia una particolare idrofobina di classe I, Vmh2, prodotta dal fungo edibile *Pleurotus ostreatus*. Vmh2 è stata ampiamente caratterizzata sia in forma solubile che aggregata e può essere estratta sia dal micelio che dal brodo di coltura nel quale il fungo cresce. Sfruttando le competenze acquisite dal mio gruppo di ricerca il presente lavoro verte sulla ricerca di nuove idrofobine esplorando nuove fonti come quelle da ambiente, marino, e sulla caratterizzazione e possibile applicazione in diversi settori sia delle nuove proteine individuate che dell'idrofobina Vmh2.

B. NUOVE IDROFOBINE DA FUNGHI MARINI

B1. Funghi marini come fonte di nuove idrofobine

E' stato sviluppato un metodo di screening per isolare nuove idrofobine da 23 ceppi di funghi marini, forniti dalla Mycotheca Universitatis Taurinensis (MUT) di Torino. Inizialmente sono state indagate le migliori condizioni di crescita (temperatura, nutrienti e salinità) per ognuno dei ceppi. La seconda parte dello screening è stata incentrata sulla messa a punto di protocolli di estrazione per entrambe le classi di idrofobine sia dai miceli che dai terreni di coltura. I protocolli sviluppati hanno permesso di estrarre sei putative idrofobine, in quantità adeguate ed in forma omogenea per le analisi successive. Successivamente sono state analizzate le loro capacità di funzionalizzare superfici e di stabilizzare emulsioni. La capacità di cambiare la bagnabilità del silicio cristallino e la stabilità dei film ai differenti lavaggi con etanolo 60% e successivamente con SDS caldo al 2% ha permesso di discriminare tra le sei idrofobine isolate due appartenenti alla classe II e quattro alla classe I. Tra le proteine isolate, un'idrofobina di classe II ha mostrato avere la migliore capacità emulsionante, in presenza di una miscela acqua-olio, formando un'emulsione stabile anche dopo un mese.

B2. Caratterizzazione di due idrofobine di classe I estratte da funghi marini

Pac2 e Pac3 sono idrofobine di classe I estratte rispettivamente dai funghi marini *Penicillium roseopurpureum* e *Acremonium sclerotigenum*. I livelli di produzione sono stati ottimizzati modificando i parametri di crescita: una bassa temperatura (20°C) e una alta concentrazione salina (30g/L) sono state determinanti per ottenere una resa proteica di 7 mg/L per Pac2 e 20 mg/L per Pac3. Entrambe le proteine sono state estratte dal brodo di crescita ed è stato necessario uno "step" aggiuntivo al protocollo di purificazione, un'estrazione in metanolo-cloroformio, per rimuovere contaminanti lipidici e pigmenti che avrebbero potuto interferire con la caratterizzazione delle proteine. Per entrambe le proteine è stata studiata la capacità di auto-assemblare formando strutture di tipo amiloide sia in 60% etanolo che in tamponi acquosi. Questo studio è stato effettuato mediante analisi delle variazioni della struttura secondaria delle proteine, la verifica della capacità di legare il colorante ThT in seguito alla formazione di strutture β -amiloide e infine tramite analisi TEM e AFM che hanno permesso la visualizzazione delle differenti morfologie delle fibrille formate.

Pac2 in etanolo 60% ha formato un film compatto di aggregati sulla mica mentre su HOPG strutture simili a fibrille, mentre Pac3 ha mostrato un comportamento opposto sulle stesse superfici. Inoltre anche fibrille preformate in soluzioni acquose di entrambe le proteine hanno mostrato avere differente affinità per le superfici. I risultati ottenuti hanno mostrato sia che le superfici possono influenzare diversamente la formazione di fibrille delle idrofobine e sia che le fibrille già mature possono interagire con affinità differente alle superfici.

C. APPLICAZIONI DELL'IDROFOBINA VMH2 PRODOTTA DAL FUNGO *PLEUROTUS OSTREATUS*

C1. Un approccio proteomico per l'identificazione rapida e affidabile del sangue

La capacità auto-assemblante dell'idrofobina Vmh2 è stata impiegata per funzionalizzare la piastrina di acciaio utilizzata nella spettrometria MALDI-TOF. Questo permette di immobilizzare sulla piastrina la tripsina, un enzima proteolitico generalmente usato nelle analisi di proteomica, per poter sviluppare un sistema di idrolisi in-situ rapido ed efficace. Studi precedenti hanno dimostrato che lo strato di Vmh2 è in grado di immobilizzare in modo non covalente la tripsina nella sua forma attiva permettendo l'idrolisi di proteine modello e di campioni complessi in soli cinque minuti comparati all'idrolisi in soluzione che dura 16 ore.

Come ulteriore prova di funzionalità di questo metodo è stato idrolizzato sangue non pretrattato sia di cavallo che di uomo in modo da individuare peptidi specie specifici. Tali peptidi sono stati individuati anche in miscele miste di sangue, infatti analisi MALDI-TOF-TOF hanno confermato le sequenze amminoacidiche dei peptidi individuati. Inoltre, la sensibilità del sistema è stata verificata esaminando un campione estratto da una piastrina insanguinata, proveniente da una reale scena del crimine, conservata per circa dieci anni. L'identificazione di peptidi relativi alla specie umana ha permesso di ipotizzare un concreto utilizzo di questa metodica per analisi forensi.

C2. Rilevazione rapida e ultrasensibile di trombina utilizzando l'idrofobina Vmh2 fusa ad una proteina fluorescente

E' stato messo a punto un sistema di espressione ricombinante dell'idrofobina Vmh2 fusa alla proteina fluorescente verde GFP, con sito di idrolisi riconosciuto dalla proteasi trombina, utilizzando come ospite il lievito *Pichia pastoris*. I cloni positivi sono stati selezionati monitorando l'intensità di fluorescenza emessa dalla proteina fusa secreta nel brodo di coltura. Successivamente la proteina fusa è stata purificata ottenendo una resa di 50mg L⁻¹ ed è stata caratterizzata in comparazione a Vmh2 tal quale, valutando l'abilità di assemblare all'interfaccia idrofilica-idrofobica e su superfici come il polistirene formando fibrille di tipo amiloide. Verificata la sua capacità di aderire al polistirene, la proteina è stata immobilizzata su piastrine multipozzetto costituite dallo stesso materiale. Ottimizzati i parametri di immobilizzazione, il sistema è stato utilizzato per monitorare la presenza della proteasi trombina che riconosce il sito di idrolisi tra Vmh2 e la GFP. L'avvenuta idrolisi è stata rilevata mediante saggi di fluorescenza in modo da valutare in base alla diminuzione di intensità di fluorescenza la quantità di trombina aggiunta nel pozzetto. Per valutare il reale utilizzo di questo biosensore è stata determinata la concentrazione di trombina anche in campioni reali di plasma di pazienti non malati.

D. STUDIO DELL'ATTIVITÀ ANTIBIOFILM DELLE IDROFOBINE PAC3 E VMH2 CONTRO STAPHYLOCOCCUS EPIDERMIDIS

Staphylococcus epidermidis è un batterio gram positivo che rappresenta il maggior componente della flora batterica che colonizza la cute e le membrane mucose. Questo batterio riesce ad aderire anche a dispositivi medici come protesi o cateteri, mediante formazione di bio-film, diventando un significativo patogeno nosocomiale soprattutto in pazienti predisposti. Le adesioni microbiche alle superfici sono processi complessi, influenzati da diversi fattori fisico-chimici, e dalla produzione di proteine o polisaccaridi. Recentemente è stata rivolta grande attenzione alla funzionalizzazione di superfici mediante biomolecole per inibire la formazione di biofilm batterici. Per tale motivo sfruttando la capacità autoassemblante delle idrofobine Pac3 e Vmh2 su supporti di diversa natura, è stata analizzata la capacità di prevenire la formazione del biofilm formato da *S. epidermidis*. Esperimenti condotti hanno mostrato che la formazione del biofilm è stata ridotta dalla presenza dei "layers" di entrambe le HFBs depositate nei pozzetti delle piastre di polistirene utilizzate per la crescita del batterio. Inoltre è stato verificato che un aumento della quantità di idrofobina depositata porta ad una proporzionale riduzione del biofilm batterico. In particolare Pac3 ha mostrato migliori prestazioni rispetto a Vmh2 anche a concentrazioni molto basse. Strati di idrofobine formati su altre superfici, generalmente usate nel settore biomedico, come il vetro, il titanio, l'acciaio e il teflon, sono state analizzate per ampliare la gamma di applicazioni. La formazione del "layer" proteico è stata verificata mediante variazione dell'angolo di contatto della superficie ed in tutti i casi è stata riscontrata una diminuzione della formazione del biofilm batterico sulla superficie funzionalizzata. Infine, mediante analisi con microscopio a fluorescenza, è stata osservata la riduzione dello spessore del biofilm, a fronte di un'invariata vitalità cellulare, evidenziando così che questi "layer" hanno proprietà antibiofilm, non antibatterica.

E. CONCLUSIONI

In conclusione con il presente progetto ho conseguito i seguenti risultati:

- Lo sviluppo di un metodo di screening per selezionare nuove idrofobine da ceppi fungini isolati da ambiente marino
- La caratterizzazione di due idrofobine di classe I nella loro forma solubile e aggregata verificando come superfici di natura diversa possano influenzare la formazione di strutture di tipo amiloide
- L'utilizzo dei "layers" formati dall'idrofobina di classe I Vmh2 per immobilizzare in modo efficiente enzimi proteolitici in modo da sviluppare sistemi rapidi per analisi forensi
- L'efficiente produzione della proteina di fusione ricombinante Vmh2-GFP da poter utilizzare come biosensore
- L'utilizzo dei "layers" assemblati da due diverse idrofobine per inibire i bio-films microbici per produrre dispositivi medici funzionalizzati

SUMMARY

Hydrophobins (HFBs) are small fungal surface-active proteins, which self-assemble spontaneously into amphipathic layers at air-water and water-environment interfaces, playing a key role in different fungal life cycles. Their properties have been demonstrated useful in biotechnological applications of several industrial fields. The knowhow about HFBs can be enforced by the discovery and characterization of new members of this family, thus also broadening the opportunities of their uses. Generally, environmental stressful conditions of fungal growth may induce the production of specific proteins, also endowed with peculiar features. In this view, the marine habitat can be fruitfully explored.

Some selected marine fungi from Mycoteca Universitatis Taurinensis (MUT) were screened to identify new HFBs. Extraction methods were set up to isolate secreted or cell wall associated HFBs, allowing the identification of six new putative HFBs. Four of them formed very stable layers on silicon chips, whereas one of them was endowed with remarkable emulsification capacity.

Two of the isolated HFBs, Pac2 and Pac3, were characterized in their soluble and aggregate forms. Using different techniques, i.e. circular dichroism, dynamic light scattering and fluorescence assay, Pac3 showed a higher propensity to form amyloid fibrils than Pac2. In addition, microscopy analysis allowed us to infer that the interaction of these proteins with specific surfaces can be crucial in the fibril formation and the assembly morphology.

Furthermore, some different applications of the HFB Vmh2 from *Pleurotus ostreatus*, extensively studied in the research group where this PhD project has been carried out, were improved or developed.

The Vmh2 layer was exploited to easily coat the sample-loading steel plate used in MALDI-TOF mass spectrometry to immobilize by adsorption a proteolytic enzyme in his active form, to achieve in-situ digestion of complex biological samples, i.e. the whole blood. This method allowed us to discriminate species-specific peptides in few minutes, encouraging its use in the forensic field. Moreover, a similar approach can be applied to analyse the distribution of biomolecules in biological tissues using the powerful tool of MALDI Imaging mass spectrometry (IMS). In particular, a rat brain tissue has been analysed identifying some putative metabolites and lipids.

Recombinant Vmh2, fused to the GFP (Green Fluorescence Protein), was heterologously produced in the yeast *Pichia pastoris*. Since the two proteins were linked by the cutting site of the protease thrombin, this construct was used as the active biological element in the realization of a thrombin biosensor.

Finally, the anti-biofilm activity of the Pac3 and Vmh2 layers against the nosocomial bacteria *Staphylococcus epidermidis* was analysed on different surfaces generally used in medical field. Pac3 showed better performances than Vmh2, reducing tenfold the biofilm thickness and preserving the cell vitality.

On the whole this work contributes to strengthen the knowledge of this family of proteins, broadening the practical perspectives.

CHAPTER 1

1. INTRODUCTION

1.1. Investigation of marine environment for interesting products

The marine environment is a rich source of biological and chemical diversity. Oceans cover more than 70% of the world's surface (Duarte et al., 2012) and represent an untapped resource for discovery of new compounds endowed with biological activities, which can be relevant from the point of view of the industry. It is estimated that marine and coastal environments host about 90% of all organisms living on earth and this biodiversity was only partly explored. However, in the last decades, the attention has been focused on the marine environment biodiversity studying plants, animals, invertebrates and especially microorganisms such as bacteria, fungi, microalgae and cyanobacteria. The marine ecosystems are complex and dynamic and the growth of microorganisms is greatly affected by the environment and its changes. Salinity, light, pressure, temperature and nutrients, are some of the environmental variables that determine the evolution of microorganisms that populate the marine environment. Thanks to their adaptation to this unique and different habitat, they produce a wide variety of novel compounds interesting in pharmaceutical, cosmetic, chemical and agrichemical fields. It is also important to preserve the vitality of the extracted species and reproduce their growth on a laboratory scale.

New methods of sampling and cultivation for promising microorganisms and biotechnological processes for selected compounds should be developed. The challenge facing the biotechnology industry in the next millennium is to develop novel screening technique to identify new sources of marine bio products (Kiuru et al., 2014).

1.1.1. Marine fungi as source of novel industrial molecules

Demand of bio-molecules of industrial interest, especially enzymes, mainly of microbial origin, is ever increasing owing to their applications in a wide variety of processes. Among the microorganisms, filamentous fungi are widely used in industrial applications. Their biotechnological uses include the production of enzymes, vitamins, polysaccharides, pigments, lipids and others.

Taxonomic and habitat diversity form the basis for exploration of marine fungal biotechnology. Studies on the molecular diversity of the micro-eukaryotic community have shown that fungi occupy a central position in a large number of marine habitats. Environmental surveys using molecular tools have shown the presence of fungi in deep-sea habitats, pelagic waters, coastal regions, hydrothermal vent ecosystem, anoxic habitats and ice-cold regions. Majority of the environmental phylotypes could be grouped within *Ascomycota*, *Basidiomycota* and *Chytridiomycota* (Manohar and Raghukumar, 2013). The basic knowledge on marine fungi (e.g., their distribution and their ecological role) is still scarce, also because many of the fungi are difficult to propagate in culture because their life cycle can be dependent on a symbiotic interaction (Duarte et al., 2012). Indeed, marine fungi like marine bacteria often live as symbionts in algae or marine invertebrates, especially sponges. Collection of these marine fungi usually requires the collection of the host or supporting material (e.g., algae, marine invertebrates, sediment or water) (Kiuru et al., 2014). Marine fungi form an ecological and not a taxonomic group. Among them, it is possible to identify two main categories. The obligate marine fungi grow and sporulate exclusively in seawater and the facultative marine fungi originate from fresh water or

terrestrial place and endured physiological adaptations that allowed them to grow and sporulate in the marine environment (Raghukumar, 2008). As a more general classification of these microorganisms, the term “marine-derived fungi” is often used because most of the fungi isolated from marine samples are not demonstrably classified as obligate or facultative marine microorganisms (Bonugli-Santos et al., 2015).

In spite of the terrestrial fungi which have been extensively studied, their marine counterpart are still unexplored. Recently they have attracted great attention because the unique physico-chemical properties of the marine environment (e.g. salinity, pH, temperature and hydrostatic pressure) may have conferred them special physiological adaptations. They are potential candidates for the production of novel enzymes, biosurfactants, polysaccharides, polyunsaturated fatty acids and secondary metabolites. (Swathi et al., 2013; Smitha et al 2014; Imhoff, 2016). The advances in discovering enzymes from marine-derived fungi and their biotechnological relevance were discussed in the recent review of Bonugli-Santos et al., 2015. Among the marine organisms with biotechnological potentials, there are comparatively few requests and patent records for fungi. However, considering the time line related to the field of marine mycology (Figure1), including the current advances in this area, a significant increase in patent applications should be observed in a near future.

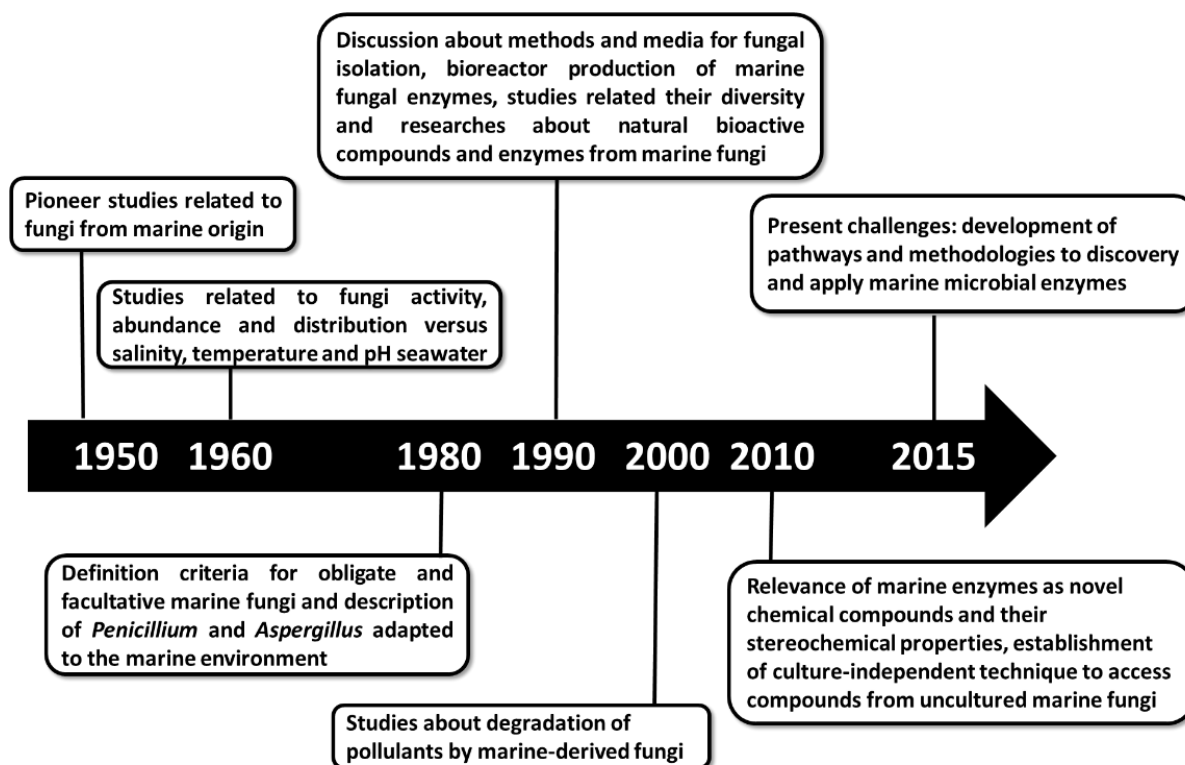


Figure 1: Timeline of marine mycology: a brief account of the relevant scientific events related to marine-derived fungi and their applications. (Bonugli-Santos et al., 2015)

1.1.2. Biosurfactant molecules: the hydrophobins

In the era of green technology, particular interest was given to biosurfactants because they offer many advantages over their synthetic counterparts thanks to their biodegradable and environmentally friendly nature. They are amphiphilic molecules mainly produced by microorganisms (including bacteria, yeast and fungi) and occur in nature as diverse groups comprising glycolipids, lipopeptides and lipoproteins, fatty acids, phospholipids, and proteins, too. Their applications range from cosmetic, pharmaceutical and food processes (Bhardwaj et al., 2013). A particular class of amphiphilic fungal proteins, the hydrophobins, have been described as the most surface-active proteins known (Cooper and Kennedy, 2010), thanks to their self-assembling capability at the hydrophobic hydrophilic interfaces. Their activity is similar to that of the traditional biosurfactants, but the surface activity of hydrophobins is only dependent by their peculiar amino acid sequence (Wosten and De Vocht, 2000).

1.2. Hydrophobins

1.2.1. General features

Hydrophobins are small-secreted proteins produced by filamentous fungi. The first gene encoding a hydrophobin was discovered during the study of the fruiting body development of the fungus *Schizophyllum commune*. Wessels and co-authors (Wessels et al., 1991a) noted the presence of a gene abundantly expressed during a particular growth phase. This gene was associated to a small protein containing a large portion of hydrophobic amino acids, since the name hydrophobin (Dons et al., 2004; Wessels et al., 1991b). The biochemical feature of these proteins is the presence of eight conserved residues of cysteines that form four disulfide bridges, which connect C1-C6, C2-C5, C3-C4, and C7-C8. Despite the conserved pattern of cysteines, the amino acid sequences of hydrophobins show low identity even when they belong to the same species. However, the relative positions of the polar and non-polar amino acids seems quite preserved, determining a hydrophobicity pattern typical of these proteins. These features emphasize that the cysteines are crucial for protein structure, providing a scaffold for the other residues that can confer different and specific properties to each hydrophobin. By aligning the known amino acid sequences from the first cysteine, these proteins can be divided into two main classes based on the different lengths of the inter-cysteine space and on the clustering of hydrophobic and hydrophilic groups. In particular, until now, class II hydrophobins are observed only in the ascomycetes and have a conserved length of the inter-cysteine spaces, while class I are produced in both ascomycetes and basidiomycetes species and the inter-cysteine space is more variable (Figure 2).

Class I hydrophobins

```

SC4  CNSG-PVQ--CCNETTT--VANAQ-KQGLLGG----LLGVVV---GPITGLVGLNCSF---ISVVGV---LTGNSCTA-QTVCCDHVTONG-----LVN--VGC
PRI2 CNNG-SLQ--CCNSSMTQDRGNLQIAQGVLGGLLGGLLGLGGLLDLVDLNLALIGVCCSP---ISIVG-----NANTCTQ-QTVCCSNNNFNG-----LIA--LGC
SC3  CTTG-SLS--CCNQVQS---ASSSEVTALLG----LLGIV---LDLNVLVGIGSCSP---LTVIG---VGGSGGSA-QTVCENTQFNG-----LIN--IGC
ABH1 CDVG-EIH--CCDTQQT----PDHTSAAASG--LLGVP---INLGAFLGFDCTP---ISVLG---VGGNCAA-CPVCTGNQFTA-----LINA-LDC
EAS  CSID-DYKPYCCQSMG---PAGSPGL-----LNLIP---VDLSASLG--C-----VVG---VIGSQCGA-SVKCKDDVTNTGNSFLINA-ANC
HCF1 CAVGSQIS--CCTNSS-----GSD-----ILGNV-----LGGSCLLDN--VSLISSLN-----SNCPAGNTECCPS-NQDG-----TLNINVSC
MPG1 CGAEKVV--CCNSKELK--NSKSGAE-----IPIDV-----LSGCKNIPINILTNQLI--PINNFCSD-TVSCSSGEQIG-----LVN--IQG
RODA  CGDQAQLS--CCNKATYAG-DVTDIDEGILAGTLKNLIGGGS---GTEGLGLFNQCSKLDLQIPVIGIPIQALVQKCKQ-NIAQCCNSPSDASG--SLIGLGLP

```

Class II hydrophobins

```

HFBI  CPTG-LFSNFCATQVVLGVLGLDCKVPSQNVYDGTDFRNVCAKTA-QPLCCVAP-VAGQALLC
HFBI  CPTG-LFSNFCATNVLDLIGVDCRKTPTIAVDTGAIQAHCAASKGS-KPLCCVAP-VADQALLC
SRH1  CPNG-LYSNFCGANVLGVAALDCHTTPRVDVLTGPIFQAVCAEAGGKQPLCCVVP-VAGQDLLC
CU    CTGL-LQKSPCCNTDILGVANLDCGPPSVPTSPSQFQASCVADGGRSARCOTLS-LLGLALVC
CRP   CSST-LYSEACCATDVLGVADLDCETVPETPTSASSFESICATSG-RDAKCTIP-LLGQALLC
MGP   CSG--LYGSAQCCATDILGLANLDCGQPSDAPVDADNFSEICAAIG-QRARCCVLP-ILDQGILC
HCF6  CPAN---RVPCQLSVLGVADVTCASPSGLTSVSAFEADCANDG-TTAQCCLIP-VLGLGLFC
HYD4  CPDGGILGTQCCSLDLVGVLSGECSSPSKTPNSAKEFQEIQAASG-QKARCCFLSEVFTLGAFC

```

Figure 2: Amino acid sequence comparison of class I and II hydrophobins. Amino acids between the first and last Cys residues are shown. The conserved Cys residues are highlighted with the conserved disulphide-bonding pattern indicated with brackets. (Sunde et al., 2008)

These characteristics of the sequences determine some differences in the properties of the proteins. Indeed class I hydrophobins assemble into insoluble polymeric layers composed of fibrillar structures known as rodlets, looking like amyloid proteins. These layers are extremely stable (resisting to hot 2% sodium dodecyl sulphate), can only be solubilized with harsh acid treatments (formic acid or trifluoroacetic acid) and the soluble forms can polymerize back into rodlets under appropriate conditions. Otherwise, the layers formed by class II hydrophobins lack the fibrillary rodlet morphology and can be solubilized with organic solvents and detergents (Bayry et al., 2012). However, self-assembly and disassembly of class II hydrophobins can be repeated even after dissociation of the membrane by TFA. This shows that both classes of hydrophobins are highly resilient to this type of treatment.

Schematic representations of the three dimensional structure of class I and class II hydrophobins were reported in Figure 3. The 3D structure of the soluble state of the class I hydrophobins EAS (*Neurospora crassa*), DewA (*Aspergillus nidulans*), MPG1 (*Magnaporthe grisea*) and RodA (*Aspergillus fumigatus*) (Kwan et al., 2006; Morris et al., 2012, 2013; Rey et al., 2013; Pille et al., 2014) and the class II hydrophobins HFBI, HFBI (Trichoderma reesei), and NC2 (*N. crassa*) (Hakanpää et al., 2004, 2006a, b; Ren et al., 2013) has been solved. Both types of hydrophobins contain a four-stranded β -barrel core. Class II hydrophobins are compact and contain two short loops (L1 and L3), and a loop (L2) containing an α -helical structure. Class I hydrophobins show more variation in the length and structure of the loops. For example, L1 and L3 of EAS are unstructured, while L2 contains β -sheet structure. In contrast, the loops L1 and L2 of DewA, RodA and MPG1 contain α -helical structure (Wösten and Scholtmeijer 2015).

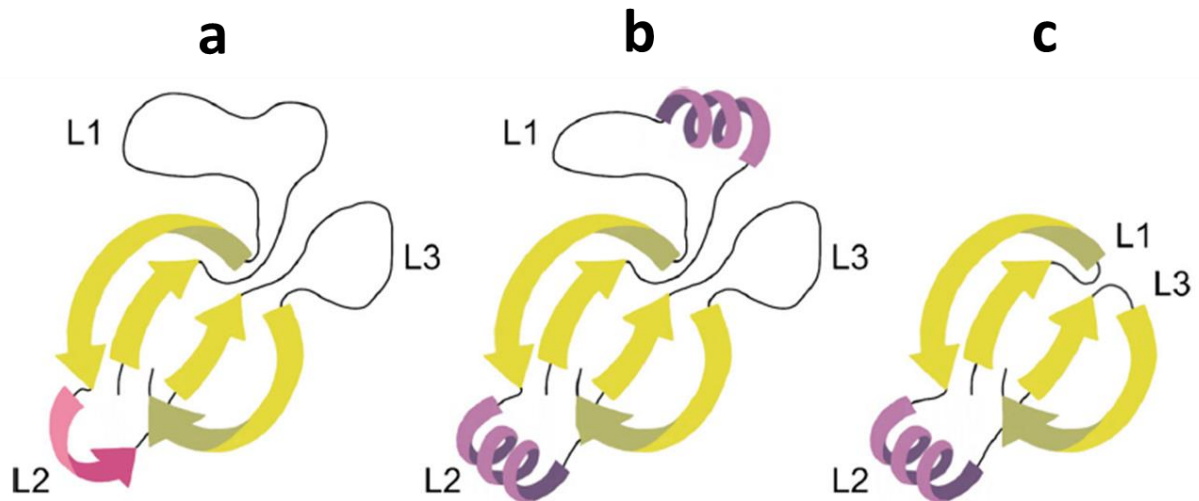


Figure 3: Schematic representation of the 3D structure of class I (a) EAS, (b) DewA, RodA, and MPG1 and class II (c) HFBI, HFBII, and NC2 hydrophobins. (Wösten & Scholtmeijer 2015)

1.2.2. Biological roles

Analysis of completed fungal genomes indicate that hydrophobins exist as small gene families (Sunde et al., 2008). Different hydrophobins are expressed at different stages in the fungus life cycle fulfilling several functions for their development. Many fungal functions are related to the surface activity of hydrophobins that self-assemble into an amphipathic membrane at hydrophilic hydrophobic interfaces (Fig. 4A,B). These layers can facilitate the aerial growth of fungi lowering the surface tension of the substrate thereby allowing the hyphae to grow into the air (Fig. 4C). The aerial hyphae continue to secrete hydrophobins, which assemble at the hyphal surface exposing a hydrophobic side, thus the hyphae become water repellent. During the aerial growth, the assembled hydrophobin layer are lined with the cavities in fruiting bodies to prevent that water fills these cavities (Fig. 4D). Similarly, hydrophobins assemble at the surfaces of spores developed from differentiated aerial hyphae (Fig. 4E). The coating of spores by hydrophobins facilitates their dispersal in the air and prevents desiccation. Moreover, hydrophobins mediate the attachment of fungi to hydrophobic solid substrates, such as the surface of a host, playing a role in symbiosis, and infections (Fig. 4F). Moreover, the hydrophobin layer prevents immune recognition of conidiospores and their clearance by neutrophils and macrophages in the early stages of infections (Zampieri et al., 2010). In figure 4 a model of the biological roles of hydrophobins during growth and development of filamentous fungi was reported.

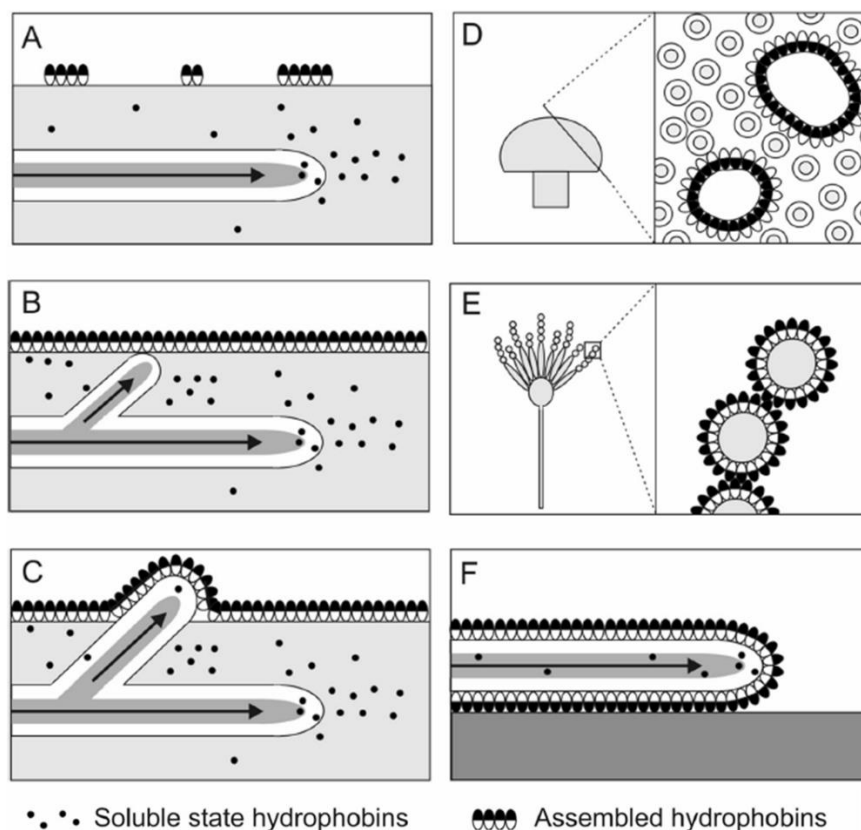


Figure 4: Biological role of fungal hydrophobins during liquid and aerial growth (Wösten & Scholtmeijer 2015)

1.2.3. Applications

Hydrophobins can be useful for several applications due to their physicochemical characteristics such as hydrophobicity and self-assembling (Khalessi et al., 2014).

At first, these properties have been exploited to modify different kinds of surfaces easily changing the wettability of both hydrophilic and hydrophobic surfaces such as glass, mica, parafilm and Teflon (Wosten et al., 1994; Mackay al., 2001).

Both classes of hydrophobins can be used to disperse hydrophobic materials in water replacing synthetic surfactants to create Teflon suspensions (Lumsdon et al., 2005) or to stabilize materials with electrochemical properties such as two-dimensional crystalline graphene sheets and multiwalled carbon nanotubes (MWCNT) (Laaksonen et al., 2010; Wang et al., 2010b; Gravagnuolo et al., 2015a), Wang et al., 2010c; Yang et al., 2013). Hydrophobins are also capable to stabilize emulsions such as oil droplets in water (Lumsdon et al., 2005; Reger et al., 2011; Askolin et al., 2006). Their use was proposed in creams and ointments for cosmetic, pharmaceutical purposes and in food applications (Hektor and Scholtmeijer 2005) improving the stability of physical and sensory properties of aerated products such as ice-creams or mayonnaise reducing also the amount of fat and/or calories (Cox et al., 2007, 2009; Tchuenbou-Magaia et al., 2009).

Hydrophobins offer a non-covalent alternative to the conventional surface modification methods. They functionalize substrates that can be used to immobilize peptides and proteins (Wang et al., 2007, 2010a, c; Qin et al., 2007; Hou et al., 2009; Zhang et al., 2011a, b, c, d; Longobardi et al., 2015). These amphiphilic layers can immobilize antibodies to improve the attachment of human endothelial cells to a

biocompatible surface (Zhang et al. 2011d) and cells like *Saccharomyces cerevisiae* on hydrophobic silicon-based materials, to improve the efficiency of metabolites productions (Nakari-Setälä et al., 2002). Moreover, hydrophobins did not seem to be neither toxic nor cytotoxic or immunogenic (Janssen et al., 2002; Janssen et al., 2004) making them really interesting for biomedical applications. Hydrophobins can also be used to immobilize inorganic compounds (Laaksonen et al., 2009, 2010).

Furthermore, hydrophobins can be used to produce recombinant proteins that can be purified via one-step extraction systems. (Linder et al., 2001). Many other applications of hydrophobins have been patented (Rink and Scholtmeijer 2005; Li Fet et al., 2015).

However, the applications of hydrophobins can be limited due to the low yield of production and purification. The required hydrophobin purity is directly correlated to the application of interest. For some applications, it is not necessary to reach the highest purity. For example, a crude extract containing a trace amount of hydrophobin may be sufficient as a foaming agent. In contrast, a highly pure hydrophobin is needed to be used as an additive in foodstuff and medicines (Khalesi et al., 2015). Most hydrophobins cannot yet be produced in gram per liter quantities hampering their use in technical applications. However, BASF succeeded to produce the hydrophobins H*Protein A and H*Protein B in sufficient amounts for large-scale applications. This brings the potential of hydrophobins in applications in daily life nearby.

1.3. Class I hydrophobin from *Pleurotus ostreatus*: Vmh2

The basidiomycetes *Pleurotus ostreatus* is a commercially important edible mushroom, also used as a source of proteins and other chemicals for industrial applications (Giardina et al., 1996). The family of genes coding for *P. ostreatus* hydrophobins is large and complex and the function of the encoded proteins is regulated by different developmental stages (Penas et al., 2009). A hydrophobin produced and secreted by *P. ostreatus* mycelia has been identified as Vmh2 and it has been purified and extensively studied by our research group.

Vmh2 seems to be the most hydrophobic hydrophobin characterized so far. The pure protein is not soluble in water, but in ethanol solution, whereas the most studied class I hydrophobins, such as SC3 and EAS, can be dissolved in water up to 1 mg/mL (Longobardi et al., 2012). The presence of carbohydrates, i.e. cyclodextrins, maltohexaose, and glucose, strongly increases the Vmh2 solubility in water but also its propensity to self-assembly with respect to the pure protein dissolved in less polar solvent (60% ethanol), not prone to self-assembly (Armenante et al., 2010). Structural and functional properties of the protein as a function of the environmental conditions have been determined. Solvent polarity, pH, temperature, and the presence of calcium ions trigger the protein transition across amyloid structural states (Longobardi et al., 2012). A study on Vmh2 soluble and aggregated forms is reported in Gravagnuolo et al., 2016 showing that Vmh2 does not form fibrillar aggregates at HHI but exhibits spherical and fibrillar assemblies whose ratio depends on the protein concentration when freshly solubilized at $\text{pH} \geq 7$. Moreover, Vmh2 spontaneously self-assembles into isolated, micrometer long, and twisted amyloid fibrils and this process is promoted by acidic pH, temperature, and Ca^{2+} ions.

Vmh2 layer prepared on the hydrophobic Teflon membrane in different conditions were characterized by the FT-IR analysis suggesting the best preparation conditions of the Vmh2 hydrophobin layer in terms of surface homogeneity (Portaccio et al.,

2015). Results, suggest that a slow aggregation process favours the formation of a uniform layer with a higher β -sheet contribution.

The natural capability to self-assemble on different surfaces has been exploited. Silicon is the most used solid support in all micro- and nanotechnologies developed for the integrated circuits industry. The ability of Vmh2 to form stable biofilm on hydrophobic silicon was verified, suggesting the possibility to use it as mask in micromachining processes for the realization of microsystems (De Stefano et al., 2007) and for the biological passivation of porous silicon, a nanostructured material usable in the development of some devices (De Stefano et al., 2008). The structural conformation of Vmh2 self-assembled into nanometric films (Houmadi et al., 2012) and its capability to adsorb enzymes in their active form, onto the bio-hybrid surface (Rea et al., 2012; De Stefano et al., 2009) have been explored.

The protein film has been also exploited to easily and homogeneously coat the sample-loading steel plate used in MALDI-TOF mass spectrometry. The functionalized surface was able to absorb peptides and proteins whereas salts or denaturants can be washed out allowing fast and high-throughput on-plate desalting prior to MS analysis (Longobardi et al., 2014). Trypsin has also been immobilized on Vmh2-coated MALDI wells in order to perform on-plate digestion of protein mixtures. The immobilized trypsin is active and able to perform the complete hydrolysis of substrate more quickly than the free enzyme (Longobardi et al., 2015).

The production of biofunctionalized graphene by exfoliation of a low-cost graphite source using Vmh2 in ethanol-water media was obtained. Gravagnuolo et al., 2015a described a one-step method for the exfoliation, stabilization and functionalization of graphene by Vmh2. As a potentially scalable approach, this method could enable massive production of biofunctionalized graphene, which could be a valuable material for the upcoming diffusion of new nanobiotechnologies in the global biomedical market. Vmh2 amphiphilic layer has been also used as a simple and rapid method for glass coating, modifying the WCA of super-hydrophilic glass up to 60°. This functionalized surface, highly homogeneous, was tested in microarray technology adsorbing stably a fluorescent protein and quantum dots by micro-patterning (Gravagnuolo et al., 2015b).

In addition, this protein plays a key role in one-step synthesis of hybrid protein-gold nanoparticles that were used to interact with protein and antibodies (Politi et al., 2015). Exploiting the capability of Vmh2 to interact naturally with glucose, it has been demonstrated that these nanoparticles are able to recognise this carbohydrate in aqueous solutions to monitor its concentration (Politi et al., 2016).

The production of hydrophobins fused to the enzymes is an interesting tool for the development of self-immobilizing enzymes useful for high throughput analyses. In this regard the enzyme glutathione-S-transferase (GST) fused to Vmh2 was exploited to develop a biosensor to quantify toxic compounds, such as the pesticides molinate and captan, in aqueous environmental samples. The achieved results have shown that this biosensor was able to detect low amounts of toxic compounds, in the order of femtomoles (Piscitelli et al., 2016).

1.4. Work description

This PhD project has been split into three main sections:

Isolation and characterizations of new hydrophobins from marine fungi

- Optimisation of culture growth conditions for marine fungi and set up of extraction techniques to isolate both classes of hydrophobins
- Characterization of two selected class I hydrophobins

Applications of the class I hydrophobin Vmh2

- Development of a proteomic approach through the MALDI-TOF mass spectrometry using the assembled layers of Vmh2 to immobilize the proteolytic enzyme trypsin and to hydrolyse *in situ* samples of different complexity
- Heterologous expression of the Vmh2 fused to GFP (Green fluorescent protein) in *Pichia pastoris* and use of the recombinant protein to develop a biosensor to detect thrombin

Use of hydrophobin coatings for antibiofilm activity

- Use of assembled layers of two different class I hydrophobins to inhibit biofilm formation of the nosocomial pathogen *Staphylococcus epidermidis*

1.5. References

- Armenante A, Longobardi S, Rea I, De Stefano L, Giocondo M, Silipo A, Molinaro A, Giardina P.** (2010) The *Pleurotus ostreatus* hydrophobin Vmh2 and its interaction with glucans. *Glycobiology* 20: 594-602.
- Askolin S, Linder MB, Scholtmeijer K, Tenkanen M, Penttilä ME, de Vocht ML, Wösten HAB.** (2006) Interaction and comparison of a class I hydrophobin from *Schizophyllum commune* and class II hydrophobins from *Trichoderma reesei*. *Biomacromolecules* 7:1295–1301.
- Bayry J, Aimanianda V, Guijarro JI, Sunde M, Latge JP.** (2012) Hydrophobins-Unique Fungal Proteins. *PLoS Pathog* 8(5): e1002700.
- Bhardwaj G, Cameotra SS, Chopra HK.** (2013) Biosurfactants from Fungi: A Review. *Pet Environ Biotechnol* 4:6.
- Bonugli-Santos RC, dos Santos Vasconcelos MR, Passarini MRZ, Vieira GAL, Lopes VCP, Mainardi PH, dos Santos JA, de Azevedo Duarte L, Otero IVR, da Silva Yoshida AM, Feitosa VA, Pessoa Jr A, Sette LD.** (2015) Marine-derived fungi: diversity of enzymes and biotechnological applications. *Front. Microbiol.*6:269.
- Cooper A, Kennedy MW.** (2010) Biofoams and natural protein surfactants. Review. *Biophysical Chemistry* 151:96–104.
- Cox AR, Aldred DL, Russell AB.** (2009) Exceptional stability of food foams using class II hydrophobin HFBII. *Food Hydrocoll* 23:366-376.
- Cox AR, Cagnol F, Russell AB, Izzard MJ.** (2007) Surface properties of class II hydrophobins from *Trichoderma reesei* and influence on bubble stability. *Langmuir*.
- De Stefano L, Rea I, Armenante A, Giardina P, Giocondo M, Rendina I.** (2007) Self Assembled Biofilm of Hydrophobins Protects the Silicon Surface in the KOH Wet Etch Process. *Langmuir* 23:7920-7922.
- De Stefano L, Rea I, Giardina P, Armenante A, Rendina I.** (2008) Protein-modified porous silicon nanostructures. *Adv Mater* 20:1529–1533.
- De Stefano L, Rea I, De Tommasi E, Rendina I, Rotiroti L, Giocondo M, Longobardi S, Armenante A, Giardina P.** (2009) Bioactive modification of silicon surface using self-assembled hydrophobins from *Pleurotus ostreatus*. *Eur. Phys. J. E. Soft Matter* 30:181-185.
- Dons JJM, Springer J, de Vries SC, Wessels JGH.** (1984) Molecular cloning of a gene abundantly expressed during fruiting body initiation in *Schizophyllum commune*. *J. Bacteriol.*157:802–808.
- Duarte K, Rocha-Santos TAP, Freitas AC, Duarte AC.** (2012) Analytical techniques for discovery of bioactive compounds from marine fungi. *Trends in Analytical Chemistry*, 34:97-110.
- Giardina P, Aurilia V, Cannio R, Marzullo L, Amoresano A, Siciliano R, Pucci P, Sannia G.** (1996) The gene, protein and glycan structures of laccase from *Pleurotus ostreatus*. *Eur. J. Biochem* 235:508-515.
- Gravagnuolo AM, Morales-Narváez E, Longobardi S, da Silva ET, Giardina P, Merkoçi A.** (2015a) In Situ Production of Biofunctionalized Few-Layer Defect-Free Microsheets of Graphene. *Adv. Funct. Mater.* 25: 2771-2779.
- Gravagnuolo AM, Morales-Narváez E, Santos Matos CR, Longobardi S, Giardina P, Merkoçi A.** (2015b) On-the-Spot Immobilization of Quantum Dots, Graphene Oxide, and Proteins via Hydrophobins. *Adv. Funct. Mater.* 25: 6084-6092.
- Gravagnuolo AM, Longobardi S, Luchini A, Appavou MS, De Stefano L, Notomista E, Paduano L, Giardina P.** (2016) Class I Hydrophobin Vmh2 Adopts Atypical Mechanisms to Self-Assemble into Functional Amyloid Fibrils. *Biomacromolecules* 17:954-64.

Hakanpää J, Paananen A, Askolin S, Nakari-Setälä T, Parkkinen T, Penttilä ME, Linder MB, Rouvinen J. (2004) Atomic resolution structure of the HFBII hydrophobin, a self-assembling amphiphile. *J Biol Chem* 279:534–539.

Hakanpää J, Szilvay GR, Kaljunen H, Maksimainen M, Linder MB, Rouvinen J. (2006a) Two crystal structures of *Trichoderma reesei* hydrophobin HFBI—the structure of a protein amphiphile with and without detergent interaction. *Protein Sci* 15:2129–2140.

Hakanpää J, Linder MB, Popov A, Schmidt A, Rouvinen J. (2006b) Hydrophobin HFBII in detail: ultrahigh-resolution structure at 0.75 Å. *Acta Crystallogr D Biol Crystallogr* 62:356–367.

Hektor HJ, Scholtmeijer K. (2005) Hydrophobins: proteins with potential. *Curr Opin Biotechnol* 16:434–439.

Hou S, Li X, Feng XZ, Wang R, Wang C, Yu L, Qiao MQ. (2009) Surface modification using a novel type I hydrophobin HGFI. *Anal Bioanal Chem* 394:783–789.

Houmadi S, Rodriguez RD, Longobardi S, Giardina P, Fauré MC, Giocondo M, Lacaze E. (2012) Self-assembly of hydrophobin protein rodlets studied with atomic force spectroscopy in dynamic mode. *Langmuir* 28:2551–57.

Imhoff JF. (2016) Natural Products from Marine Fungi—Still an Underrepresented Resource. *Marine Drugs* 14–19.

Janssen MI, van Leeuwen MBM, Scholtmeijer K, van Kooten TG, Dijkhuizen L, Wösten HAB. (2002) Coating with genetic engineered hydrophobin promotes growth of fibroblasts on a hydrophobic solid. *Biomaterials* 23:4847–4854.

Janssen MI, van Leeuwen MBM, van Kooten TG, de Vries J, Dijkhuizen L, Wösten HAB. (2004) Promotion of fibroblast activity by coating with hydrophobins in the β -sheet end state. *Biomaterials* 25:2731–2739.

Kiuru P, D’Auria MV, Muller CD, Tammela P, Vuorela H, -Kauhaluoma JY. (2014) Exploring Marine Resources for Bioactive Compounds. *Planta Med* 80:1234–1246.

Khalesi M, Mandelings N, Shokribousjein Z, Riveros-Galan D, Verachtert H, Gebruers K, Delvigne F, Vankelecom I, Derdelinckx G. (2014) Biophysical characterisation of hydrophobin enriched foamate. *Cerevisia* 38:129–134.

Khalesi M, Gebruers K and Derdelinckx G. (2015) Recent advances in fungal hydrophobin towards using in industry. *Protein* 34:243–255

Kwan AHY, Winefield RD, Sunde M, Matthews JM, Haverkamp RG, Templeton MD, Mackay JP. (2006) Structural basis for rodlet assembly in fungal hydrophobins. *Proc Natl Acad Sci USA* 103:3621–3626.

Laaksonen P, Kainlauri M, Laaksonen T, Shchepetov A, Jiang H, Ahopelto J, Linder MB. (2010) Interfacial engineering by proteins: exfoliation and functionalization of graphene by hydrophobins. *Angew Chem Int Ed* 49:4946–4949.

Laaksonen P, Kivioja J, Paananen A, Kainlauri M, Kontturi K, Ahopelto J, Linder MB. (2009) Selective nanopatterning using citrate-stabilized Au nanoparticles and cysteine-modified amphiphilic protein. *Langmuir* 25:5185–5192.

Li F, You Z, Rishton V. (2015) Hydrophobin composition and process for treating surfaces. Patent WO 2015051121 A1.

Linder M, Selber K, Nakari-Setälä T, Qiao M, Kula M-R, Penttilä M. (2001) The hydrophobins HFBI and HFBII from *Trichoderma reesei* showing efficient interactions with nonionic surfactants in aqueous two-phase systems. *Biomacromolecules* 2:511–517.

- Longobardi S, Picone D, Ercole C, Spadaccini R, De Stefano L, Rea I, Giardina P.** (2012) Environmental conditions modulate the switch among different states of the hydrophobin Vmh2 from *Pleurotus ostreatus*. *Biomacromolecules* 13(3):743-50.
- Longobardi S, Gravagnuolo AM, Rea I, De Stefano L, Marino G, Giardina P.** (2014) Hydrophobin-coated plates as matrix-assisted laser desorption/ionization sample support for peptide/protein analysis. *Anal Biochem* 449:9–16.
- Longobardi S, Gravagnuolo AM, Funari R, Della Ventura B, Pane F, Galano E, Amoresano A, Marino G, Giardina P.** (2015) A simple MALDI plate functionalization by Vmh2 hydrophobin for serial multi-enzymatic protein digestions. *Anal Bioanal Chem.* 407(2):487-96.
- Lumsdon SO, Green J, Stieglitz B.** (2005) Adsorption of hydrophobin proteins at hydrophobic and hydrophilic interfaces. *Colloids Surf B Biointerfaces* 44:172–178.
- Mackay JP, Jacqueline K, Matthews M, Winefield RD, Mackay LG, Haverkamp RG, Templeton MD.** (2001) The hydrophobin EAS is largely unstructured in solution and functions by forming amyloid-like structures. *Structure* 9:83–91.
- Manohar CS, Raghukumar C.** (2013) Fungal diversity from various marine habitats deduced through culture-independent studies. *FEMS Microbiol Lett* 341:69–78.
- Morris VK, Kwan AH, Mackay JP, Sunde M.** (2012) Backbone and sidechain ¹H, ¹³C and ¹⁵N chemical shift assignments of the hydrophobin DewA from *Aspergillus nidulans*. *Biomol NMR Assign* 6:83–86.
- Morris VK, Kwan AH, Mackay JP, Sunde M.** (2013) Analysis of the structure and conformational states of DewA gives insight into the assembly of the fungal hydrophobins. *J Mol Biol* 425:244–256.
- Nakari-Setälä T, Azeredo J, Henriques M, Oliveira R, Teixeira J, Linder M, Penttilä M.** (2002) Expression of a fungal hydrophobin in the *Saccharomyces cerevisiae* cell wall: effect on cell surface properties and immobilization. *AEM* 68:3385–3391.
- Peñas MM, Rust B, Larraya LM, Ramírez L, Pisabarro AG.** (2009) Differentially regulated, vegetative-mycelium-specific hydrophobins of the edible basidiomycete *Pleurotus ostreatus*. *Appl Environ Microbiol.* 68: 3891-3898.
- Pille A, Kwan AH, Cheung I, Hampsey M, Amanianda V, Delepierre M, Latgé JP, Sunde M, Guijarro I.** (2014) ¹H, ¹³C and ¹⁵N resonance assignments of the RodA hydrophobin from the opportunistic pathogen *Aspergillus fumigatus*. *Biomol NMR assign.*
- Piscitelli A, Pennacchio A, Longobardi S, Velotta R, Giardina P.** (2016) Vmh2 hydrophobin as a tool for the development of "self-immobilizing" enzymes for biosensing. *Biotechnol Bioeng.* 9999:1-7.
- Politi J, De Stefano L, Longobardi S, Giardina P, Rea I, Methivier C, Pradier CM, Casale S, Spadavecchia J.** (2015) Vmh2 plays a key role in one-step synthesis of hybrid protein-gold nanoparticles. *Colloids Surf B Biointerfaces.* 136:214-21.
- Politi J, De Stefano L, Rea I, Gravagnuolo AM, Giardina P, Methivier C, Casale S, Spadavecchia J.** (2016) One-pot synthesis of a gold nanoparticle-Vmh2 hydrophobin nanobiocomplex for glucose monitoring. *Nanotechnology.* 27:195701.
- Portaccio M, Gravagnuolo AM, Longobardi S, Giardina P, Rea I, De Stefano L, Cammarota M, Lepore M.** (2015) ATR FT-IR spectroscopy on Vmh2 hydrophobin self-assembled layers for Teflon membrane bio-functionalization. *Applied Surface Science* 351:673–680.
- Qin M, Wang LK, Feng XZ, Yang YL, Wang R, Wang C, Yu L, Shao B, Qiao MQ.** (2007) Bioactive surface modification of mica and poly(-dimethylsiloxane) with hydrophobins for protein immobilization. *Langmuir* 23:4465–4471.

- Raghukumar C.** (2008) Marine fungal biotechnology: an ecological perspective. *Fungal Diversity* 31: 19-35.
- Rea I, Giardina P, Longobardi S, Porro F, Casuscelli V, Rendina I, De Stefano L.** (2012) Hydrophobin Vmh2-glucose complexes self-assemble in nanometric biofilms. *J. R. Soc. Interface* 9:2450-56.
- Reger M, Sekine T, Okamoto T, Hoffmann H.** (2011) Unique emulsions based on biotechnically produced hydrophobins. *Soft Matter* 7:8248.
- Ren Q, Kwan AH, Sunde M.** (2013) Solution structure and interface driven self-assembly of NC2, a new member of the Class II hydrophobin proteins. *Proteins* 1.
- Rey AA, Hocher A, Kwan AH, Sunde M.** (2013) Backbone and sidechain 1H, 13C and 15N chemical shift assignments of the hydrophobin MPG1 from the rice blast fungus *Magnaporthe oryzae*. *Biomol NMR Assign* 7:109–112.
- Rink R, Scholtmeijer K.** (2005) Method for coating an object with hydrophobin at low temperatures. Patent WO 2005068087 A2.
- Smitha S, Correya NS, Philip R.** (2014) Marine fungi as a potential source of enzymes and antibiotics. *International Journal of Research in Marine Sciences* 3: 5-10.
- Sunde M, Kwan AHY, Templeton MD, Beever RE, Mackay JP.** (2008) Structural analysis of hydrophobins. *Review. Micron* 39:773–784.
- Swathi J, Narendra K, Sowjanya KM, Satya AK.** (2013) Marine fungal metabolites as a rich source of bioactive compounds. *African Journal of Biochemistry Research* 7:184-196.
- Tchuenbou-Magaia FL, Norton IT, Cox PW.** (2009) Hydrophobins stabilised air-filled emulsions for the food industry. *Food Hydrocolloids* 23:1877–1885.
- Wang R, Yang J-Y, Qin M, Wang L-K, Yu L, Shao B, Qiao M-Q, Wang C, Feng X-Z.** (2007) Biocompatible hydrophilic modifications of poly(dimethylsiloxane) using self-assembled hydrophobins. *Chem Mater* 19:3227–3231.
- Wang X, Wang H, Huang Y, Zhao Z, Qin X, Wang Y, Miao Z, Chen Q, Qiao M.** (2010a) Non covalently functionalized multi-wall carbon nanotubes in aqueous solution using the hydrophobin HFBI and their electroanalytical application. *Biosens Bioelectronics* 26:1104–1108.
- Wang Z, Huang Y, Li S, Xu H, Linder MB, Qiao M.** (2010b) Hydrophilic modification of polystyrene with hydrophobin for time-resolved immunofluorometric assay. *Biosens Bioelectronics* 26:1074–1079.
- Wang Z, Wang Y, Huang Y, Li S, Feng S, Xu H, Qiao M.** (2010c) Characterization and application of hydrophobin-dispersed multiwalled carbon nanotubes. *Carbon* 48:2890–2898.
- Wessels JG, de Vries OM, Asgeirsdottir SA, Springer J.** (1991a) The thn mutation of *Schizophyllum commune*, which suppresses formation of aerial hyphae, affects expression of the Sc3 hydrophobin gene. *J. Gen. Microbiol.* 137:2439–2445.
- Wessels JG, de Vries OM, Asgeirsdottir SA, Schuren J.** (1991b). Hydrophobin genes involved in formation of aerial hyphae and fruit bodies in *Schizophyllum*. *Plant Cell.* 3:793–799.
- Wösten HAB, Schuren FHJ, Wessels JGH.** (1994) Interfacial self-assembly of a hydrophobin into an amphipathic protein membrane mediates fungal attachment to hydrophobic surfaces. *EMBO J* 13:5848–5854.
- Wösten HAB, de Vocht ML.** (2000) Hydrophobins, the fungal coat unravelled. *Biochimica et Biophysica Acta* 1469: 79-86.
- Wösten HAB, Scholtmeijer K.** (2015) Applications of hydrophobins: current state and perspectives. Mini review. *Appl Microbiol Biotechnol.*

Yang W, Ren Q, Wu Y-N, Morris VK, Rey AA, Braet F, Kwan AH, Sunde M. (2013) Surface functionalization of carbon nanomaterials by self-assembling hydrophobin proteins. *Biopolymers* 99:84–94.

Zampieri F, Wösten HAB, Scholtmeijer K. (2010) Creating Surface Properties Using a Palette of Hydrophobins. *Review. Materials* 3:4607-4625.

Zhang XL, Penfold J, Thomas RK, Tucker IM, Petkov JT, Bent J, Cox A, Campbell RA. (2011a) Adsorption behaviour of hydrophobin and hydrophobin/surfactant mixtures at the air-water interface. *Langmuir* 27:11316–11323.

Zhang XL, Penfold J, Thomas RK, Tucker IM, Petkov JT, Bent J, Cox A, Grillo I. (2011b) Self-assembly of hydrophobin and hydrophobin/surfactant mixtures in aqueous solution. *Langmuir* 27:10514–10522.

Zhang XL, Penfold J, Thomas RK, Tucker IM, Petkov JT, Bent J, Cox A. (2011c) Adsorption behavior of hydrophobin and hydrophobin/ surfactant mixtures at the solid-solution interface. *Langmuir* 27: 10464–10474.

Zhang M, Wang Z, Wang Z, Feng S, Xu H, Zhao Q, Wang S, Fang J, Qiao M, Kong D. (2011d) Immobilization of anti-CD31 antibody on electro-spun poly(ϵ -caprolactone) scaffolds through hydrophobins for specific adhesion of endothelial cells. *Coll Surf B: Biointerf* 85:32–39.

CHAPTER 2

2. ISOLATION AND CHARACTERIZATIONS OF NEW HYDROPHOBINS FROM MARINE FUNGI

One of the challenges of the green technology is to find natural bio-molecules suitable for industrial applications in order to minimize the use and generation of hazardous substances. Recently many investigations have been focused on the marine environment because it is an untapped rich source of biological and chemical diversity to discover new compounds with intriguing activities. Therefore novel screening technologies, production and extraction techniques should be addressed to marine micro/organisms. Thanks to these premises, the aim of the work described in this chapter has been the exploration of the marine environment to identify new producers of a particular class of fungal self-assembling proteins, the hydrophobins, which in the recent decades have received considerable attention for their use in several industrial fields.

This chapter has been split in two sections:

- The first section is focused on the screening of some marine fungi to isolate, with appropriate extraction methods, new hydrophobins.
- In the second section two class I hydrophobins isolated during the previous screening have been characterized in solution and aggregate form.

2.1. Marine fungi as source of new hydrophobins



Contents lists available at ScienceDirect

International Journal of Biological Macromolecules

journal homepage: www.elsevier.com/locate/ijbiomac

Marine fungi as source of new hydrophobins

Paola Cicatiello^a, Alfredo Maria Gravagnuolo^a, Giorgio Gnani^b, Giovanna Cristina Varese^b, Paola Gardina^{a,*}^a Department of Chemical Sciences, University of Naples Federico II, via Cintia 4, I-80126 Naples, Italy^b Department of Life Sciences and Systems Biology, University of Turin, viale P.A. Mattioli 25, I-10125 Turin, Italy

ARTICLE INFO

Article history:
Received 22 June 2016
Accepted 11 August 2016
Available online 12 August 2016

Keywords:
Biosurfactants
Marine microorganisms
Self-assembly
Surface wettability
Emulsion
Protein coating

ABSTRACT

Hydrophobins have been described as the most powerful surface-active proteins known. They are produced by filamentous fungi and exhibit a distinct amphiphilic structure determining their self-assembly at hydrophilic-hydrophobic interfaces and surfactant properties which have been demonstrated to be useful for several biotechnological applications. The marine environment represents a vast natural resource of new molecules produced by organisms growing in various stressful conditions. This study was focused on the screening of 100 marine fungi from *Mycoteca Universitatis Taurinensis* (MUT) for the identification of new hydrophobins. Four different methods were set up to extract hydrophobins of class I and II, from the mycelium or the culture broth of fungi. Six fungi were selected as the best producers of hydrophobins endowed with different characteristics. Their ability to form stable amphiphilic films and their emulsification capacity in the presence of olive oil was evaluated.

© 2016 Elsevier B.V. All rights reserved.

1. Introduction

Hydrophobins (HFBs), small proteins (about 100 amino acids) typical of filamentous fungi, have been described as the most powerful surface-active proteins known and their activity is intrinsic to the proteins themselves [1,2]. Indeed, on one side of their molecular surface, some exposed hydrophobic aliphatic side chains form a flat hydrophobic patch, whilst polar or charged residues are confined to the other side [3,4]. The hydrophobic patch could be involved in interaction with an identical protein partner that obscures the hydrophobic region. This allows miscibility with the bulk water phase until reaching an air–water interface or other non-polar surface, where they probably dissociate and re-orient with the hydrophobic surface exposed to the interface [5]. Several features of fungal development have been attributed to these proteins [6], e.g. coating of spores, aerial hyphae and fruiting bodies with a water-repellent and adhesive layer allowing the fungus to escape from the liquid medium and to live in adhesion on different surfaces [7]. HFBs show very little conservation of their sequence, apart from the pattern of eight Cys residues implicated in the formation of four disulfide bridges (Cys1–Cys6, Cys2–Cys5, Cys3–Cys4, Cys7–Cys8) [8]. They have been split in two groups, class I and class II, based on

structural differences and properties of the aggregates they form [9]. Class I HFBs form highly insoluble aggregates that have the appearance of distinct rodlets and, similarly to amyloid fibrils, are characterized by cross β -structure [10]. These assemblies show outstanding stability and can be depolymerized in 100% trifluoroacetic acid (TFA) whereas class II HFBs form less stable polymers that are soluble in some organic solvents or SDS aqueous solution, and lack the rodlet appearance of class I HFBs [11]. Both types of HFBs have been used for several biotechnological applications, such as dispersion of hydrophobic materials, foam stabilization in food products, surface coating and modification of the surface wettability, immobilization of enzymes, peptides, antibodies and nanomaterials on various surfaces [12–15]. The marine environment host a huge biodiversity of (micro) organisms, and fungi make up a large part of them [16]. Marine fungi form an ecological, and not a taxonomic group. These species live in a stressful habitat, under cold, lightless, high-pressure conditions or other types of mechanical stress. Their capability to survive in different environmental conditions makes them attractive to isolate new molecules [17–19]. The aim of the present study is to identify marine fungi as source of HFBs.

* Corresponding author at: Department of Chemical Sciences, Complesso Universitario Monte S. Angelo, Via Cintia 4, 80126 Naples, Italy.
E-mail address: giardina@unina.it (P. Gardina).

2. Material and methods

2.1. Marine fungi

Marine fungi were isolated and identified from the seagrass *Posidonia oceanica*, the green alga *Flabellia petiolata* and the brown alga *Padina pavonica* collected nearby Elba Island in the Mediterranean Sea as previously described [20–22] and are preserved at the *Mycoteca Universitatis Taurinensis* (MUT).

2.2. Culture conditions

Each marine fungal strain was maintained through periodic transfer on agar plate at 20 °C. The strains were grown in multiwell plates (9.5 cm² cell growth area) in 3 different liquid media XNST30 (malt extract 3 g/L; yeast extract 3 g/L; NaCl 30 g/L; 10 g/L glucose and 5 g/L peptone), PDY15 (24 g/L potato dextrose; 5 g/L yeast extract and 15 g/L NaCl) and WM (10 g/L glucose; 2 g/L peptone; 1 g/L (NH₄)₂SO₄; 0.5 g/L MgSO₄·7H₂O; 0.875 g/L KH₂PO₄; 0.125 g/L K₂HPO₄; 0.1 g/L CaCl₂·2H₂O; 0.1 g/L NaCl; 0.05 g/L MnCl₂; 0.001 g/L FeSO₄) at 2 different temperatures (20–28 °C) in triplicate for 10 days. The inoculum was carried out by addition of mycelium disks (5 mm diameter) taken from actively growing cultures on agar plates in 7.5 mL of medium or by adding 0.5 mL of a suspension in 0.9% NaCl, 0.1% Tween 80 of mycelium mechanically broken by glass beads. In order to extract sufficient amounts of HFBs, marine fungi were grown in 100 mL conical flasks containing 50 mL of the selected medium. Fungi were grown in the dark at 200 rpm for 10 days.

2.3. Extraction of class I and class II HFBs from the culture broth

Proteins were aggregated by air bubbling, using a Waring blender. Foam was collected and treated with 20% trichloroacetic acid (TCA) and was centrifuged after 12 h incubation at 4 °C in static. In order to extract class I HFB candidates, the obtained precipitate was treated by 100% TFA in a bath sonicator, dried using a stream of nitrogen and then dissolved in a 60% ethanol solution, while it was directly treated by 60% ethanol to dissolve class II HFBs.

2.4. Extraction of class I and class II HFBs from the mycelium

To extract Class II HFBs, mycelia were washed by water and proteins were extracted using 60% ethanol in a bath sonicator and, after centrifugation, the supernatant was collected.

To extract class I HFBs, mycelia were firstly washed by 2% SDS, several times by water and once by 60% ethanol to remove soluble proteins, contaminants and the detergent. The residue was freeze-dried, treated by TFA using a bath sonicator to extract the protein from the wall of the mycelium. After centrifugation of the TFA extract, the supernatant was dried using a stream of nitrogen, dissolved in 60% ethanol and centrifuged again. The new supernatant was lyophilized and proteins were extracted at the interphase using a chloroform:methanol:water mixture 1:2:2 v/v in a bath sonicator. After centrifugation, the precipitate was freeze-dried, treated by TFA in a bath sonicator, dried in a stream of nitrogen and dissolved in 60% ethanol.

2.5. Analysis of the purified proteins

Protein concentrations were evaluated using the PIERCE 660 nm Protein Assay kit using bovine serum albumin as standard. The purity and the molecular weight of the extracted samples were evaluated by SDS-PAGE (15% acrylamide), and silver stained.

2.6. Water contact angle analysis of the functionalized surfaces

Contact angle measurements were performed on a KSV Instruments LTD CAM 200 Optical Contact Angle Meter coupled with drop shape analysis software. Each contact angle was calculated as the average of two drops of 5 μL, spotted on different points of the crystalline silicon chip.

2.7. Evaluation of emulsifying properties of HFBs

HFBs were dissolved in 50 mM phosphate buffer pH 7 at 0.05 mg ml⁻¹. Solutions were mixed by vortexing for 2 min with olive oil (25% v/v) and left standing for 24 h. To evaluate the emulsification capacity of the samples the height of the emulsion phase was monitored.

3. Results and discussion

3.1. Growth conditions of marine fungi

Twenty-three fungi were selected from a pool of 100 marine fungal strains on the base of the ability to produce foam during the growth in shaken cultures, thus indicating the production of biosurfactants. The list of these strains is reported in Table 1.

Subsequently, the growth conditions of the selected fungi in liquid medium were optimized in multiwell plates changing parameters such as the temperature, 20 and 28 °C, and the composition of the culture broths. Three cultural broths, commonly used for fungal growth, XNST30, PDY15 and WM, characterized by different C/N ratio and salt concentrations, were tested. The growths were performed at two temperatures, 20 and 28 °C, in triplicate for 10 days. Most of the strains grew in more than one condition, however the best combinations of parameters were selected on the basis of the abundance of the produced mycelia (Table 1). Three strains, MUT 4871, 4857 and 4860, only grew when the culture broths were inoculated by addition of mycelia mechanically broken by glass beads, not by addition of mycelium disks from agar plates. When results were comparable, the WM poor medium was preferentially selected to reduce the presence of contaminant molecules in the purified samples.

3.2. Extraction of class I and class II HFBs

In order to extract sufficient amounts of HFBs, marine fungi were grown in conical flasks for 10 days and separated from the culture broths by filtration. Four different extraction methods were set up to extract HFBs belonging to Class I and Class II from both the mycelium and the culture broth, were set up (Fig. 1). The capability of HFBs to migrate at the water/air interface was exploited to extract the secreted proteins by bubbling the culture broth, while the cell wall associated proteins were isolated from the dried mycelium by solvent extraction. The requirement of the TFA treatment to solubilize the Class I HFBs was exploited to discriminate between the two classes. Since *Coprinellus* sp. MUT 4897 belongs to the basidiomycetes which exclusively produce class I HFBs [9], the extraction methods for this class were only used in this case.

Adequate amounts of putative HFBs were extracted from 6 strains, and analyzed by SDS-PAGE (Fig. 2). The developed procedures allowed us to obtain quite homogeneous protein samples. The molecular weights of the extracted proteins ranged between 11 and 35 kDa, as observed in most of the known HFBs.

3.3. Analysis of the HFB functions

To test the ability of these putative HFBs to self-assemble into a stable amphiphilic layer and to functionalize a solid surface, the

Table 1

List of the screened fungal strains with their MUT code and the original substrate of isolation. The asterisks indicate conditions in which they grew. The grey boxes correspond to the best growth conditions in which proteins were extracted.

MUT accession number and strain	Original substrate	XNST30		PDY15		WM	
		28°C	20°C	28°C	20°C	28°C	20°C
4777 <i>Apiospora mantagnei</i>	<i>F. petiolata</i>	*					
4857 <i>Verrucocladosporium dirinae</i>	<i>F. petiolata</i>		*		*		*
4858 <i>Sporormiaceae</i> sp.	<i>F. petiolata</i>	*	*	*	*	*	*
4859 <i>Rousoellaceae</i> sp.2	<i>F. petiolata</i>		*		*		*
4860 <i>Massarina</i> sp.1	<i>F. petiolata</i>						*
4861 <i>Microascaceae</i> sp.1	<i>F. petiolata</i>	*					
4863 <i>Massarina</i> sp.2	<i>F. petiolata</i>		*		*		
4864 <i>Microascus cirrosus</i>	<i>F. petiolata</i>	*	*	*	*		
4868 <i>Myceliophthora verrucosa</i>	<i>F. petiolata</i>	*	*	*	*	*	*
4871 <i>Gibellulopsis nigrescens</i>	<i>F. petiolata</i>	*	*	*	*	*	*
4872 <i>Acremonium sclerotigenum</i>	<i>F. petiolata</i>	*	*	*	*	*	*
4877 <i>Penicillium expansum</i>	<i>F. petiolata</i>		*		*		*
4878 <i>Myceliophthora verrucosa</i>	<i>F. petiolata</i>	*	*	*	*	*	*
4879 <i>Arthopyrenia salicis</i>	<i>F. petiolata</i>	*					
4883 <i>Biatrispora</i> sp.	<i>F. petiolata</i>		*		*		*
4885 <i>Microascus trigonosporus</i>	<i>F. petiolata</i>		*		*		*
4886 <i>Rousoellaceae</i> sp.1	<i>F. petiolata</i>		*		*		*
4887 <i>Massarina rubi</i>	<i>F. petiolata</i>				*		*
4892 <i>Penicillium roseopurpureum</i>	<i>P. pavonica</i>		*		*		*
4894 <i>Didymellaceae</i> sp.1	<i>P. pavonica</i>	*					
4897 <i>Coprinellus</i> sp.	<i>P. pavonica</i>						*
5039 <i>Penicillium chrysogenum</i>	<i>P. oceanica</i>		*		*		*
5169 <i>Penicillium brevicompactum</i>	<i>P. pavonica</i>		*		*		*

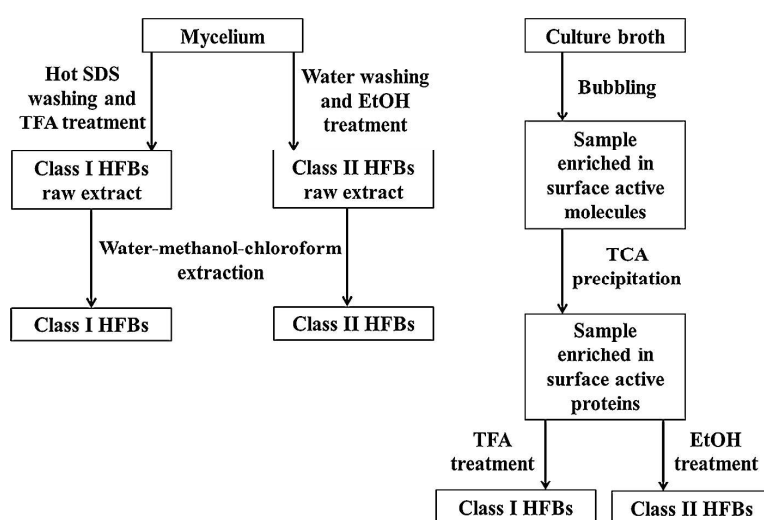
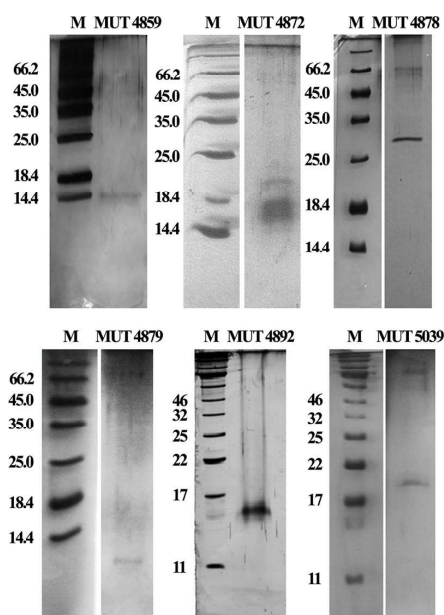


Fig. 1. Scheme of the procedures set up to extract Class I or Class II HFB, associated to the mycelium wall or secreted in the culture broth.

Table 2

Strains selected as producers of new HFBs, classification and yield of the purified proteins.

MUT accession number and strain	Source	HFB class	Production yield, mgL ⁻¹
4859 <i>Rousoellaceae</i> sp. 2	Culture broth	I	2
4872 <i>Acremonium sclerotigenum</i>	Culture broth	I	10
4878 <i>Myceliophthora verrucosa</i>	Culture broth	II	5
4879 <i>Arthopyrenia salicis</i>	Mycelium	II	5
4892 <i>Penicillium roseopurpureum</i>	Culture broth	I	3
5039 <i>Penicillium chrysogenum</i>	Mycelium and culture broth	II	12

**Fig. 2.** SDS-PAGE analysis of the extracted proteins. M is the molecular weight marker, the MUT code of the strain from which the protein was extracted, is reported in each panel.

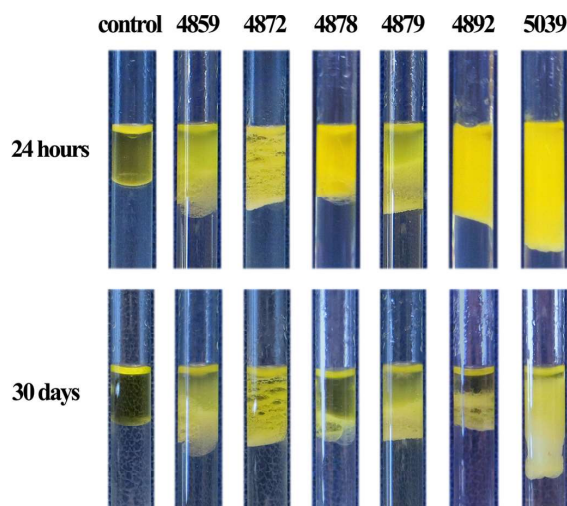
samples were deposited on crystalline silicon chips, dried at 60° C, and washed by a 60% ethanol solution or hot SDS at 2%. The change of the wettability was evaluated by the contact angle of a sessile water drop before and after the functionalization and upon the washing steps (Fig. 3). The 4 putative Class I HFBs formed a stable layer, resistant to 60% ethanol and hot SDS, confirming that they belong to that class. On the other hand the layers of the other two putative HFBs were removed after mild washing in 60% ethanol, confirming that they belong to the Class II HFBs. A list of the selected strains with the corresponding HFB class and production yield is shown in Table 2.

Furthermore, the emulsification capacity of each of the extracted protein was tested in the presence of olive oil upon agitation by vortex. All the six putative HFBs were able to produce water/oil emulsions (Fig. 4). Their stability was followed during one month at room temperature showing that the putative Class II HFB from the *Penicillium chrysogenum* MUT 5039 is the most surface-active protein identified in this study.

4. Conclusions

Twenty three marine fungi, out of 100, have been selected for their ability to produce foam in shaken culture. Afterwards four extraction methods have been set up to isolate secreted or cell wall associated HFBs of Class I or II, allowing the identification of 6

MUT	After deposition	After washing by 60% ethanol	After washing by hot 2% SDS
Control	88 ± 1°	87 ± 2°	79 ± 1°
4859	10 ± 1°	63 ± 6°	47 ± 4°
4872	26 ± 2°	54 ± 5°	58 ± 1°
4878	25 ± 5°	70 ± 2°	83 ± 1°
4879	6 ± 1°	61 ± 2°	45 ± 1°
4892	8 ± 1°	44 ± 3°	33 ± 2°
5039	16 ± 1°	67 ± 3°	75 ± 3°

Fig. 3. WCA analysis of crystalline silicon surface upon functionalization using the extracted HFBs and washings using different solutions.**Fig. 4.** Aqueous emulsions of the extracted proteins (0.05 mg mL⁻¹) in the presence of 25% olive oil. Each solution was vortexed for 2 min, left standing and imaged after 24 h and 30 days.

new putative HFBs which show promising properties for biotechnological applications. The purity and the Mw of the proteins have been assessed by SDS-PAGE. On the basis of the stability of the amphiphilic layer that they form on a crystalline silicon chip, it has been confirmed that 4 of them belong to the Class I and 2 proteins to the Class II of the HFB family. One of them was endowed with

remarkable emulsification capacity tested on a mixture of water and olive oil.

The use of marine species could enable the large scale and sustainable production of HFBs exploiting the natural resource of widely available seawater for their cultivation.

Acknowledgments

The authors would like to thank dr. Luca De Stefano and dr. Jane Politi of the Institute for Microelectronics and Microsystems, Unit of Naples, National Council of Research, for their assistance in the water contact angle measurements.

This work was supported by grant from the Ministero dell'Università e della Ricerca Scientifica—Industrial research project “Development of green technologies for production of BIO-chemicals and their use in preparation and industrial application of POLImeric materials from agricultural biomasses cultivated in a sustainable way in Campania region (BioPoliS)PONO3PE.00107.1, funded in the frame of Operative National Programme Research and Competitiveness 2007–2013 D. D. Prot. N. 713/Ric. 29/10/2010.

References

- [1] A. Cooper, M.W. Kennedy, Biofoams and natural protein surfactants, *Biophys. Chem.* 151 (2010) 96–104, <http://dx.doi.org/10.1016/j.bpc.2010.06.006>.
- [2] W. Wohlleben, T. Subkowski, C. Bollschweiler, B. von Vacano, Y. Liu, W. Schrepp, et al., Recombinantly produced hydrophobins from fungal analogues as highly surface-active performance proteins, *Eur. Biophys. J.* 39 (2010) 457–468, <http://dx.doi.org/10.1007/s00249-009-0430-4>.
- [3] J. Hakanpää, A. Paananen, S. Askolin, T. Nakari-Setälä, T. Parkkinen, M. Penttilä, et al., Atomic resolution structure of the HFBII hydrophobin, a self-assembling amphiphile, *J. Biol. Chem.* 279 (2004) 534–539, <http://dx.doi.org/10.1074/jbc.M309650200>.
- [4] A.H. Kwan, R.D. Winefield, M. Sunde, J.M. Matthews, R.G. Haverkamp, M.D. Templeton, et al., Structural basis for rodlet assembly in fungal hydrophobins, *Proc. Natl. Acad. Sci. U. S. A.* 103 (2006) 3621–3626, <http://dx.doi.org/10.1073/pnas.0505704103>.
- [5] H. a Wösten, M.L. de Vocht, Hydrophobins, the fungal coat unravelled, *Biochim. Biophys. Acta* 1469 (2000) 79–86 <http://www.ncbi.nlm.nih.gov/ubmed/10998570>.
- [6] H.A. Wösten, Hydrophobins: multipurpose proteins, *Annu. Rev. Microbiol.* 55 (2001) 625–646, <http://dx.doi.org/10.1146/annurev.micro.55.1.625>.
- [7] S. Zhang, Y.X. Xia, B. Kim, N.O. Keyhani, Two hydrophobins are involved in fungal spore coat rodlet layer assembly and each play distinct roles in surface interactions, development and pathogenesis in the entomopathogenic fungus, *Beauveria bassiana*, *Mol. Microbiol.* 80 (2011) 811–826, <http://dx.doi.org/10.1111/j.1365-2958.2011.07613.x>.
- [8] J. Bayry, V. Aimanianda, J.I. Guijarro, M. Sunde, J.-P. Latgé, Hydrophobins—unique fungal proteins, *PLoS Pathog.* 8 (2012) e1002700, <http://dx.doi.org/10.1371/journal.ppat.1002700>.
- [9] M.B. Linder, G.R. Szilvay, T. Nakari-Setälä, M.E. Penttilä, Hydrophobins: the protein-amphiphiles of filamentous fungi, *FEMS Microbiol. Rev.* 29 (2005) 877–896, <http://dx.doi.org/10.1016/j.femsre.2005.01.004>.
- [10] I. Macindoe, A.H. Kwan, Q. Ren, V.K. Morris, W. Yang, J.P. Mackay, et al., Self-assembly of functional, amphipathic amyloid monolayers by the fungal hydrophobin EAS, *Proc. Natl. Acad. Sci. U. S. A.* 109 (2012) E804–11, <http://dx.doi.org/10.1073/pnas.1114052109>.
- [11] V. Lo, Q. Ren, C. Pham, V. Morris, A. Kwan, M. Sunde, Fungal hydrophobin proteins produce self-assembling protein films with diverse structure and chemical stability, *Nanomaterials* 4 (2014) 827–843, <http://dx.doi.org/10.3390/nano4030827>.
- [12] H.A.B. Wösten, K. Scholtmeijer, Applications of hydrophobins: current state and perspectives, *Appl. Microbiol. Biotechnol.* 99 (2015) 1587–1597, <http://dx.doi.org/10.1007/s00253-014-6319-x>.
- [13] M. Khalesi, K. Gebruers, G. Derdelinckx, Recent advances in fungal hydrophobin towards using in industry, *Protein J.* 34 (2015) 243–255, <http://dx.doi.org/10.1007/s10930-015-9621-2>.
- [14] A.M. Gravagnuolo, E. Morales-Narváez, C.R.S. Matos, S. Longobardi, P. Giardina, A. Merkoçi, On-the-spot immobilization of quantum dots, graphene oxide, and proteins via hydrophobins, *Adv. Funct. Mater.* 25 (2015) 6084–6092, <http://dx.doi.org/10.1002/adfm.201502837>.
- [15] E. Patel, P. Cicatiello, L. Deininger, M.R. Clench, G. Marino, P. Giardina, et al., A proteomic approach for the rapid, multi-informative and reliable identification of blood, *Analyst* 141 (2016) 191–208, <http://dx.doi.org/10.1039/c5an02016f>.
- [16] L. Panno, M. Bruno, S. Voyron, A. Anastasi, G. Gnani, L. Miserere, et al., Diversity, ecological role and potential biotechnological applications of marine fungi associated to the seagrass *Posidonia oceanica*, *New Biotechnol.* 30 (2013) 685–694, <http://dx.doi.org/10.1016/j.nbt.2013.01.010>.
- [17] S.K. Satpute, A.G. Banpurkar, P.K. Dhakephalkar, I.M. Banat, B.A. Chopade, Methods for investigating biosurfactants and bioemulsifiers: a review, *Crit. Rev. Biotechnol.* 30 (2010) 127–144, <http://dx.doi.org/10.3109/07388550903427280>.
- [18] G.M. König, S. Kehraus, S.F. Seibert, A. Abdel-Lateff, D. Müller, Natural products from marine organisms and their associated microbes, *ChemBioChem* 7 (2006) 229–238, <http://dx.doi.org/10.1002/cbic.200500087>.
- [19] R. Nicoletti, A. Trincone, Bioactive compounds produced by strains of *penicillium* and *talaromyces* of marine origin, *Mar. Drugs* 14 (2016), <http://dx.doi.org/10.3390/md14020037>.
- [20] G. Gnani, E. Ercole, L. Panno, A. Vizzini, G.C. Varese, Dothideomycetes and Leotiomycetes sterile mycelia isolated from the Italian seagrass *Posidonia oceanica* based on rDNA data, *Springerplus* 3 (2014) 508, <http://dx.doi.org/10.1186/2193-1801-3-508>.
- [21] L. Garzoli, G. Gnani, F. Tamma, S. Tosi, G.C. Varese, A.M. Picco, Sink or swim: updated knowledge on marine fungi associated with wood substrates in the Mediterranean Sea and hints about their potential to remediate hydrocarbons, *Prog. Oceanogr.* 137 (2015) 140–148, <http://dx.doi.org/10.1016/j.pcean.2015.05.028>.
- [22] A. Micheluz, S. Manente, V. Tigrini, V. Prigione, F. Pinzari, G. Ravagnan, et al., The extreme environment of a library: xerophilic fungi inhabiting indoor niches, *Int. Biodeterior. Biodegrad.* 99 (2015) 1–7, <http://dx.doi.org/10.1016/j.ibiod.2014.12.012>.

CHAPTER 3

3. APPLICATIONS OF THE CLASS I HYDROPHOBIN VMH2

The class I hydrophobin Vmh2 isolated from the basidiomycete fungus *Pleurotus ostreatus* has been thoroughly studied in the last ten years in the research group where this PhD project has been developed. A broad characterization of the wild type and recombinant Vmh2, both in solution and on surfaces, has been carried out in order to investigate on the use of this protein in different applications. One of them concerns the ability of the Vmh2 layer to efficiently immobilize enzymes. Indeed Vmh2 spontaneously forms stable and homogeneous layers on different surfaces, capable to immobilize enzymes preserving their active form.

In particular, the Vmh2 layer has been employed to functionalize the sample plate used in MALDI-TOF mass spectrometry, to immobilize different enzymes widely used in proteomics (proteases, glycosidases and phosphatases) in order to carry out *in-situ* multi-enzymatic reactions. Using this lab-on-plate approach the proteolytic reactions were performed quicker than those in solution, only 5 minutes against 12 hours of incubation, obtaining a high level of sequence coverage of standard proteins (bovine serum albumin and ovalbumin) and biological complex samples, such as milk. On this basis, the work described in the first two sections of this chapter has been carried out, in collaboration with Fingermark Research Group of Dr. Simona Francese at Sheffield Hallam University, Sheffield, UK.

- In the first section a preliminary approach to improve the resolution and detection of the mass spectrometry MALDI Imaging (IMS) technique, through the use of Vmh2-coated-supports is described.
- In the second section, the Lab-on-plate approach is employed to analyse whole blood of different species (human and horse) and to individuate the species-specific peptides for forensic analysis.

Self-assembling protein layers are also promising candidates for the fabrication of biosensors, being their use as platforms for enzyme immobilization rapidly gathering attention. Moreover, if the enzyme of interest is genetically fused to a self-assembling protein, the ease of obtaining adhesive film is conjugated with the strength of the covalent immobilization. In this view, a system for recombinant production in *Escherichia coli* of Vmh2 fused to the enzyme glutathione-S-transferase (GST) has been established with the aim of overproducing the Vmh2 hydrophobin and increasing its solubility. Furthermore the Vmh2-GST fused protein has been used to develop a GST based biosensor to quantify toxic compounds, such as the pesticides molinate and captan, in aqueous environmental samples.

- The third section of this chapter is focused on the heterologous expression of Vmh2 fused to GFP (Green fluorescent protein) in the yeast *P. pastoris* to develop a smart and effective tool for the study of Vmh2 self-assembling. Moreover, since the two proteins were linked by the specific cutting site of the thrombin, the fusion protein was used as the active biological element in the realization of a thrombin biosensor. My main contribution to this work was given during the cloning and purification of the recombinant fused protein.

3.1. The use of the Vmh2 layer in MALDI-IMS

(Matrix Assisted Laser Desorption/Ionization Imaging Mass Spectrometry)

Introduction

The MALDI-IMS is a powerful tool to study and determine the distribution of hundreds of unknown compounds in a single analysis, allowing the acquisition of cellular expression profiles maintaining cellular and molecular integrity. This technique can detect, identify and localize lipids, peptides, proteins, drugs and metabolites (Cillero-Pastor and Heeren, 2013). In the recent years, remarkable improvements of this technique have been achieved by making it more sensitive and robust to perform molecular investigations directly on intact tissue sections without the use of antibodies or radioactive probes. In the Figure 1 an IMS experiment is illustrated. Briefly, a thin tissue section is mounted on a conductive target surface. After the matrix application, the tissue section is irradiated by the laser in an array pattern to generate the mass spectrum for each ablated spot correlated to specific x, y coordinates. Then the selected ions are mapped across the tissue to create images that can be combined to create a multiplex ion image (Peggi and Caprioli, 2013).

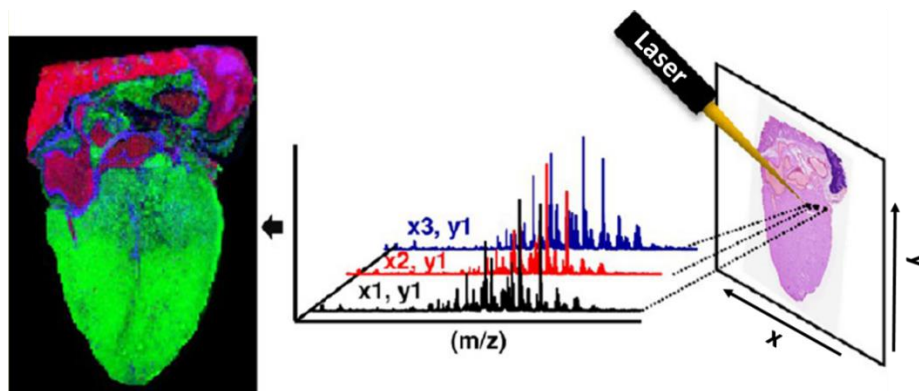


Figure 1. Overview of an IMS experiment. (Peggi and Caprioli, 2013)

The problems related to this technique are numerous including the storage, handling and deposition of the tissue, and the kind of matrix to use and how it has to be used. In Figure 2 an experimental workflow is reported, describing the parameters that should be considered when designing an IMS experiment (Peggi and Caprioli, 2013).

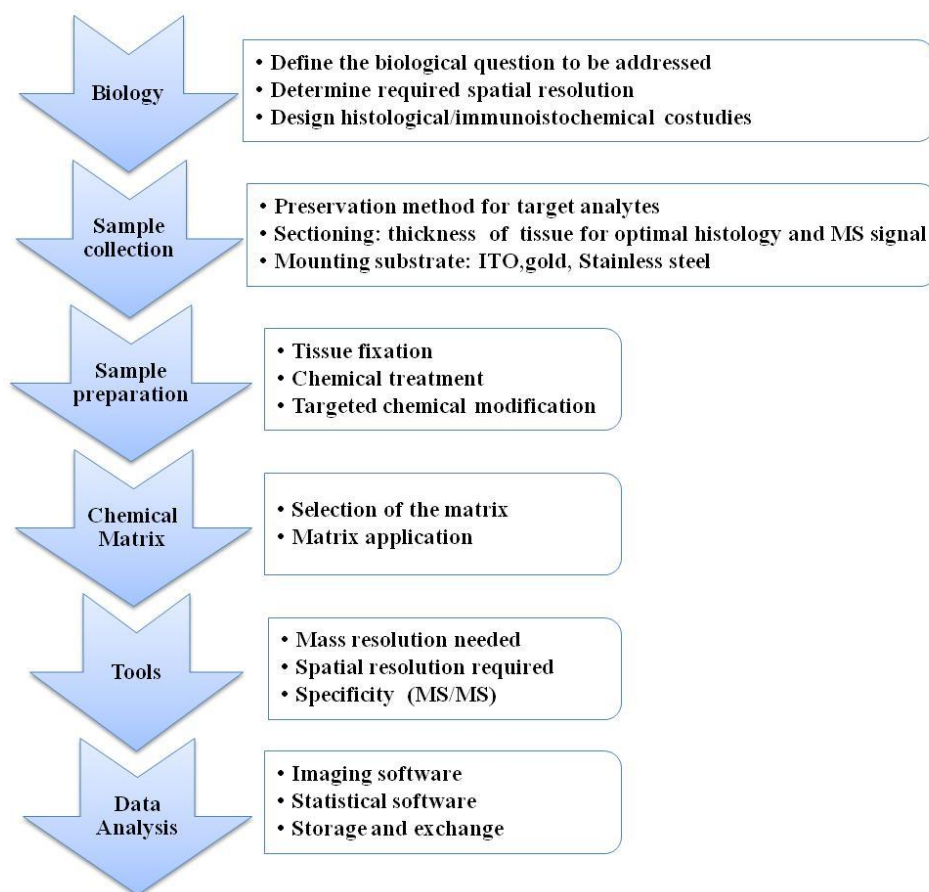


Figure 2. *Experimental workflow for an IMS analysis. (Peggi and Caprioli, 2013)*

Different approaches can be used according to the molecule to analyse. For the identification of proteins, a top down approach involves a direct analysis of the whole proteins, while a bottom up approach involves a proteolytic digestion to generate peptides whose fragmentation leads to the identification of the original protein (Schone et al., 2013).

The use of a Vmh2 layer to blot the tissue on the IMS support could make easier both the sample collection and preparation phases and optimize the resolution of the acquired images. Indeed the biomolecules of the tissue can be immobilized on the Vmh2 pre-coated slides, which can be washed to remove possible contaminants, in order to obtain quickly and easily, with good S/N ratio, the specific distribution of peptides, proteins, metabolites or lipids.

Moreover, based on the previous works, the Vmh2 layer could be used to produce pre-covered supports to immobilize proteolytic enzymes for a bottom-up approach of MALDI-IMS (Longobardi et al., 2015).

Materials and Methods

The slides coated with ITO (Indium Tin Oxide) were functionalized with Vmh2. 0.2 mL of 0.1 mg/mL Vmh2 in 60% ethanol solution were deposited on the slide covering the whole surface. After the complete evaporation of the protein incubated at 60°C, washes with 60% ethanol to remove the protein excess were performed. A second deposition was repeated in the same way. A glass slide, on which a slice of rat brain tissue was previously deposited (10µm thickness), was put in contact for 5 minutes with the Vmh2 coated slide applying a slight pressure to favour the deposition by blotting. The α -cyano-4-hydroxycinnamic acid was used as matrix dissolved in a solution containing in the ratio 7:3 100% acetonitrile: 0.5% trifluoroacetic acid at a concentration of 5 mg/mL. Five layers of matrix were deposited using the SunCollect autosprayer (KR Analytical) at a flow rate of 2µL/min. The data and analysis of MALDI MSI images were recorded in positive ion mode with a range from 40 to 2000 Da using a Bruker autoflex III Smartbeam. The laser power was 35% with a resolution of 100 micron.

Results

The blotting of the tissue on the Vmh2 coated slide was observed with the naked eye. The carried out trials were analysed in a range of m/z ratio up to 2000 in order to verify the presence of lipids or small metabolites. An acquired image related to the molecular representation of the ion at m/z ratio of 104 could be attributed to a low molecular weight neurotransmitter metabolite, i.e. the γ -aminobutyric acid (GABA) (Fujimura and Miura, 2014) (Figure 1a). In addition, other two images were acquired, related to the distribution of signals with m/z ratio of 632 and 660, which could be attributed to lipid molecules (Figure 1b,c).

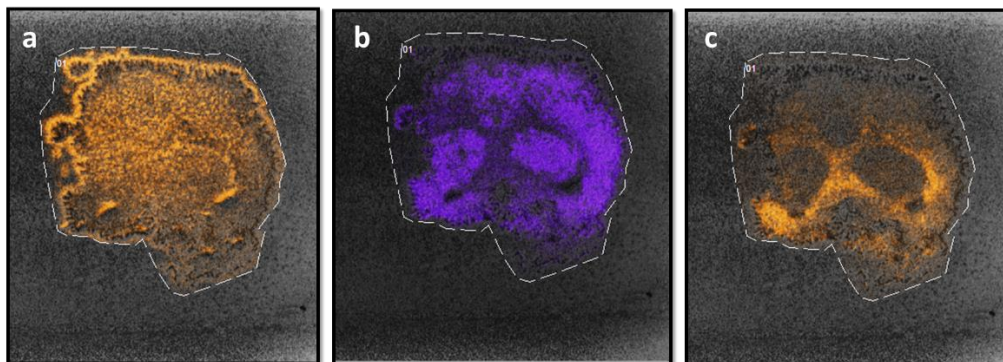


Figure 1: a), b) and c) are respectively the images corresponding to the signals with m/z ratio of 104, 632 e 660

The encouraging results obtained can represent a proof of concept for further investigations. In particular, the Vmh2 layer could be used to immobilize proteolytic enzyme directly on the MALDI-IMS support to perform an *in-situ* digest.

References

Angel PM and Caprioli RM. (2013) Matrix-Assisted Laser Desorption Ionization Imaging Mass Spectrometry: in situ molecular mapping. *Biochemistry* 52(22): 3818-3828.

Cillero-Pastor B and Heeren RMA. (2013) Matrix-Assisted Laser Desorption Ionization Mass Spectrometry Imaging for peptide and protein analysis: a critical review on tissue digestion. *J. Proteome Res.* 13(2): 325-335.

Fujimura Y and Miura D. (2014) MALDI Mass Spectrometry Imaging for visualizing in situ metabolism of endogenous metabolites and dietary phytochemicals. *Metabolites* 4:319-346.

Schöne C, Höfler H, Walch A. (2013) MALDI imaging mass spectrometry in cancer research: combining proteomic profiling and histological evaluation. *Clin Biochem* 46(6):539-45.

3.2 A proteomic approach for the rapid, multi-informative and reliable identification of blood



Cite this: *Analyst*, 2016, **141**, 191

A proteomic approach for the rapid, multi-informative and reliable identification of blood†

E. Patel,^{‡a} P. Cicatiello,^{‡b} L. Deininger,^a M. R. Clench,^a G. Marino,^b P. Giardina,^b G. Langenburg,^c A. West,^d P. Marshall,^d V. Sears^e and S. Francese^{*a}

Blood evidence is frequently encountered at the scene of violent crimes and can provide valuable intelligence in the forensic investigation of serious offences. Because many of the current enhancement methods used by crime scene investigators are presumptive, the visualisation of blood is not always reliable nor does it bear additional information. In the work presented here, two methods employing a shotgun bottom up proteomic approach for the detection of blood are reported; the developed protocols employ both an in solution digestion method and a recently proposed procedure involving immobilization of trypsin on hydrophobin Vmh2 coated MALDI sample plate. The methods are complementary as whilst one yields more identifiable proteins (as biomolecular signatures), the other is extremely rapid (5 minutes). Additionally, data demonstrate the opportunity to discriminate blood provenance even when two different blood sources are present in a mixture. This approach is also suitable for old bloodstains which had been previously chemically enhanced, as experiments conducted on a 9-year-old bloodstain deposited on a ceramic tile demonstrate.

Received 30th September 2015,
Accepted 17th November 2015

DOI: 10.1039/c5an02016f

www.rsc.org/analyst

Introduction

The detection of blood in stains or fingermarks at crime scenes can be an invaluable piece of evidence in the investigation of violent crimes. Crime Scene Investigators (CSI) have several enhancement classes of techniques available to visualize the presence of blood including optical, spectroscopic and chemical development methods.¹ In addition to limitations in common to all of the three classes of methods, chemical techniques are actually only presumptive methods thus occasionally leading to false positives. These methods have been extensively reviewed by Sears¹ and all were reported to exhibit a lack of specificity; even haem-reactive compounds, the most specific class of blood reagents, may give false positives as horseradish, leather and other extracts from plant material² show the same peroxidase activity exhibited by haem in

human blood. For this reason, we have previously reported a rapid and specific Matrix Assisted Laser Desorption Ionisation mass spectrometric method to detect blood in stains and map this biofluid in bloodied fingermarks.³ With this method, the mass-to-charge ratio (m/z) of both haem and intact Haemoglobin were employed to reliably confirm the presence of blood. The method was applied to a real crime scene stain proving successful in less than five minutes of preparation and acquisition time. Since blood provenance is also a forensic question of interest and as the m/z of haem would not permit the determination of the blood source, the m/z of intact Haemoglobin chains were exploited to distinguish between equine, human and bovine blood, based on the small differences in the protein amino acid sequence.³ However, although the detection of blood at a molecular level provides much higher specificity and reliability, intact protein analysis by MALDI mass spectrometry suffers from mass resolution and mass accuracy issues which may become significant, especially if blood is mixed with other biofluids or protein sources.

The use of a bottom up proteomic approach increases the reliability of protein identification because the mass accuracy that can be achieved on the protein-deriving peptides is much higher (a few parts per million). This approach would also enable the detection of additional blood specific proteins, besides Haemoglobin, allowing specificity and confidence in the determination of the blood presence to be further enhanced. The literature already contains many reports

^a Biomolecular Research Centre, Sheffield Hallam University, Howard Street S1 1WB, Sheffield, UK. E-mail: s.francese@shu.ac.uk; Tel: +44 (0)1142256165

^b Dipartimento di Scienze Chimiche, Università di Napoli Federico II, via Cinthia I-80126 Naples, Italy

^c Bureau of Criminal Apprehension, 1430 Maryland Avenue East, St Paul, Minnesota MN 55106, USA

^d GlaxoSmithKline, Gunnels Wood Road, Stevenage, SG1 2NY, UK

^e Centre for Applied Science and Technology, Home Office, St Albans, ALA 9HQ, UK

† Electronic supplementary information (ESI) available. See DOI: 10.1039/c5an02016f

‡ These authors have equally contributed to the manuscript.



attempting to map the proteome of plasma and serum. Different authors concur on the extreme complexity of these matrices with plasma being particularly challenging due to the wide⁴ range of concentrations of the proteins present (spanning 9 orders of magnitude) and the huge heterogeneity due to a variety of protein glycoisoforms. In 2010, Liunbruno *et al.*⁵ extensively reviewed the literature covering the mapping of the blood proteome with all the techniques employed up to that point in time and the corresponding number of obtained protein identifications.⁵ The majority of the methods employed separation techniques (gel based or liquid chromatography) hyphenated with mass spectrometry, in both on-line and off-line approaches, employing Electrospray and MALDI respectively as mass spectrometry techniques. Amongst the techniques used, the combination of 2D gel electrophoresis and mass spectrometry was reported to be able to identify 289 plasma proteins in 2002;⁴ cation exchange coupled to capillary gradient reverse phase liquid chromatography combined to mass spectrometry of digested peptides contributed to the identification of 490 blood serum proteins.⁶ These numbers have further increased when depletion and sample enrichment methods were preliminarily employed. In a 2005 collaborative study coordinated by HUPO involving 35 laboratories, up to 3020 plasma/serum proteins were identified using a range of hyphenated techniques;⁷ since the start of the HUPO project the number of identified proteins has rapidly increased to populate a database (<http://www.plasmaproteome-database.org/>) of 10546 proteins.⁸ None of the approaches reported in the literature so far has involved the direct application of MALDI MS on enzymatically digested blood. This is understandable as in all of the previous reports the aim was to map the entirety of the blood proteome for medical and diagnostic purposes. However, in a forensic context, the detection of a handful of blood specific proteins *via* the more reliable bottom up proteomic approach using MALDI MS would be more than appropriate. Furthermore, in forensic science, provided that reliability of the evidence is not compromised, speed is paramount to investigations; the hyphenated methods reported can be very labour intensive and time consuming, especially since some of them have employed preliminary purification to remove the most abundant proteins (*e.g.* albumin and Haemoglobin). For these reasons, in our laboratories, we have optimized a method for the digestion of blood-stains followed by direct MALDI MS analysis; the method couples high mass accuracy, within the peptide mass fingerprinting stage, as well as further confirmatory analysis by Tandem Mass Spectrometry. A classical in-solution digestion protocol was optimized for blood stains by investigating the optimal concentration of trypsin to employ as well as the optimal digestion time. The performance of this method was then critically compared to that of a second method employing Vmh2 hydrophobin to preliminarily coat the MALDI target plate. This protein belongs to the class I hydrophobins and it has been demonstrated to homogeneously self-assemble on hydrophilic or hydrophobic surfaces⁹ and to subsequently strongly bind proteins, including enzymes in their active form

such as trypsin.¹⁰ The use of Vmh2 has been recently proposed as a lab-on-plate approach as a simple and effective desalting method enabling decrease in the proteolysis time and increase of the peptides signal-to-noise (S/N) for tryptic digestion.¹¹

It was found that both methods could be successfully used to: (i) reliably detect the presence of blood in stains, (ii) determine the blood provenance even when two different blood sources were mixed and (iii) to identify the presence of this biofluid in a 9-year-old sample that had been pre-treated with acid black 1,^{12,13} a protein dye used for the unspecific enhancement/visualisation of blood. As it is discussed in this manuscript, the present data will no doubt impact on the effectiveness of forensic practice by providing much more reliable and informative evidence, thus empowering both investigations (of cold cases too) and judicial debates.

Experimental

Materials

ALUGRAMSIL G/UV₂₅₄ aluminium sheets, acetonitrile (ACN), Ammonium Bicarbonate (AmBic), trifluoroacetic acid (TFA), trypsin from bovine pancreas and alpha-cyano 4 hydroxycinnamic acid (CHCA) were obtained from Sigma-Aldrich (Dorset, UK). Trypsin Gold was purchased from Promega, Southampton (UK) whereas Rapigest™ SF was purchased from Waters (Elstree, UK). Defibrinated horse blood was obtained from FisherScientific (USA). Unistik® 3 Neonatal & Laboratory single use lancet were obtained from Owen Mumford (Oxford, UK). Vmh2 ethanolic solution was prepared as previously described.¹⁰

Instrumentation and data acquisition

Calibration over a 600–2800 Da mass range was performed prior to analysis using phosphorous red. MALDI IMS/MS data were acquired in positive ion mode from 600 to 3000 Da at a mass resolution of 10 000 FWHM using a SYNAPT G2™ HDMS system (Waters Corporation, Manchester, UK) operating with a 1 KHz Nd:YAG laser. Full scan mass spectra were manually acquired over 45 seconds; all experiments were carried out in duplicate. The laser energy was set to 250 arbitrary units on the instrument; with laser energy increased to 270 arbitrary units for MALDI IMS-MS/MS experiments. MS/MS analyses were conducted *in situ* on the most intense peaks. Fragmentation was carried out in the transfer region of the instrument, post ion mobility separation, therefore product ions retain the same drift time as the precursor ion. Collision energies ranging between 60–80 eV were used to obtain the best signal to noise ratio for product ions.

Methods

Preparation and digestion of blood samples and enzymatic digestions. For the in solution experiments, 10 µl of horse and human blood were spread individually (2 cm²) onto a clean



white ceramic tile. The tile was covered and placed into the environmental chamber for 5 hours at 25 °C and 60% humidity. Blood was then extracted from the ceramic tile by pipetting 70 µl of 50% ACN solution onto the dried blood regions. The extract was transferred to an eppendorf and 50/50 ACN/H₂O was added up to 1 mL in volume; the eppendorf was subsequently placed in an ultrasonic bath for 10 min at 45 kHz frequency. Forty µl of 40 mM AmBic (pH 8) was added to 10 µl of the extracts from horse and human blood. Nine µl of 20 µg mL⁻¹ Trypsin Gold including 0.1% RapigestTM SF were subsequently added and were allowed to digest for 1 hour at 37 °C and 5% CO₂. Proteolysis was stopped by the addition of 2 µl 5% aqueous trifluoroacetic acid (TFA_{aq}). 0.5 µl of each in solution digest were spotted onto a well target plate with 0.5 µl 10 mg mL⁻¹ CHCA (50/50 ACN/0.5% TFA_{aq} containing 4.8 µl aniline) matrix solution spotted on top.

For enzymatic digestions performed using the lab-on-plate approach, 10 µl of defibrinated horse blood was spread across pre-cut 2 cm² ALUGRAMSIL G/UV_{2.54} aluminium sheets pre-treated as previously described.¹⁴ These were sealed in petri dishes with parafilm and placed in an environmental chamber for 5 hours at 25 °C and 60% relative humidity. Under full ethical approval (HWB-BRERG23-13-14), human blood was obtained from the tip of the index finger using a Unistik® 3 Neonatal & Laboratory single use lancet (UK) and blood was then prepared as described for horse blood. The MALDI plates were preliminarily functionalized with Vmh2 hydrophobin and subsequently immobilized with trypsin from bovine pancreas as previously described.¹⁰ The aluminium sheets with dried blood were carefully rolled into a glass vial, covered with 1 mL 50% ACN solution and ultra-sonicated for 10 min. One µl of sample was spotted on Vmh2-adsorbed enzyme wells (MALDI plate) contained immobilized trypsin. The on plate digest reaction was carried out for 5 min at room temperature. The reaction was stopped by the addition of 0.5 µl 10 mg mL⁻¹ CHCA matrix solution. After mass spectrometric analysis the Vmh2 coating was removed by washing the MALDI plate with 10% TFA (and gently polishing the surface) followed by washing with 100% acetonitrile, water, and 100% acetone.

Blood provenance determination. Ten µl of horse blood was mixed with 10 µl of human blood. The mixture was digested using the in solution and lab-on-plate protocols reported above. Samples were submitted to MALDI MS analysis upon completion of the proteolysis.

Analysis of a 9-year-old bloodstain. Blood extracts were obtained from a ceramic tile exhibiting a 9-year-old bloody handprint, previously enhanced with acid black 1, by rubbing a swab previously wetted with 70/30 ACN/H₂O over the sample region. The swab tip was cut and sonicated for 10 min in 1 mL 70/30 ACN/H₂O to release the proteins. Twenty µl of the supernatant were dried under a stream of nitrogen and re-dissolved in 20 µl of 50 mM AmBic (pH 8) under sonication (10 min). The blood extracts were subsequent digested in solution or on the hydrophobin coated plate as previously described.

Data analysis. Mass spectra obtained from MassLynxTM (Waters Corporation, Manchester, UK) were either converted

into txt files and imported into mMass,^{15,16} an open source multiplatform mass spectrometry software, or processed directly within MassLynxTM by means of peak smoothing, baseline correction and peak centroiding. ExPasy (<http://www.expasy.org/>) was employed to generate *in silico* peptide lists of known proteins present in horse and human blood. *In silico* peptide lists were generated by selecting “*Equus caballus*” or “*Homo sapiens*” as taxonomy for the two blood types investigated. Mass lists were generated by selecting “*monoisotopic*”, “*MH*⁺”, “*trypsin higher specificity*”, “*2 missed cleavages*” and “*methionine oxidation*”. Peptide lists were imported into mMass (an open source multiplatform mass spectrometry software) to create an “in house” and local reference library. Mass lists including known matrix (or matrix cluster, adduct) and trypsin autolysis *m/z* were used to preliminarily assign peaks and therefore exclude them from subsequent peptide assignment. Peak assignments in mMass were performed automatically using the “*compound search*” tool and the in house created library by setting the tolerance at 10 ppm with a “*max charge*” of 1 and ticking the box “*monoisotopic*”. Prior to peak assignment search, spectra were smoothed and de-isotoped. Peak assignment was not accepted if the S/N was lower than 3 : 1. Spectral processing consisted of smoothing, baseline correction and lock mass based mass correction. Prior to performing an MS/MS Mascot (Matrix Science, London, UK) search, spectra were processed using MassLynxTM with the MaxEnt 3 algorithm to deisotope and enhance the S/N.¹⁷ Queries were searched against the “*Swiss-Prot*” database with parent and fragment ion tolerances set to 50 ppm and 0.1 Da respectively. Two missed cleavages were also selected.

Results and discussion

Although detection of blood at crime scenes or on evidential items is often a crucial piece of intelligence in the investigation of criminal offences, current forensic visualization methods do not offer the desired level of specificity.³ This may result in incomplete or even in missing crucial information. In this paper the development of a rapid bottom up proteomic method offering blood-specific signatures is reported. The developed methodology employs a recently proposed procedure involving immobilization of trypsin on hydrophobin Vmh2 coated MALDI plates,¹⁰ (“lab-on-plate” approach). Although other methods for immobilizing trypsin for enzymatic digestion have been reported we have found the use of Vmh2 to be very straightforward and have optimized the reported protocols for the detection and identification of blood. MALDI MS profiles of blood were acquired from both in solution digest and the lab-on plate digest for comparative purposes. In order to optimise both methodologies, defibrinated horse blood was preliminarily employed. Both optimized methods yielded blood specific peptide signatures including those from myoglobin and the two chains of Haemoglobin with a mass accuracy lower than 8 ppm (Table 1). In general, relevant peptide intensities are greater within the 1 hour in



Table 1 Peptide mass fingerprinting of equine blood from in solution and lab on plate digests

Horse proteins	Peptide <i>m/z</i>	Sequence	In solution relative error (ppm)	Lab-on-plate relative error (ppm)
Myoglobin	2232.0865	¹²⁰ HPGDFGADAQGAMTKALELF R ₁₄₀	—	-2.3296
Haemoglobin beta	2326.2037	⁹ AAVLALWDKVNEEEVGGALGR ₃₀	-5.7174	-0.2579
	1999.9218	⁴ 1FFDSFGDLSNPGAVMGNPK ₅₉	-6.0002	6.3002
	1930.0293	⁶⁶ KVLHSFGEGVHHLNLK ₈₂	-5.4403	-7.9791
	1801.9343	⁶⁷ VLHSFGEGVHHLNLK ₈₂	-7.5474	—
	1449.7961	¹³³ VVAGVANALAHKYH ₁₄₆	-7.3803	-0.6207
	1426.6849	¹²¹ DFTPELQASYQK ₁₃₂	-4.2756	—
	1358.6546	¹⁸ VNEEEVGGALGR ₃₀	-6.0353	-1.6928
	1274.7255	³¹ LLVVYPWQR ₄₀	-7.8448	-1.0198
	1265.8303	¹⁰⁵ LLGNLVVVLAR ₁₁₆	-7.3469	—
	2043.0042	¹³ AAWSKVGGHAGEFGAEALER ₃₂	-3.3773	-0.0978
Haemoglobin alpha	1499.7237	¹⁸ VGGHAGEFGAEALER ₃₂	-7.4680	-1.1335
	1833.8918	⁴² TYFPFHDLSHGSAQVK ₅₇	-7.1432	-0.0545

solution digest; however the majority of peptides are still present employing the 5 minutes lab-on-plate digestion with generally a much better mass accuracy (Fig. 1A, B and Table 1). Since high throughput is always one of the “desirables” for any new forensic protocol, the method employing Vmh2 is highly relevant since it has been observed that the proteolysis is most efficient if the sample is allowed to digest for no longer than 5 minutes. The optimized methodologies were subsequently applied to whole human blood. The digestion of whole human blood using the classic in solution method resulted in a number of tentative protein identifications. In addition to peptides resulting from Haemoglobin α (α Hb) and β (β Hb), a

number of other proteins were detected including complement C3, apolipoprotein A-1, alpha-1-antitrypsin, haemopexin, serotransferrin and alpha-2-macroglobulin (Table 2). As seen in Table 2, the number of peptides originating from α Hb and β Hb is marginally greater in the in solution digest compared to the immobilized digest. However it is apparent that there are peptides from proteins such as myoglobin, haemopexin and serotransferrin detected only *via* the on lab-on-plate digest. Interestingly, using both methods, it was possible to tentatively assign multiple peptides to Erythrocyte membrane protein band (EPB) 3 and 4.2. The significance of this is that EPB 3 is specific to human blood. In the case of whole human

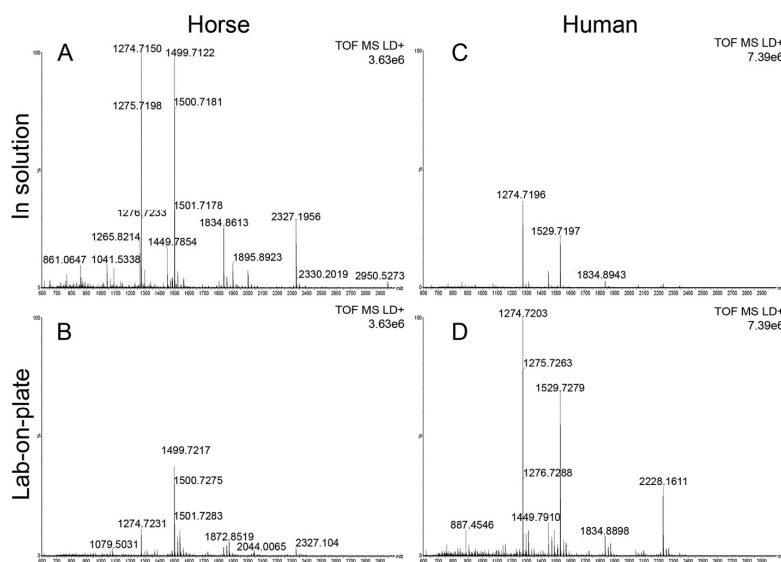


Fig. 1 MALDI MS spectrum of digested blood. Panels 1A and 1B show the MALDI spectra of equine blood digested in solution and *via* the lab-on-plate approach respectively. Panels 1C and 1D show the MALDI spectra of whole human blood digested in solution and *via* the lab-on-plate approach respectively.



Table 2 Peptide mass fingerprinting of whole human blood from in solution and lab-on-plate digests

Human proteins	Peptide <i>m/z</i>	Sequence	In solution relative error (ppm)	Lab-on-plate relative error (ppm)
Haemoglobin beta	767.4886	⁶¹ VKAHGKK ₆₇	-4.5603	-10.8144
	952.5098	² VHLTPEEK ₉	-4.5143	-5.5642
	1274.7255	³² LLVVYPWTR ₄₁	-1.8827	-4.0793
	1314.6648	¹⁹ VNVDEVGGEALGR ₃₁	-4.3357	0.1521
	1378.7001	¹²² EFTPPVQAAYQK ₁₃₃	2.8287	-10.0094
	1449.7961	¹³⁴ VVAGVANALAHKYH ₁₄₇	-3.5177	-3.1728
	1669.8907	⁶⁸ VLGAFSDGLAHLNDLTK ₈₃	-5.0901	-10.7192
	1866.0119	² VHLTPEEKSAVTALWGK ₁₈	-1.1253	—
	2058.9477	⁴² FFESFGDLSTPDAMGNPK ₆₀	-2.7198	-2.3312
	2228.1669	¹⁰ SAVTALWGKVNDEVGGEALGR ₃₁	-2.2439	-2.4683
Haemoglobin alpha	2529.2190	⁸⁴ GTFATLSELHCDKLVDPENFR ₁₀₅	-0.0790	-8.1052
	1071.5543	³³ MFLSFPTTK ₄₁	-1.7731	-1.6798
	1087.6258	⁹² LRVDPVNFK ₁₀₀	-1.6549	-0.5516
	1171.6681	² VLSPADKTNVK ₁₂	-6.9132	—
	1529.7342	¹⁸ VGAHAGEYGAEALER ₃₂	-4.5105	-3.7915
	1833.8918	⁴² TYFPHFDLSHGSAQVK ₅₇	-2.3447	-3.7624
	2043.0042	¹³ AAWGKVGVAHAGEYGAEALER ₃₂	-5.9226	-3.1815
	2341.1836	⁴² TYFPHFDLSHGSAQVKGHGK ₆₂	-2.6055	-2.5200
	2582.2707	¹⁸ VGAHAGEYGAEALERMFLSFPTTK ₄₁	-1.1230	-6.5059
	2996.4894	⁶³ VADALNTAVAHVDDMPNALSALSDLHAHK ₉₁	-3.5374	-3.1370
Myoglobin	1685.8679	¹³⁵ ALELFRKDMASNYK ₁₄₈	—	-5.1012
	887.4581	⁸⁴² NEQVEIR ₈₄₈	-3.0423	-3.2677
Complement C3	1334.7096	⁶⁷² SVQLTEKRMDK ₆₈₂	8.1665	-6.6681
	1087.6357	¹⁵⁹² EALKLEEK ₁₆₀₀	-10.7572	-9.6539
Apolipoprotein A-I	1215.6215	²²⁰ ATEHLSTLSEK ₂₃₀	-4.1131	—
	1230.7092	²⁴⁰ QGLLPVLESFK ₂₅₀	-0.9750	-2.1938
	1723.9449	¹⁴¹ QKVEPLRAELQEGAR ₁₅₅	-3.7704	-4.0024
	1815.8507	⁴⁸ DSGRDYVSQFEGSALGK ₆₄	7.2693	7.8200
	1833.8918	⁴² TYFPHFDLSHGSAQVK ₅₇	-2.3447	-3.7624
	1908.9847	¹⁵⁸ LHELQEKLSPLGEEMR ₁₇₃	-4.0859	—
	1318.6758	²⁴⁸ LGMFNIQHCKK ₂₅₈	-0.3033	5.4600
Haemopexin	965.4430	⁴⁰³ VDGALCMEK ₄₁₁	-5.9040	9.4257
	1060.5785	⁸⁴ ELISERWK ₉₁	—	-1.8857
Serotransferrin	1070.5741	²¹⁴ GEVPPRYPR ₂₂₂	—	2.6154
	1068.5506	⁶¹ KASYLDCIR ₆₉	—	9.7328
EPB 4.2	1855.8683	⁵³¹ EGYGYTGAFRCLVEK ₅₄₆	-0.1616	-0.6465
	949.4771	⁴⁵⁴ EKMEREK ₄₆₀	5.0554	8.3203
	1048.5455	⁴⁵¹ VEKEKMER ₄₅₈	-0.1907	5.2453
EPB 3	1079.5745	²⁰⁵ WSQPVHVAR ₂₁₃	-9.4481	—
	1113.4881	⁴²⁸ CEDITQNYK ₄₃₆	1.7063	—
	1258.7001	⁴⁴⁶ EVLERVEKEK ₄₅₅	-2.3834	1.9861
Alpha 2-Macroglobulin	949.4771	²⁸⁴ AAATLMSER ₂₉₂	5.0554	8.3203
	1328.6852	⁷³¹ SVTHANALTMGK ₇₄₃	—	-2.7847
	1334.7215	³⁵⁰ LSFVKVDSHFR ₃₆₀	-0.7492	—

blood, the overall relevant peptides intensities were lower within the in solution digest (Fig. 1C) in comparison to the on plate digest (Fig. 1D); this is probably due to the analyses being performed on whole human blood as opposed to a defibrinated sample (less complex) as in the case of the equine blood.

A close evaluation of the data on its performance, in comparison with an optimized in solution digestion of the minimum duration of 1 hour (Fig. 1A and B), shows that the lab-on-plate protocol enabled the detection of the same number of blood proteins but less blood protein-derived peptides (10/13 of the peptides from myoglobin, α Hb and β Hb observed in in solution digest). However the slightly fewer number of peptides detected is outweighed by the considerably reduced digestion time for the lab-on-plate approach.

As can be seen in Table 2 there are instances in which only one peptide could be putatively assigned to a protein (*i.e.* in the case of myoglobin, alpha-1-antitrypsin and alpha-2-macroglobulin). This is not standard practice in proteomics whereby, for increased identification reliability, at least two peptides should be assigned to a single protein. In the view of these authors, this is not an issue preventing to claim the presence of blood; based on the experiments carried out, we suggest the presence of two or more peptides from α Hb and β Hb and another blood protein (*i.e.* myoglobin or serotransferrin) to be the proposed minimum for the confident identification of blood.

Encouraged by these data, the focus was moved onto investigating the opportunity to provide information of the provenance of blood. These authors have already reported



preliminary data on blood provenance by MALDI-MS;³ an intact protein detection approach that was employed that, whilst successful in the instances investigated, may suffer from mass resolution and mass accuracy issues, thus reducing the level of reliability of the scientific evidence provided. At least one criminal case has been widely reported in the UK (Regina vs. Mrs Susan May),¹⁸ in which determining with certainty the provenance of the blood detected would have resulted in a better informed or speedier outcome. The importance of determining blood provenance is further testified by a case from the USA reported 1996. Here the blood of the dog shot together with his owners aided the conviction of two men of murder; in this case it took a DNA test (in the first trial ever in the country to use animal DNA as evidence) to prove the presence of canine blood on the jacket of one of the murderers.¹⁹ Already the comparison of the peptides obtained for equine and human blood (Fig. 1A, D and Tables 1, 2) demonstrate this as a feasible approach to determine blood provenance with a much higher specificity than previously shown.³ To further demonstrate robustness of the method, the lab-on-plate approach was applied to a sample made from mixing both equine and human blood.

Fig. 2 shows the peptide mass spectral profiles obtained from in solution (Fig. 2A) and lab-on-plate (Fig. 2B) digests of a mixture of human and equine blood. Although overall signal intensity is higher within the in solution digest spectrum,

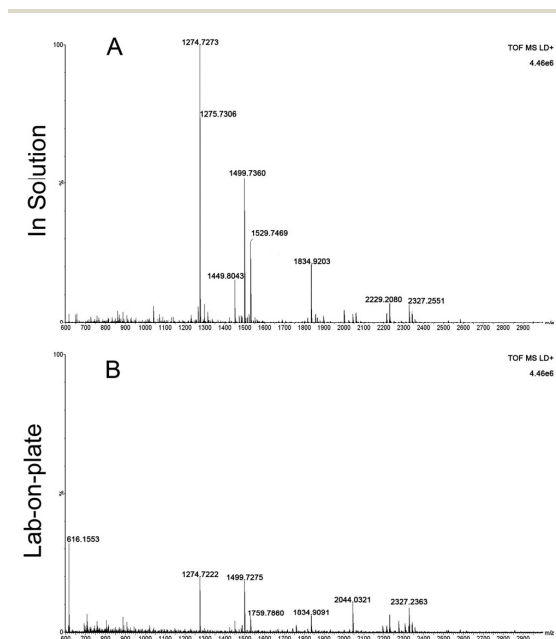


Fig. 2 MALDI MS spectrum of mixed digested blood. Panels A and B show the mass spectral profile of whole human blood mixed with defibrinated horse blood using the in solution and the lab-on-plate approach respectively.

both digestion protocols enabled the detection of blood peptide markers specific to each species and putatively assigned peptides are shown in Table S1 (ESI†). A number of tryptic peptides originating from α Hb and β Hb were present. However, due to the extensive sequence homology between the two species, it was not possible to solely use the m/z of these protein derived peptides or even the confirmed presence of β Hb tryptic peptide at m/z 1274.7260 *via* MALDI-IMS-MS/MS analysis of the peptide ion (Fig. 3A) as markers for species differentiation. However, subjected to MS/MS analysis, the tryptic peptide at m/z 1499.7237 was identified as equine α Hb with Mascot score of 99 (Fig. 3B). Furthermore, the tryptic peptide m/z 1815.9024 originating from myoglobin was also detected in the same spectra. This peptide is specific to the equine protein sequence thus more robustly confirming the presence of blood from equine provenance. Additionally, as expected from the *in silico* digestions, the detection of the human EPB 4.2 peptides, at m/z 949.4771 and 1113.4881 (present in the 1 hour in solution digest and *via* the rapid lab-on-plate hydrolysis), as well as that of serotransferrin at m/z 1529.7529, indicated the further presence of human blood thus enabling to claim the sample to be of mixed provenance, as well as indicating the individual species contributing to the blood sample under investigation. The authors would like to note that although there is a significant sequence homology between EPB 4.2 and α -2-macroglobulin within humans and chimpanzees, the indication of EPB 4.2 to be specific to human within this discussion is only with respect to equine

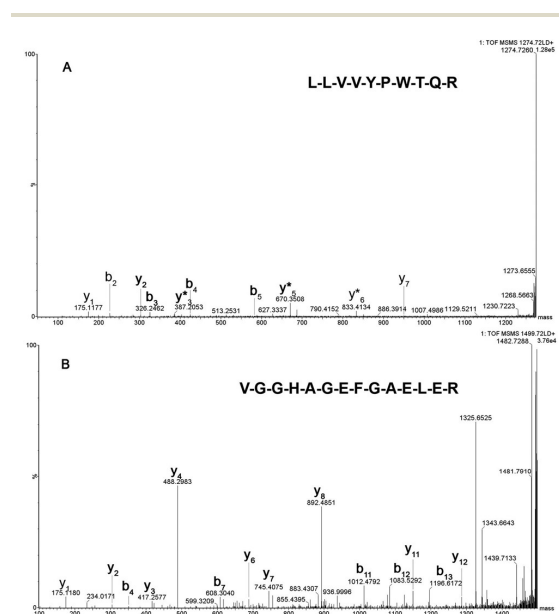


Fig. 3 MALDI-IMS-MS/MS of tryptic peptides m/z 1274 (3A) and m/z 1499.7237 (3B), identified *via* Mascot as β Hb and α Hb respectively. Both b and y ions are annotated with y* representing the y-NH₃ fragment ion.



blood. Both the in solution and the lab-on-plate approaches were successful in determining the double source of blood, and the considerably shorter digestion time within the lab-on-plate makes this the preferred method once again.

Finally, a method that is applicable not only to fresh bloodstains but also to much older ones would be highly desirable in the review of cold cases. Therefore the Vmh2 lab-on-plate method was tested, in comparison with the classic optimized in solution protocol, on a 9-year-old bloody handprint which was deposited on a ceramic tile and stored at room temperature (Fig. 4A(i and ii)). Spectra acquired from the analysis of the extract digested in solution (Fig. 4B) and *via* on plate hydrolysis (Fig. 4C) are shown, with corresponding expanded mass regions in the m/z range 1000–2000. A number of relevant tryptic peptides are present including α Hb peptides m/z 1087.6258, 1529.7342 and β Hb peptides m/z 1274.7255 and 1449.7961 to name a few (Table S2†). Data obtained indicated that blood presence confirmation was possible with the in solution approach, though both EBP 4.2 (indicating that the blood may be of human origin) and Complement C3 were

identified by one peptide only each. The lab-on-plate approach did not allow the detection of the Complement C3 protein (which is not highly specific to blood in any case) and also enabled the detection only one EBP 4.2 peptide. The authors suggest that in these cases, the lab-on-plate approach should still be used first for its rapidity. However for confirmatory purposes, as a tryptic digestion generates numerous peptides resulting in complex mixtures, often with overlapping signals, cross validation and identification using LC/MS/MS may be beneficial.

In addition to the ability to detect blood reliably and from such an old sample, it is very important to note that the bloodied handprint was preliminarily, 9 years ago, enhanced with acid black 1, a commonly used protein stain for blood enhancement. Successful blood confirmation in this instance demonstrates feasibility of the protocol to be integrated in the forensic workflow for blood enhancement/visualisation. The data obtained suggest that the acid black 1 does not interfere with the analyses, rather, that it may slow down degradation of the blood proteins over time.

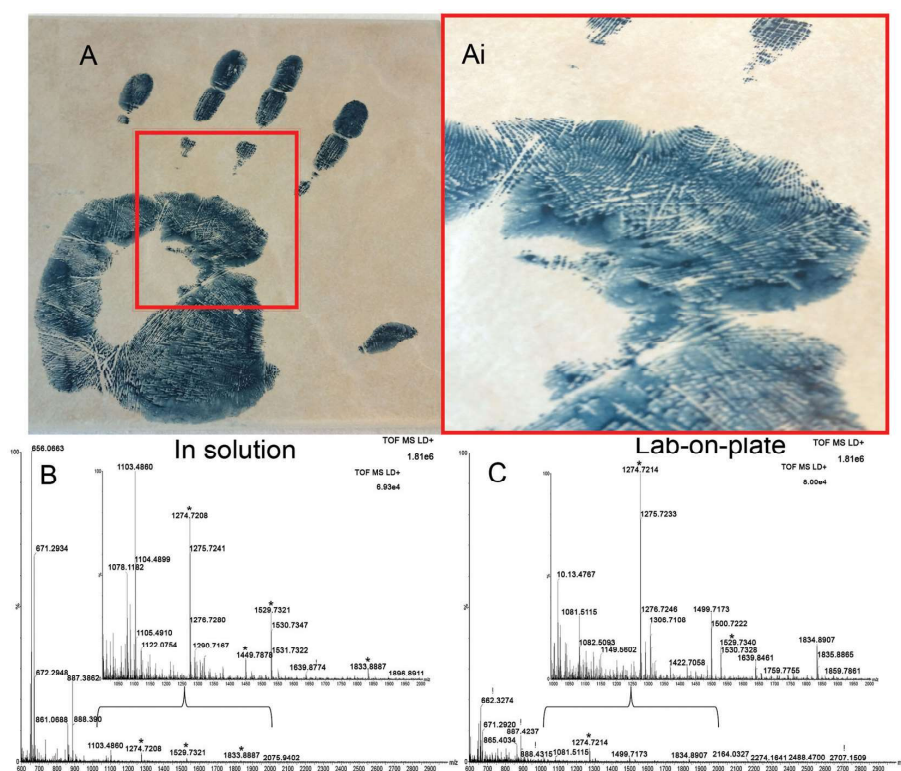


Fig. 4 Confirmation of the presence of blood from a 9-year-old forensically treated sample. Panels A and Ai show the bloodied handprint and magnified region from which the blood was swabbed respectively (the blue-black colour is due to the treatment with the protein stain Acid black 1). Panels B and C show the mass spectral profiles of the extracts digested in solution and *via* the lab-on-plate approach respectively.

Conclusions

The shotgun method illustrated in this report will have a significant impact on forensic practice as well as on the overall criminal justice system by generating more robust and informative evidence. This is due to the high specificity of the method against current presumptive tests prone to generate false positives. Furthermore the recovery of simultaneous information on blood provenance will both empower and speed up investigations as well as strengthening judicial debates. The study also crucially highlights compatibility with the necessary and prior application of blood enhancement techniques in combination with the analysis of very old blood samples, thus opening up new forensic opportunities for the review of cold cases. The lab-on-plate approach was shown to additionally offer rapid results (5 minutes only proteolysis time) which, in an operational forensic context, is a highly desirable feature. These studies are currently being expanded in our laboratories and include the reliable mapping of blood signatures on fingermark ridges using MALDI MS Imaging in order to link the suspect (through the biometric information) to the crime. Finally, validation has also been planned whereby the requirement for the minimum number of blood peptide signatures for both blood detection and blood provenance determination will be provided through a blind study in collaboration with the Minnesota Bureau of Criminal Apprehension.

Acknowledgements

The authors gratefully acknowledge BBSRC and GlaxoSmithKline for the BBSRC Industrial Case Award funding the Ph.D. studentship of E. P. The European COST Action programme BM1104 'Mass Spectrometry Imaging: New Tools for Healthcare Research' is also gratefully acknowledged for funding a 3 month Short Term Scientific Mission of PhD student P. C. at the Biomolecular Research Centre, Sheffield Hallam University.

References

- 1 V. Sears, in *Advances in Fingerprint Technology*, ed. H. Lee and R. Gaensslen, CRC Press, 2013.
- 2 M. Stoilovic, *Forensic Sci. Int.*, 1991, **51**, 289–296.
- 3 R. Bradshaw, S. Bleay, M. R. Clench and S. Francese, *Sci. Justice*, 2014, **54**, 110–117.
- 4 N. L. Anderson and N. G. Anderson, *Mol. Cell. Proteomics*, 2002, **1**, 845.
- 5 G. Liumbruno, A. D'Alessandro, G. Grazzini and L. Zolla, *J. Proteomics*, 2010, **73**, 483–507.
- 6 J. N. Adkins, S. M. Varnum, K. J. Auberry, R. J. Moore, N. H. Angell, R. D. Smith, D. L. Springer and J. G. Pounds, *Mol. Cell. Proteomics*, 2002, **1**, 947.
- 7 G. S. Omenn, *Proteomics: Clin. Appl.*, 2007, **1**, 769–779.
- 8 V. Nanjappa, J. K. Thomas, A. Marimuthu, B. Muthusamy, A. Radhakrishnan, R. Sharma, A. Ahmad Khan, L. Balakrishnan, N. A. Sahasrabudde, S. Kumar, B. N. Jhaveri, K. V. Sheth, R. Kumar Khatana, P. G. Shaw, S. M. Srikanth, P. P. Mathur, S. Shankar, D. Nagaraja, R. Christopher, S. Mathivanan, R. Raju, R. Sirdeshmukh, A. Chatterjee, R. J. Simpson, H. C. Harsha, A. Pandey and T. S. K. Prasad, *Nucleic Acids Res.*, 2014, **42**, D959.
- 9 L. De Stefano, I. Rea, E. De Tommasi, I. Rendina, L. Rotiroti, M. Giocondo, S. Longobardi, A. Armenante and P. Giardina, *Eur. Phys. J. E*, 2009, **30**, 181–185.
- 10 S. Longobardi, A. Gravagnuolo, R. Funari, B. Della Ventura, F. Pane, E. Galano, A. Amoresano, G. Marino and P. Giardina, *Anal. Bioanal. Chem.*, 2015, **407**, 487–496.
- 11 S. Longobardi, A. M. Gravagnuolo, I. Rea, L. De Stefano, G. Marino and P. Giardina, *Anal. Biochem.*, 2014, **449**, 9–16.
- 12 V. Sears and T. Prizeman, *Journal of Forensic Identification*, 2000, **50**, 470–480.
- 13 V. Bowman, V. Sears, H. Bandey, S. Bleay, L. Fitzgerald, A. Gibson, S. Hardwick, A. Hart, D. Hewlett, T. Kent and S. Walker, *nonsynonymous HOPSDB*, 2nd edn, 1998.
- 14 R. Wolstenholme, R. Bradshaw, M. R. Clench and S. Francese, *Rapid Commun. Mass Spectrom.*, 2009, **23**, 3031–3039.
- 15 M. Strohal, M. Hassman, B. Kosata and M. Kodicek, *Rapid Commun. Mass Spectrom.*, 2008, **22**, 905–908.
- 16 M. Strohal, D. Kavan, P. Novak, M. Volny and V. Havlicek, *Anal. Chem.*, 2010, **82**, 4648–4651.
- 17 M. C. Djidja, S. Francese, P. M. Loadman, C. W. Sutton, P. Scriven, E. Claude, M. F. Snel, J. Franck, M. Salzet and M. R. Clench, *Proteomics*, 2009, **9**, 2750–2763, DOI: 10.1002/pmic.200800624, DOI: 10.1002/pmic.200800624.
- 18 CCRC report-Statement of reasons, <http://www.susanmay.co.uk/ccrc.htm>, (accessed July 2015).
- 19 Forensic Files-Historic cases, chief evidence, <https://www.youtube.com/watch?v=q8jL8S2yIe8>, (accessed July 2015).



Proteins	Peptide <i>m/z</i>	Sequence	In solution Relative error (ppm)	Lab-on-plate Relative error (ppm)
Hemoglobin beta (human & equine)	1274.7255	³² LLVVYPWTR ₄₁	1.4120	-2.5103
Serotransferrin (human)	1529.7529	⁵⁸⁸ KPVEEYANCHLAR ₆₀₀	-3.4646	-7.9097
EPB4.2 (human)	1113.4881	⁴²⁸ CEDITQNYK ₄₃₆	-1.7063	-5.0292
	949.4771	⁴⁵⁴ EKMEREK ₄₆₀	-1.3691	-2.5277
Alpha 2-Macroglobulin (human)	1334.7215	³⁵⁰ LSFVKVDSHFR ₃₆₀	9.2154	1.1987
Hemoglobin alpha (equine)	1499.7237	¹⁸ VGGHAGEFGAEALER ₃₂	8.7349	2.6671
	1833.8918	⁴² TYFPFDLSHGSAQVK ₅₇	-	9.1608
Myoglobin (equine)	1815.9024	² GLSDGEWQQVLNVWGK ₁₇	-0.6608	1.8723

Table S1 Peptide mass fingerprinting of whole human blood mixed with defibrinated equine blood from in solution and lab on plate digests. Table reports human and equine blood specific signatures

Blood proteins	Peptide <i>m/z</i>	Sequence	In solution Relative error (ppm)	Lab-on-plate Relative error (ppm)
Hemoglobin alpha	974.5418	⁹ TNVKAAWGK ₁₇	-	4.8227
	1087.6258	⁹² LRVDPVNFK ₁₀₀	-5.4246	-3.8616
	1529.7342	¹⁸ VGAHAGEYGAEALER ₃₂	-1.5035	0.3268
	1833.8918	⁴² TYFPHDLSHGSAQVK ₅₇	-2.5083	-0.5998
	2043.0042	¹³ AAWGKVGAAHAGEYGAEALER ₃₂	-	-1.5173
Hemoglobin beta	1274.7255	³² LLVVYPWTQR ₄₁	-1.7258	-3.2163
	1314.6648	¹⁹ VNVDEVGGEALGR ₃₁	-1.3691	-
	1449.7961	¹³⁴ VVAGVANALAHKYH ₁₄₇	-4.3454	-3.5867
	2058.9477	⁴² FFESFGDLSTPDVAVMGNPK ₆₀	-	-1.0199
EPB 4.2	1113.4881	⁴²⁸ CEDITQNYK ₄₃₆	-9.3400	-
	949.4771	⁴⁵⁴ EKMEREK ₄₆₀	-	1.0532
Complement C3	959.5407	¹⁵⁹² EALKLEEK ₁₅₉₉	1.3548	-

Table S2. Blood peptide signatures detected from the 9 year old treated bloodied hand print.

3.3 Rapid and ultrasensitive detection of active thrombin based on the Vmh2 hydrophobin fused to a Green Fluorescent Protein



Contents lists available at ScienceDirect

Biosensors and Bioelectronics

journal homepage: www.elsevier.com/locate/bios

Rapid and ultrasensitive detection of active thrombin based on the Vmh2 hydrophobin fused to a Green Fluorescent Protein



Alessandra Piscitelli^{a,*}, Anna Pennacchio^a, Paola Cicatiello^a, Jane Politi^b, Luca De Stefano^b, Paola Giardina^a

^a Department of Chemical Sciences, Università degli Studi di Napoli Federico II, Complesso Universitario Monte S. Angelo, via Cinthia, 4, 80126 Naples, Italy

^b Unit of Naples–Institute for Microelectronics and Microsystems, National Council of Research, 80131 Naples, Italy

ARTICLE INFO

Keywords:

Class I hydrophobin
Amyloid fibrils
Yeast heterologous expression
Protease

ABSTRACT

A fusion protein designed in order to combine the fluorescence emission of the Green Fluorescent Protein (GFP) with the adhesion ability of the class I hydrophobin Vmh2 was heterologously produced in the yeast *Pichia pastoris*. The Vmh2-GFP fusion protein has proven to be a smart and effective tool for the study of Vmh2 self-assembling.

Since the two proteins were linked by the specific cutting site of the thrombin, the fusion protein was used as the active biological element in the realization of a thrombin biosensor. When the thrombin present in the target solution specifically hydrolyzed its cleavage sequence, a consequent decrease in the fluorescence intensity of the sample could be observed. The Vmh2-GFP based assay allowed quantification of thrombin in solution with a detection limit of 2.27 aM. The specificity of the assay with respect to other proteases and proteins granted the measurement of thrombin added to healthy human plasma with same high sensitivity and a limit of detection of 2.3 aM. Further advantages of the developed biosensor are the simplicity of its design and preparation, and the low requirements in terms of samples, reagents and time.

1. Introduction

Thrombin is a crucial enzyme in blood coagulation and is an analyte which has been the subject of increasing interest in the last few years. This serine protease can directly transform soluble fibrinogen into insoluble fibrin, and can facilitate blood hemostasis (Hsieh, 1997). If the level of thrombin in the body is too high, thromboembolic diseases or even death will result, while a low amount of thrombin will induce an excessive bleeding. During the coagulation process, its concentration varies considerably, even from nM to mM (Na et al., 2015). The development of rapid, sensitive and accurate thrombin detection in real-time is essential to adjust the strategies of drug administration for certain patients with severe thrombin-related medical problems. Moreover, monitoring thrombin is of great importance in the early diagnosis of some types of disease, such as hemorrhagic or thromboembolic complications and Alzheimer's disease (Chen et al., 2016), and as a useful marker in the diagnosis of pulmonary metastasis (Hernandez-Rodriguez et al. 1997).

Numerous methods of thrombin detection have been proposed since the beginning of this century. Most of them have been based on the use of thrombin binding aptamers, which are promising candidates

as sensing elements for the development of real-time biosensors. The molecular recognition between thrombin and aptamers and/or the biosensor configuration itself have been reported in several of these studies, but as a proof-of-concept rather than as an instrument in the development of a thrombin detection method (Xu et al., 2009; Qin et al., 2015; Derkus, 2016).

Different methods have been proposed, including an optical approach (Yan et al., 2011), electrochemiluminescence (Wang et al., 2011; Lu et al., 2015), electrochemical impedance spectroscopy (Lu et al., 2015; Derkus, 2016), an electrochemical approach (Zhao et al., 2011; Xu et al., 2013), colorimetry (Liang et al., 2011), surface plasmon resonance (Yu et al., 2004; Jalit et al., 2013; Trapaidze et al., 2016), and quartz crystal microbalance with dissipation monitoring (Chen et al., 2010). Wide ranges in the Limit of Detection (LOD), spanning from nM (10^{-9} M) (Trapaidze et al., 2016; Kuang et al., 2016) down to fM (10^{-15} M) have been reported (Zhao and Gao, 2015; Heydari-Bafrooei et al., 2016). A higher sensitivity (aM, 10^{-18}) has been obtained through modifications with fluorophores (Yu et al., 2004) and the use of electrochemical impedance spectroscopy (Lu et al., 2015).

In this study, a novel method to reliably quantify the thrombin

* Corresponding author.

E-mail addresses: apiscite@unina.it (A. Piscitelli), anna.pennacchio@unina.it (A. Pennacchio), paola.cicatiello@unina.it (P. Cicatiello), jane.politi@na.imm.cnr.it (J. Politi), luca.destefano@na.imm.cnr.it (L. De Stefano), giardina@unina.it (P. Giardina).

<http://dx.doi.org/10.1016/j.bios.2016.09.052>

Received 29 July 2016; Received in revised form 13 September 2016; Accepted 14 September 2016

Available online 15 September 2016

0956-5663/ © 2016 Elsevier B.V. All rights reserved.

concentration has been developed based on the detection of thrombin effectively active in the sample. The biological element, able to detect this protease enzyme in the biosensor system proposed, was designed in order to combine the fluorescence of the Green Fluorescent Protein (GFP) with the adhesion ability of the class I hydrophobin Vmh2, linked by the specific cutting site (LVPR/GS) of the thrombin. The designed fusion protein was heterologously produced in the yeast *Pichia pastoris*. The sensing mechanism is that the thrombin present in the target solution specifically recognizes and hydrolyzes its cleavage sequence with a consequent decrease in the fluorescence intensity of the sample.

Fluorescent Proteins (FPs) are genetically encoded fluorophores, which can be easily used as fluorescent probes for the tracking of proteins, organelles or whole cells, and as the basis for the construction of biosensors (Enterina et al., 2015). Protein engineering (Chen et al., 2012) and the discovery of new FPs (Mishin et al., 2015) have expanded the possibilities of use of these biosensors. Other emerging technologies to efficiently exploit FPs include different structural approaches aimed at turning on or shifting the fluorescence emission in response to environmental changes (Enterina et al., 2015).

Class I hydrophobins are small proteins able to self-assemble into amphiphilic films at hydrophobic-hydrophilic interfaces (Linder, 2009). They efficiently adhere to different hydrophobic surfaces, such as teflon (Askolin et al., 2006), polystyrene (Wang et al., 2010), silicon (De Stefano et al., 2007, 2009) and graphene (Gravagnuolo et al., 2015), forming extremely stable films that can be dissolved only in strong acids (e.g. 100% trifluoroacetic acid, TFA). Class I hydrophobins form fibrillar structures, known as rodlets, showing many structural analogies with amyloid fibrils. Hydrophobin assemblies represent a versatile and simple method for the immobilization of proteins (De Stefano et al., 2009; Wang et al., 2010; Sun et al., 2011; Longobardi et al., 2015; Zhao et al., 2007) on diverse substrates for the development of several biotools such as biosensors (Qin et al., 2007; Zhao et al., 2009; Wang et al., 2010; Sun et al., 2011; Piscitelli et al., 2016). The class I hydrophobin Vmh2 from the basidiomycete fungus *Pleurotus ostreatus* is able to spontaneously form stable and homogeneous layers on hydrophilic or hydrophobic surfaces, changing their wettability (De Stefano 2007), and has been efficiently exploited for several different applications (Longobardi et al., 2015; Gravagnuolo et al., 2015; Piscitelli et al., 2016).

The fluorescent assay developed in this study is a promising alternative approach compared to the analytical methods currently used to detect thrombin in the plasma. In fact, it allows a reliable and sensitive measurement of the analyte of interest in less than 20 min and without the need for specialized personnel, costly equipment or an excessive amount and manipulation of blood.

2. Materials and methods

2.1. Materials

Reagents were purchased from Sigma-Aldrich (Saint Louis, Missouri, USA). Expression vectors and yeast strains were purchased from Biogrammatix, Ltd (Las Palmas Dr, Carlsbad, CA, USA). DNA restriction and modifying enzymes were supplied by Promega (Madison, WI, USA). The fusion protein encoding gene was synthesized by Thermo Fischer Scientific (Waltham, Massachusetts, USA). Culture media were bought from BD Difico (Becton Drive, Franklin Lakes, NJ USA). The human factor Xa was purchased from New England Biolabs (Ipswich, MA, USA).

2.2. Vector construction

A synthetic gene encoding for the GFP from *Aequorea victoria* in frame with the thrombin cleavage site and with Vmh2 from *P. ostreatus* was designed (1008 bp) and optimized according to *P.*

pastoris codon usage. The gene product was restricted with *BsaI* and ligated into the corresponding site of the pJGG_akR vector in-frame with the α -factor (signal peptide) under the control of the constitutive GAP promoter, yielding the recombinant plasmid pJGG_Vmh2-GFP. The recombinant plasmid was linearized by *BsiWI* and transformed into *P. pastoris* BG-10.

2.3. Transformation of *P. pastoris* and screening of the clones

P. pastoris cells were collected from a solid culture and grown in 50 mL of YPD medium (10g l⁻¹ yeast extract, 20g l⁻¹ bacto tryptone, 20g l⁻¹ glucose) at 28 °C on a rotary shaker (150 rpm) over night. The overnight culture was diluted 1:5000 in fresh medium and grown overnight up to 1.3–1.5 OD₆₀₀. Next, the cells were sedimented by centrifugation at 2000 rpm at 4 °C for 5 min, resuspended in YPD, 0.02 M HEPES, 0.04 M DTT, and shaken at 30 °C for 25 min at 100 rpm. Then the cell suspension was diluted 1:10 with cold H₂O and the cellular pellet washed with cold H₂O, and cold 1 M sorbitol. The cell pellet was then resuspended in 1 M sorbitol and mixed with the linearized transforming DNA plasmid (up to 0.5 μ g). *P. pastoris* transformation was performed by electroporation with a Bio-Rad Micro-Pulser apparatus (BioRad, Hercules, California, USA), as specified by the manufacturer. Immediately afterwards, 1 mL of Recovery Media (1:1 YPD: sorbitol) was added to the electroporation cuvette and the whole content was transferred to a sterile tube. The tube was then incubated at 28 °C for 3 h under shaking conditions. The cell suspension was spread on YPD plates containing 900 μ g mL⁻¹ of G418 and incubated for 3–7 days at 28 °C until colony formation. The colonies were collected, inoculated in Minimal Dextrose Medium (MD) (13g l⁻¹ Yeast Nitrogen Base with ammonium sulfate w/o aminoacids, 4 \times 10⁻⁴ g l⁻¹ biotin, 20g l⁻¹ glucose), and grown at 28 °C on a rotary shaker (250 rpm). Aliquots were daily withdrawn and assayed for cell density and for GFP fluorescence emission using the Synergy H4 (Biotek Instruments, Winooski, Vermont, USA) acquiring data through top-reading mode. The excitation wavelength was fixed at 450 nm and emission spectra were recorded between 460 and 560 nm. The emission spectra were then corrected by subtracting the blank (the supernatant of the wild-type *P. pastoris* strain).

2.4. Expression and purification of the fusion protein Vmh2-GFP

Pre-inoculum preparation of the recombinant selected clone was performed at 28 °C overnight in MD. The pre-inoculum was diluted 1:100 in the same medium. 10g l⁻¹ Yeast Nitrogen Base (YNB) was added to the medium when the culture reached the stationary phase. The recombinant protein was recovered after 8 days and the cells were removed by centrifuging for 20 min at 7000 rpm at 4 °C. The supernatant was recovered, concentrated and dialyzed towards 50 mM Tris-HCl buffer, pH 8.0, using Centricon Centrifugal Filter Units with Ultracel YM-10 membrane (Merck, Darmstadt, Germany). The protein concentration was determined using the Bradford method (BioRad) according to the manufacturer's instructions and using BSA as the standard.

2.5. PAGE analyses

The purity of the sample and the Mw of the protein were verified by 15% SDS-PAGE, stained with Coomassie brilliant blue R-250.

Semi-denaturing PAGE was performed in the same conditions except for the reduction and heat denaturation of the samples before loading. The fluorescent protein band was visualized by exposing the gel to UV light by means of an UV transilluminator (Vilber Lourmat, Eberhardzell, Germany).

2.6. Contact angle measurement

Contact angle measurements were performed by using a KSV Instruments LTD CAM 200 Optical Contact Angle Meter: each contact angle was calculated as the average of the values obtained from three drops having the same volume (about 2 μL of a 0.1 mg mL^{-1} protein sample), spotted on different points of a polystyrene surface, air dried and washed three times with buffer.

2.7. Thioflavin assay

Vmh2-GFP (from 0.1 to 1 mg mL^{-1}) in 50 mM Tris HCl buffer, pH 8.0, was immobilized in multiwell plates (described in paragraph 2.9) and washed three times with the same buffer. 100 μL of 30 μM thioflavin (ThT) was added to the wells and incubated at room temperature for 5 min. The ThT fluorescence intensity of each sample was recorded using 435 nm excitation.

2.8. Fluorescence microscopy

Fluorescence analysis was performed by means of a Leica Z16 APO fluorescence microscope equipped with a Leica DFC300 camera (Leica, Wetzlar, Germany). A I3 filter was used for the image acquisition, consisting of a 450–490 nm band-pass excitation filter, a 510 nm dichromatic mirror, and a 515 nm suppression filter.

Confocal microscopy was performed by means of a Carl Zeiss LSM 700 apparatus using the tunable Argon 488 nm laser at 90.0% (Carl Zeiss, Oberkochen, Germany). The excitation and emission measurements for the Vmh2-GFP images were 488 and 518 nm, respectively.

2.9. Vmh2-GFP immobilization on multiwell plates

Several tests of immobilization of 100 μL of the Vmh2-GFP solutions on polystyrene multiwell plates were carried out, changing different parameters: the protein concentration, the presence of a preformed layer of native Vmh2, and the mixing of the fusion protein with the native Vmh2 (0.1 mg mL^{-1} final concentration).

After incubation at 28° C overnight, removal of the residual liquid and three washes with 50 mM Tris HCl buffer, pH 8.0 to eliminate any unbound proteins, the fluorescence of the GFP was measured in the same buffer. The immobilization yield in terms of fluorescence was calculated considering the immobilized fluorescence with respect to that incubated in the well. To assess the yield in terms of protein amount, the immobilized content was calculated as the difference between the quantity used for the immobilization and that measured in the residual liquid and in the washings.

2.10. Thrombin assay

Defined volumes (100 μL) of thrombin protease at increasing concentrations (from 450 nM to 4.5 μM) in Tris-HCl 50 mM, pH8 were added to the Vmh2-GFP coated wells and incubated at 37° C for 15 min. After two washes with 50 mM Tris-HCl buffer, pH 8.0, to remove the hydrolyzed proteins, the remaining fluorescence was measured in the same buffer.

Solutions of thrombin at varying concentrations were also added to human plasma to test the performance of the sensor in complex matrixes. Human plasma samples were collected in a citrate anticoagulated tube from healthy subjects. Fibrinogen was removed through precipitation according to the method reported in the literature (Bini et al., 2007). The protein amount of the raw plasma and of the eluted solution was evaluated by spectrophotometric measurements at 280 nm and a loss of protein content (40%) was detected after precipitation of fibrinogen.

To promote the transformation from prothrombin to thrombin, 8 nM human factor Xa in the presence of CaCl_2 (0.03 M) were added to

the plasma..

3. Results and discussion

3.1. Production and characterization of the fusion Vmh2-GFP protein

The recombinant expression system developed in this work allowed for the production and secretion in *P. pastoris* of the class I hydrophobin Vmh2 from *P. ostreatus* fused to the enhanced GFP from *A. victoria*. The secreted fusion protein Vmh2-GFP was found to be homogeneous after only two steps, concentration and dialysis, and the obtained yield was about 50 mg L^{-1} . SDS PAGE analysis displayed the presence of a unique protein band at the expected molecular weight (Fig. S1A). The functionality of the GFP moiety was confirmed both by the green fluorescence exhibited by the protein band on partially denaturing SDS-PAGE (Fig. S1B) and by the emission spectra registered for the purified protein (Fig. S1C).

With the aim of verifying the behavior of the Vmh2 moiety within the chimeric protein, its ability to reach the hydrophobic-hydrophilic interfaces, to adhere to the surface and to form amyloid-like fibrils was investigated. Bubble formation was induced by insufflating air in the protein solution, after which a 70–80% reduction of fluorescence in the solution was measured. The obtained foam was deposited on microscopy glasses, heat-dried, and analysed through fluorescence microscopy. Bubble images clearly revealed the presence of the protein at the air-water interfaces (Fig. 1A).

The ability of the Vmh2-GFP protein to adhere to the hydrophobic polystyrene surface, thus modifying its wettability, was monitored by water contact angle measurements after protein deposition and washing. The polystyrene surface, strongly hydrophobic in nature, became clearly hydrophilic (Fig. 1B) and the effect of Vmh2-GFP was more evident than that of native Vmh2, due to the higher hydrophilicity of the protein fused to Vmh2.

The formation of amyloid-like structures on the polystyrene surface was verified through Thioflavin T assay. The higher were the protein concentrations, the greater was the fluorescence intensity due to the presence of fibril-ThT complexes (Fig. 1C). Fluorescence microscope images of the fusion protein deposited on the polystyrene surface at different concentrations showed the presence of protein aggregates at all the tested concentrations, while fluorescent fibrils were detectable at protein concentrations higher than 0.05 mg mL^{-1} (Fig. 1D).

These results highlighted the finding that the Vmh2-GFP fusion protein might be a smart and effective tool for the study of Vmh2 self-assembling. Moreover, the developed recombinant expression system could allow the production and secretion of other Vmh2-fused proteins useful for the direct functionalization of different surfaces, thus expanding the range of applicability of these “self-immobilizing” proteins (Piscitelli et al., 2016).

3.2. Immobilization of the fusion protein Vmh2-GFP

Several tests of the immobilization of the fusion protein on multiwell plates were carried out using Vmh2-GFP at different concentrations (Table 1, rows S1–S6), and evaluating the effect due to the presence of a preformed layer of native Vmh2 and due to a mixture of the fusion protein with the native Vmh2 (Table 1, rows S7 and S8).

The fusion protein was easily immobilized in the polystyrene well by deposition, resulting fluorescent and tightly bound to the surface after several washes with the buffer. A noticeably high immobilization yield of the fusion protein, in terms of both the fluorescence intensity and the protein amount, was calculated in all the tested conditions, in comparison with the opportune controls (Table 1, rows C1 and C2). In relation to the protein concentration used, there was a slight increase in the immobilization yield from 0.05 to 0.1 mg mL^{-1} , while a further increase in this concentration did not affect this parameter. The immobilization yield of the fusion protein on a preformed Vmh2 layer

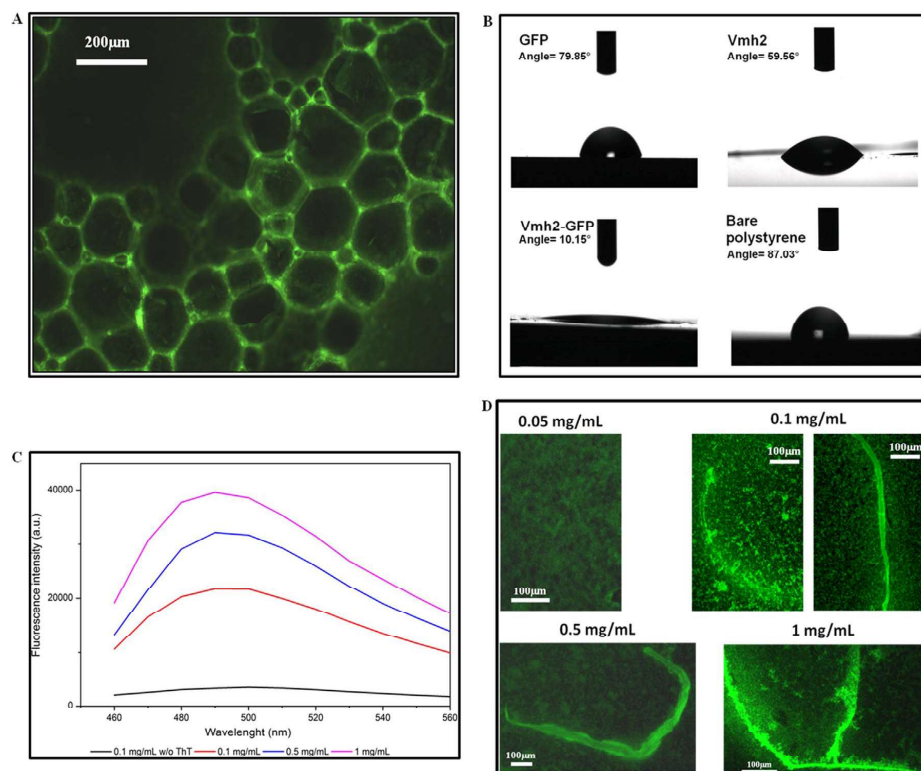


Fig. 1. Protein characterization. A. Fluorescence images of a bubble dispersion of Vmh2-GFP. B. Measurement of water contact angle of a water drop on the polystyrene surface after the deposition of GFP, Vmh2 and Vmh2-GFP. The polystyrene surface was used as a reference. C. Fluorescence spectra of 30 μ M ThT after the immobilization of different Vmh2-GFP concentrations. D. Immobilization of different Vmh2-GFP concentrations on the polystyrene surface analysed by confocal microscopy.

was lower than that obtained by its direct deposition on the polystyrene surface (Table 1, row S7 and S2). As already reported (Piscitelli et al., 2016), the yield obtained through deposition on a preformed Vmh2 layer was higher for the fusion protein than for the GFP alone (Table 1, row S7 and C1). In the case of the immobilization of mixtures of the native Vmh2 and the Vmh2-GFP fusion protein, the measured immobilization yield was lower than that obtained for each protein separately (Table 1, row S8, S2 and C3) at the same final protein concentration. This result could be ascribed to their higher propensity for assembling in bulk solution rather than for coating when the two proteins are mixed. A similar effect has been observed for mixtures of the native Vmh2 and the Vmh2-GST fusion protein (Piscitelli et al.,

2016).

The stability of the immobilized protein with respect to that of the free counterpart was also evaluated by measuring the fluorescence of Vmh2-GFP over time at two different temperatures (4 °C and room temperature). The immobilized fusion protein Vmh2-GFP was fully stable for at least 30 days, while the free protein exhibited a complete loss of fluorescence after only three days at both temperatures. These results demonstrated that the stability of the GFP noticeably increased upon immobilization.

Table 1
Immobilization yield of Vmh2-GFP.

Conditions	Sample	Immobilization yield (% mg tot)	Immobilization yield (% fluorescence intensity)
S1	Vmh2-GFP 0.05 mg mL ⁻¹	80	79
S2	Vmh2-GFP 0.1 mg mL ⁻¹	95	97
S3	Vmh2-GFP 0.2 mg mL ⁻¹	95	96
S4	Vmh2-GFP 0.5 mg mL ⁻¹	95	96
S5	Vmh2-GFP 0.7 mg mL ⁻¹	95	95
S6	Vmh2-GFP 1 mg mL ⁻¹	95	95
S7	Vmh2-GFP on Vmh2 layer	75	78
S8	Vmh2-GFP: Vmh2 mix (1:3)	70	68
C1	GFP on Vmh2 layer	20	18
C2	GFP	7	6
C3	Vmh2	90	–

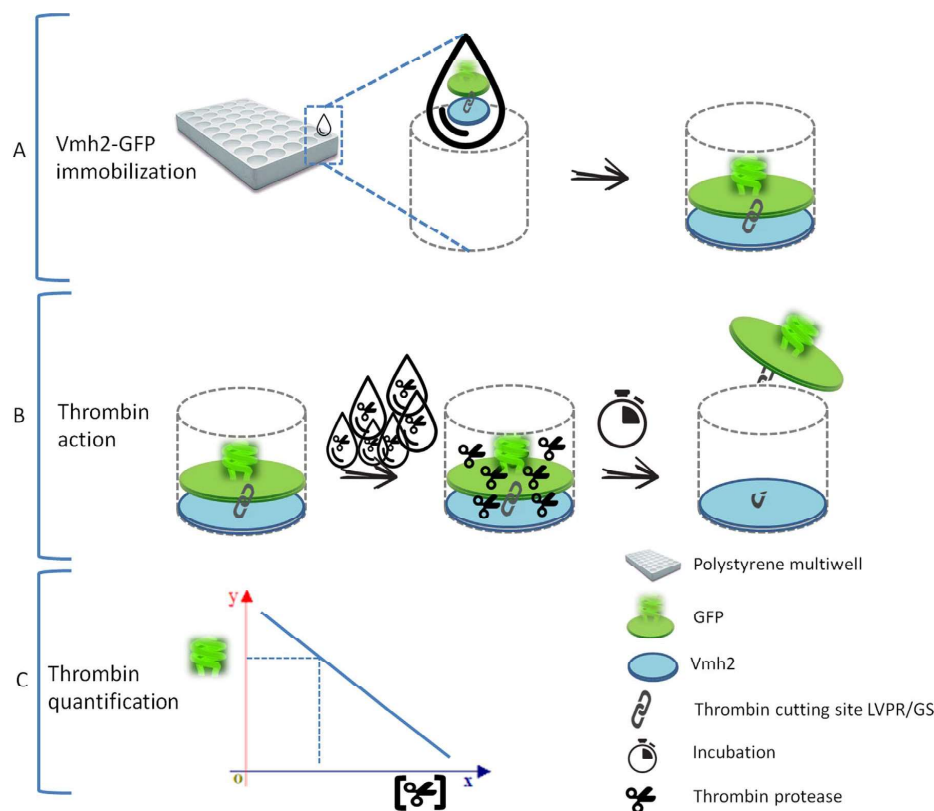


Fig. 2. Scheme of biosensor. Schematic representation of the sensing procedure for detection of thrombin.

3.3. Thrombin assay

Considering that the surface active protein Vmh2 and the fluorescent GFP moieties were linked by the thrombin recognition site, Vmh2-GFP was used to specifically detect thrombin. The protease recognizes and cleaves its specific cutting site, releasing the GFP protein bound to the polystyrene surface through Vmh2 adhesion. As expected, in the presence of increasing concentrations of thrombin, the fluorescence emission intensity decreased due to the removal of GFP (Fig. 2).

Fig. 3 shows the relationship between the percentages of fluorescence intensity measured after thrombin cleavage and the concentrations of thrombin. The results are reported in a logarithmic scale in order to highlight that fluorescence changed in a range of several orders of magnitude. When high Vmh2-GFP concentrations (0.1 and 0.2 mg mL⁻¹) were immobilized, a non-linear trend was observed (Fig. 3A and B). This phenomenon may be probably due to the existence of a non-homogeneous layer affecting the accessibility of the protease to its cleavage sites. As a fact, the presence of fibrils observed at those Vmh2-GFP concentrations (Fig. 1D) makes the film more irregular.

To verify this hypothesis, lower protein concentrations (0.05 and 0.07 mg mL⁻¹) were immobilized on the 96-well plate. At the lowest concentration of Vmh2-GFP (0.05 mg mL⁻¹), a linear trend was observed in the whole concentration range of thrombin (Fig. 3D). Therefore, it may be inferred that the presence of the fibrils affected the homogeneity of the layer and, accordingly, the protease accessibility.

Actually, the procedure set-up at the lowest Vmh2-GFP concentration showed a very large linear range, from aM to mM. To the best of our knowledge this is the widest linear range obtained for a thrombin biosensor. This remarkable result may be due to the peculiar immobilization efficiency of our sensing molecule.

The relationship between the Vmh2-GFP fluorescence and the thrombin concentration was analysed by fitting the data using the linear equation (Eq. (1)):

$$y = a + b \log x \quad (1)$$

The value of a resulting from the best fit procedure (Table S1) was compatible with the measured blank (111.5 ± 0.6 a.u.) and it can be used to estimate the LOD. The LOD was calculated as 2.3 aM, according to the $3 s_b/m$ criterion, where m is the slope of the calibration curve and s_b is the standard deviation of the blank (Table S1). This value is comparable to the lowest LOD found for thrombin detection, obtained by Lu and co-workers (2015) (2.7 aM) using a bi-functionalized aptasensor.

The specificity of this assay was tested by evaluating the effect of other proteases on the fluorescence intensity (Fig. 4A). A decrease in the fluorescence intensity was measured only in the presence of thrombin, while no decrease was detected when other proteases were used. Moreover, the presence of high concentrations of other proteins (lysozyme, or bovine serum albumin) did not affect the decrease of fluorescence intensity due to the thrombin action (Fig. 4B).

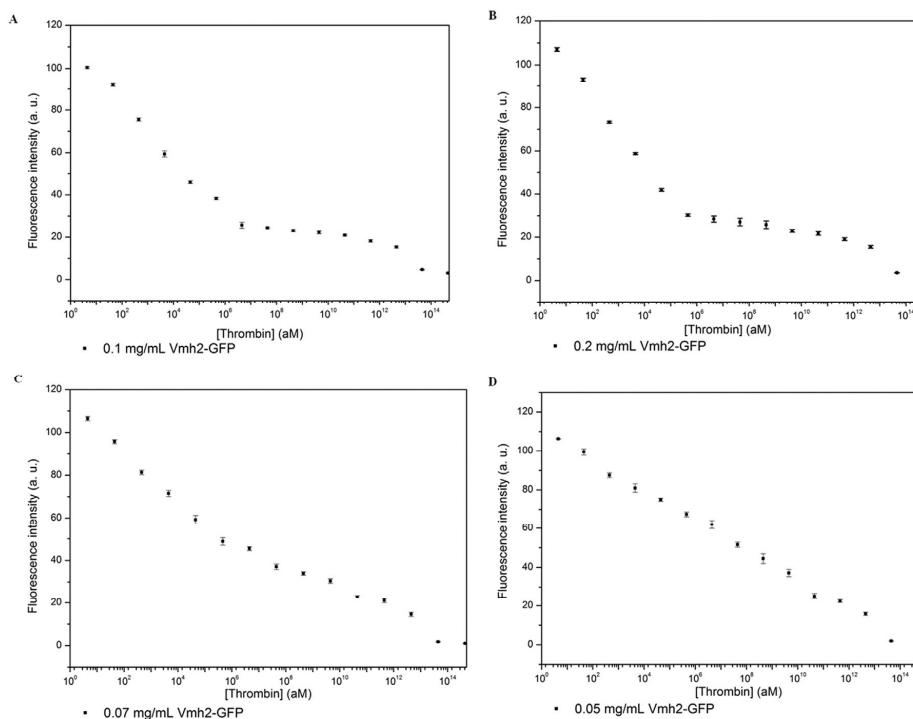


Fig. 3. Calibration curve. Logarithmic plot of the calibration curve of the fluorescence intensity emission (top reading mode) of Vmh2-GFP at 505 nm vs the thrombin concentration in Tris-HCl buffer at pH 8.0. The Vmh2-GFP immobilization was performed starting from different protein concentrations. A. 0.1 mg mL⁻¹. B. 0.2 mg mL⁻¹. C. 0.07 mg mL⁻¹. D. 0.05 mg mL⁻¹. Coefficients of variation (CV%, n=5) vary from 0.2% to 8.2%.

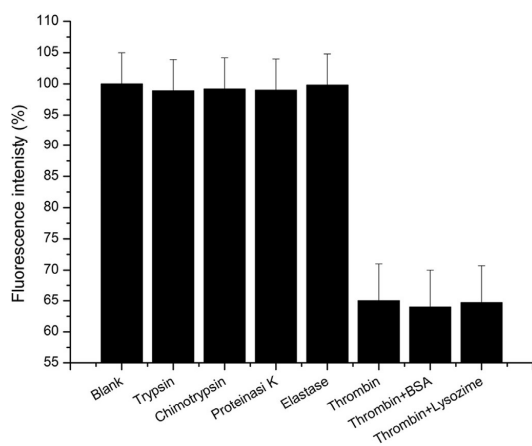


Fig. 4. Specificity of the assay. Percentage (%) of the fluorescence intensity of Vmh2-GFP in the presence of 4.5 fM of different proteases, such as thrombin, trypsin, chymotrypsin, proteinase K, elastase, and of 4.5 fM of thrombin with 3.0 μ M lysozyme or BSA.

3.4. Thrombin assay in the plasma

Since a major challenge for thrombin detection is its quantification in complex biological fluids, the same assay was performed by adding different amounts of thrombin to healthy human plasma samples. A

very similar response for thrombin in the buffer and in the plasma was observed (Fig. S2 and Table S1).

The GFP fluorescent biosensor was used to monitor the thrombin level in human plasma after the activation of its precursor prothrombin by human factor Xa (Table 2). Thrombin was also spiked in the plasma sample and its concentration was then evaluated in activated and non-activated samples (Table 2). The results obtained confirmed the reliability of this biosensor system in quantitative thrombin detection.

4. Conclusion

The first outcome of this work was the heterologous production in the yeast *P. pastoris* of the GFP protein endowed with robust adhesion ability thanks to its fusion to the class I hydrophobin Vmh2. In principle, the set-up system allows the straight immobilization of any protein fused to Vmh2 produced and secreted by *P. pastoris*.

The peculiar ability of Vmh2-GFP to adhere to surfaces allowed us to develop an alternative method for the monitoring of thrombin in biological samples, compared to those currently in use. The main advantages of this sensor include the simplicity of its design and preparation, high sensitivity, wide range of linearity and accuracy. In fact, the Vmh2-GFP based biosensor allows a reliable detection of thrombin in the aM- mM range using a small amount of blood, and requiring a low consumption of reagents and time.

Acknowledgments

This work was supported by a grant from the Ministero dell'Istruzione, dell'Università e della Ricerca –PON03PE_00107_1 Industrial research project “Development of green technologies for the

Table 2
Assay results of thrombin in plasma.

Sample	Added amount (μM)	Expected amount (μM)	Measured amount (μM)
Plasma	–	–	< LOD
Plasma+factor	–	–	$(9.89 \pm 0.06) \times 10^{-1}$
Xa			
Plasma	4.5×10^{-3}	4.5×10^{-3}	$(4.50 \pm 0.01) \times 10^{-3}$
Plasma+factor	4.5×10^{-3}	0.99	1.04 ± 0.01
Xa			
Plasma	4.5	4.5	4.40 ± 0.02
Plasma+factor	4.5	5.49	5.52 ± 0.04
Xa			

production of BIOchemicals and their use in the preparation and industrial application of POLImeric materials from agricultural biomasses cultivated in a sustainable way in the Campania region (BioPoliS)[®] funded within the framework of the Operative National Program of Research and Competitiveness 2007–2013 D.D. Prot. N. 713/Ric. 29/10/2010.

The authors would like to thank Dr. Alfredo Maria Gravagnuolo of the Department of Chemical Sciences, University of Naples, Federico II, for his helpful discussions.

Appendix A. Supplementary material

Supplementary data associated with this article can be found in the online version at <http://dx.doi.org/10.1016/j.bios.2016.09.052>.

References

- Askolin, S., Linder, M., Scholtmeijer, K., Tenkanen, M., Penttilä, M., de Vocht, M.L., Wösten, H.A., 2006. *Biomacromolecules* 7, 1295–1301.
- Bini, A., Minunni, M., Tombelli, S., Centi, S., Mascini, M., 2007. *Anal. Chem.* 79, 3016–3019.
- Chen, J., Liu, Y., Zhao, G.C., 2016. *Sensors* 16, 135. <http://dx.doi.org/10.3390/s16010135>.
- Chen, Q., Tang, W., Wang, D., Wu, X., Li, N., Liu, F., 2010. *Biosens. Bioelectron.* 26, 575–579.
- Chen, S., Chen, Z., Ren, W., Ai, H., 2012. *J. Am. Chem. Soc.* 134, 9589–9592.
- De Stefano, L., Rea, I., Armenante, A., Giardina, P., Giocondo, M., Rendina, I., 2007. *Langmuir* 23, 7920–7922.
- De Stefano, L., Rea, I., De Tommasi, E., Rendina, I., Rotiroli, L., Giocondo, M., Longobardi, S., Armenante, A., Giardina, P., 2009. *Eur. Phys. J. E: Soft. Matter* 30, 181–185.
- Derkus, B., 2016. *Biosens. Bioelectron.* 79, 901–913.
- Enterina, J.R., Wu, L., Campbell, R.E., 2015. *Curr. Opin. Chem. Biol.* 27, 10–17.
- Gravagnuolo, A.M., Morales-Narváez, E., Longobardi, S., da Silva, E.T., Giardina, P., Merkoçi, A., 2015. *Adv. Funct. Mater.* 25, 2771–2779.
- Hernandez-Rodríguez, N.A., Correa, E., Contreras-Paredes, A., 1997. *Revista del Instituto Nacional Cancerología* 43, pp. 65–75.
- Heydari-Bafrooei, E., Amini, M., Ardakani, M.H., 2016. *Biosens. Bioelectron.* 85, 828–836.
- Hsieh, K.H., 1997. *Thromb. Res.* 86, 301–316.
- Jalil, Y., Gutierrez, F.A., Dubacheva, G., Goyer, C., Coche-Guerente, L., Defranco, E., Labbé, P., Rivas, G.A., Rodríguez, M.C., 2013. *Biosens. Bioelectron.* 41, 424–429.
- Kuang, L., Cao, S.P., Zhang, L., Li, Q.H., Liu, Z.C., Liang, R.P., Qiu, J.D., 2016. *Biosens. Bioelectron.* 85, 798–806.
- Liang, G., Cai, S., Zhang, P., Peng, Y., Chen, H., Zhang, S., Kong, J., 2011. *Anal. Chim. Acta* 689, 243–249.
- Linder, M.B., 2009. *Curr. Opin. Colloid* 14, 356–363.
- Longobardi, S., Gravagnuolo, A.M., Funari, R., Della Ventura, B., Pane, F., Galano, E., Amoresano, A., Marino, G., Giardina, P., 2015. *Anal. Bioanal. Chem.* 407, 487–496.
- Lu, L., Li, J., Kang, T., Cheng, S., 2015. *Talanta* 138, 273–278.
- Mishin, A.S., Belousov, V.V., Solntsev, K.M., Lukyanov, K.A., 2015. *Curr. Opin. Chem. Biol.* 27, 1–9.
- Na, W., Liu, X., Wang, L., Su, X., 2015. *Anal. Chim. Acta* 899, 85–90.
- Piscitelli, A., Pennacchio, A., Longobardi, S., Velotta, R., Giardina, P., 2016. *Biotechnol. Bioeng.* <http://dx.doi.org/10.1002/bit.26049>.
- Qin, C., Wen, W., Zhang, X., Gu, H., Wang, S., 2015. *Analyst* 140, 7710–7717.
- Qin, M., Wang, L.K., Feng, X.Z., Yang, Y.L., Wang, R., Wang, C., Yu, L., Shao, B., Qiao, M.Q., 2007. *Langmuir* 23, 4465–4471.
- Sun, T., Qing, G., Su, B., Jiang, L., 2011. *Chem. Soc. Rev.* 40, 2909–2921.
- Trapaidze, A., Héroult, J.P., Herbert, J.M., Bancaud, A., Gué, A.M., 2016. *Biosens. Bioelectron.* 78, 58–66.
- Wang, J., Shan, Y., Zhao, W.W., Xu, J.J., Chen, H.Y., 2011. *Anal. Chem.* 83, 4004–4011.
- Wang, Z., Lienemann, M., Qiao, M., Linder, M.B., 2010. *Langmuir* 26 (11), 8491–8496.
- Xu, H., Gorgy, K., Gondran, C., Le Goff, A., Spinelli, N., Lopez, C., Defranco, E., Cosnier, S., 2013. *Biosens. Bioelectron.* 41, 90–95.
- Xu, H., Mao, X., Zeng, Q., Wang, S., Kawde, A.N., Liu, G., 2009. *Anal. Chem.* 81, 669–675.
- Yan, S., Huang, R., Zhou, Y., Zhang, M., Deng, M., Wang, X., Weng, X., Zhou, X., 2011. *Chem. Commun.* 47, 1273–1275.
- Yu, F., Persson, B., Löfås, S., Knoll, W., 2004. *J. Am. Chem. Soc.* 126, 8902–8903.
- Zhao, Q., Gao, J., 2015. *Biosens. Bioelectron.* 53, 21–25.
- Zhao, Q., Li, X.F., Le, X.C., 2011. *Anal. Chem.* 83, 9234–9236.
- Zhao, Z.X., Qiao, M.Q., Yin, F., Shao, B., Wu, B.Y., Wang, Y.Y., Wang, X.S., Qin, X., Li, S., Yu, L., Chen, Q., 2007. *Biosens. Bioelectron.* 22, 3021–3027.
- Zhao, Z.X., Wang, H.C., Qin, X., Wang, X.S., Qiao, M.Q., Anzal, J., Chen, Q., 2009. *Colloids Surf. B Biointerfaces* 71, 102–106.

Rapid and ultrasensitive detection of active thrombin based on Vmh2 hydrophobin fused to Green Fluorescent Protein

Alessandra Piscitelli, Anna Pennacchio, Paola Cicatiello, Jane Politi, Luca De Stefano, Paola Giardina

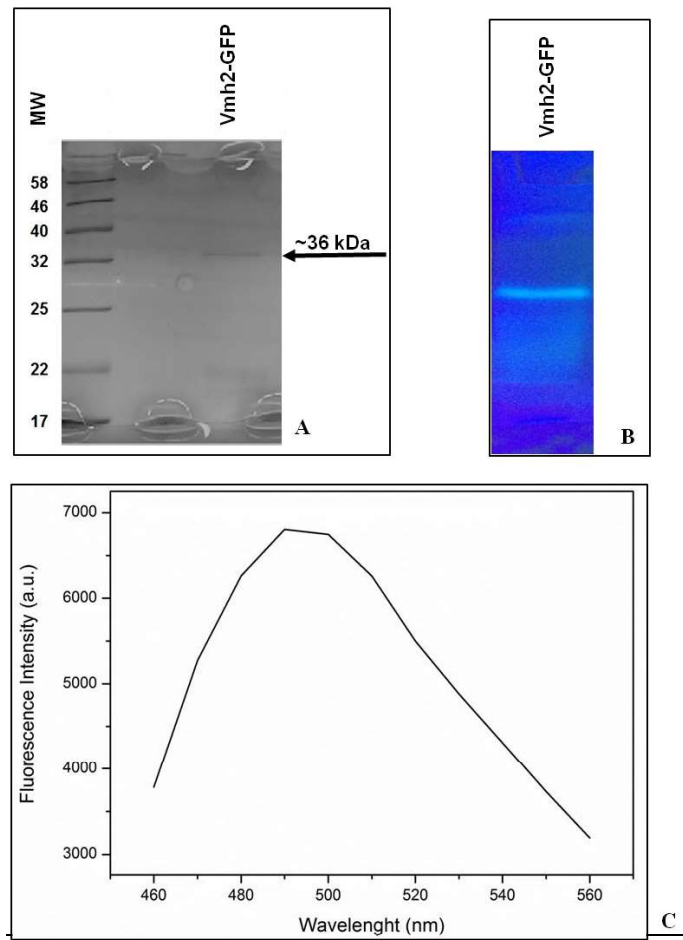


Figure S1. Characterization of Vmh2-GFP **A.** SDS PAGE; **B.** Semi denaturing PAGE; **C.** Fluorescence spectrum (excitation at 450 nm)

Table S1. Parameters of linear fitting

Buffer	Adj. R²	0.998
	Parameters	Value ± Standard Error
	Intercept	111.1± 0.9
	Slope	-7.7± 0.1
	LOD	2.27 aM

Plasma	Adj. R²	0.998
	Parameters	Value ± Standard Error
	Intercept	108.8± 0.9
	Slope	-7.5± 0.1
	LOD	2.30 aM

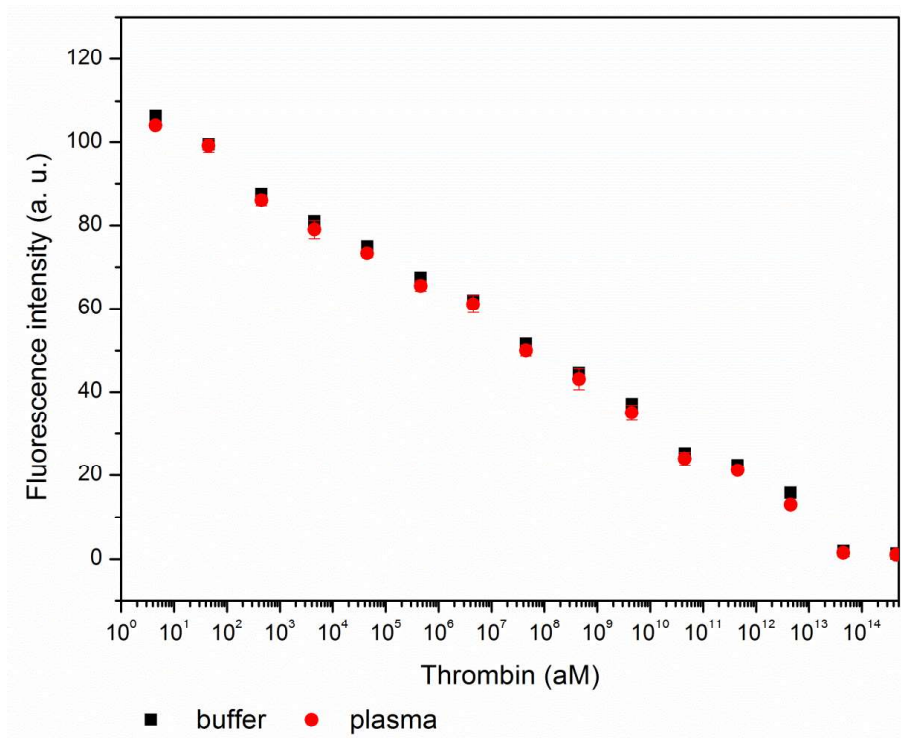


Figure S2. Logarithmic plot of the calibration curve of the fluorescence intensity of the Vmh2-GFP vs the thrombin concentrations in Tris-HCl buffer at pH 8.0 (black square) and in pretreated plasma (red circle).

CHAPTER 4

4. USE OF HYDROPHOBIN COATINGS FOR ANTI-BIOFILM ACTIVITY

A biofilm is an assemblage of microbial cells that is associated with a surface and enclosed in a matrix of primarily polysaccharide material. Biofilms may be formed on a wide variety of surfaces, including living tissues, indwelling medical devices, industrial or potable water system piping. Mature biofilms resist to a wide range of antimicrobial treatments and for this reason the discovery of new compounds able to inhibit biofilm formation is pressing. In this regard, various innovative anti-biofilm approaches have been proposed over the last few years aimed at limiting microbial adhesion to biotic and abiotic surfaces, targeting microbial signals that modulate the switch to the biofilm mode of growth, or dislodging cells from established biofilms. A promising approach to retard, repulse or attract biofilm formation is surface modification. Surface functionalization using proteins generally involve environmental friendly processes and can affect several surface properties. In particular, the use of amphiphilic proteins that form stable layers to coat surfaces can be used to prevent the biofilm formation changing the surface properties.

In this chapter the ability of two different hydrophobins, Vmh2 and Pac3, to inhibit *Staphylococcus epidermidis* biofilm has been tested on different surfaces. The interest towards this nosocomial pathogen bacterium is due to the fact that it frequently causes infections associated with implanted foreign materials.

5. Conclusions

The aim of this PhD work was focused on the discovery of novel hydrophobins and on the exploration of some of the application fields in which they can be used. The achieved results were listed below:

- New hydrophobins were isolated from marine derived fungi using *ad hoc* developed extraction methods
- Two class I hydrophobins, Pac2 and Pac3 from marine fungi, were characterized in their soluble and aggregate forms, highlighting their different interactions with surfaces of different nature
- The class I hydrophobin from *Pleurotus ostreatus*, Vmh2, was employed to coat the sample plate of MALDI-TOF mass spectrometry to set up a lab on plate approach for forensic applications. Moreover, Vmh2-coated-plates were also used for a preliminary application to MALDI-IMAGING mass spectrometry to analyse complex samples as rat brain tissue
- Vmh2 fused to the Green Fluorescence Protein was heterologously produced in *Pichia pastoris* and used to develop a thrombin biosensor
- Pac3 and Vmh2 layers were used to inhibit the biofilm formation of the nosocomial pathogen *Staphylococcus epidermidis*

Communications

Poster

- Alfredo Maria Gravagnuolo, Jane Politi, **Paola Cicatiello**, Luca De Stefano, Eden Morales, Arben Merkoci, Paola Giardina. "Self-assembled nanoscale films and complexes of the surface active protein Vmh2". 2nd edition European Symposium on Surface Science. Italy, Capri, 21-23 September 2016.
- Ekta Patel, **Paola Cicatiello**, Lisa Deininger, Malcolm Clench, Peter Marshall, Andy West, Simona Francese. "Improving the efficiency and rapidity of tryptic proteolysis: from blood to *unknown stains*". 64TH ASMS (American Society Mass Spectrometry) Conference on Mass Spectrometry and Allied Topics. Texas, San Antonio, 5-9 June 2016.

Oral presentation

- **Paola Cicatiello**, Alfredo Maria Gravagnuolo, Paola Giardina. "Marine fungi as source of protein biosurfactants". 5th International Conference on Biofoams. Sorrento, Italy, 13-16 October 2015.
- **Paola Cicatiello**, Alfredo Maria Gravagnuolo, Giorgio Gnavi, Giovanna Cristina Varese, Paola Giardina. "Novel hydrophobins from marine fungi". 9th International Conference on Fiber and Polymer Biotechnology. Osaka, Japan, 7-9 September 2016.

Publications

P1- Macellaro G, Pezzella C, **Cicatiello P**, Sannia G, Piscitelli A. (2014) Fungal laccases degradation of endocrine disrupting compounds. *Biomed Res Int.* 2014:614038.

P2- Patel E, **Cicatiello P**, Deininger L, Clench MR, Marino G, Giardina P, Langenburg G, West A, Marshall P, Sears V, Francese S. (2015) A proteomic approach for the rapid, multi-informative and reliable identification of blood. *Analyst.* 141(1):191-8.

P3- Lettera V, Pezzella C, **Cicatiello P**, Piscitelli A, Giacobelli VG, Galano E, Amoresano A, Sannia G. (2016) Efficient immobilization of a fungal laccase and its exploitation in fruit juice clarification. *Food Chem.* 196:1272-8.

P4- **Cicatiello P**, Gravagnuolo AM, Gnavi G, Varese GC, Giardina P. (2016) Marine fungi as source of new hydrophobins. *Int J Biol Macromol.* 92:1229-1233.

P5- Piscitelli A, Pennacchio A, **Cicatiello P**, Politi J, De Stefano L, Giardina P. (2016) Rapid and ultrasensitive detection of active thrombin based on the Vmh2 hydrophobin fused to a Green Fluorescent Protein. *Biosens Bioelectron.* 87:816-822.

P6- Submitted to **Biotechnology&Bioengineering**. **Paola Cicatiello**, Principia Dardano, Marinella Pirozzi, Alfredo Maria Gravagnuolo, Luca De Stefano, Paola Giardina. Self-assembly of two hydrophobins from marine fungi affected by interaction with surfaces.

Experience in foreign laboratories

February- July 2015 and August 2016: Visiting PhD student in the laboratory of Dr. Simona Francese, Biomedical Research Centre-Sheffield Hallam University (Sheffield, United Kingdom). The stage was focused on the use of hydrophobins-coated-surfaces as a proteomic tool in MALDI-TOF and MALDI IMAGING analysis.

APPENDIX

Research Article

Fungal Laccases Degradation of Endocrine Disrupting Compounds

**Gemma Macellaro, Cinzia Pezzella, Paola Cicatiello,
Giovanni Sanna, and Alessandra Piscitelli**

*Department of Chemical Sciences, University of Naples "Federico II", Complesso Universitario Monte S. Angelo,
Via Cinthia 4, 80126 Naples, Italy*

Correspondence should be addressed to Alessandra Piscitelli; apiscite@unina.it

Received 13 January 2014; Revised 12 March 2014; Accepted 31 March 2014; Published 15 April 2014

Academic Editor: Sofiane Ghorbel

Copyright © 2014 Gemma Macellaro et al. This is an open access article distributed under the Creative Commons Attribution License, which permits unrestricted use, distribution, and reproduction in any medium, provided the original work is properly cited.

Over the past decades, water pollution by trace organic compounds (ng/L) has become one of the key environmental issues in developed countries. This is the case of the emerging contaminants called endocrine disrupting compounds (EDCs). EDCs are a new class of environmental pollutants able to mimic or antagonize the effects of endogenous hormones, and are recently drawing scientific and public attention. Their widespread presence in the environment solicits the need of their removal from the contaminated sites. One promising approach to face this challenge consists in the use of enzymatic systems able to react with these molecules. Among the possible enzymes, oxidative enzymes are attracting increasing attention because of their versatility, the possibility to produce them on large scale, and to modify their properties. In this study five different EDCs were treated with four different fungal laccases, also in the presence of both synthetic and natural mediators. Mediators significantly increased the efficiency of the enzymatic treatment, promoting the degradation of substrates recalcitrant to laccase oxidation. The laccase showing the best performances was chosen to further investigate its oxidative capabilities against micropollutant mixtures. Improvement of enzyme performances in nonylphenol degradation rate was achieved through immobilization on glass beads.

1. Introduction

In the last years assessment and conservation of environmental quality have represented an interesting field of technologic applications. The main problem in industrialized states is represented by a constant and continuous pollution of soil, water-bearing stratum, surface water, and air. This is due to the introduction, in the environment, of toxic and dangerous contaminants for many organisms, including humans. In this context endocrine disrupting chemicals (EDCs) play a significant role. EDCs have been found to disturb the endogenous hormone pathway and interrupt the function of hormone receptors via estrogens-mimicking chemicals, resulting in the alteration of physiological functions, such as reproduction and development of different species, including humans [1]. EDCs are found in many products derived from cosmetic industries and working environment [2]. Many

natural chemicals (e.g., phytoestrogens, including genistein and coumestrol), found in human and animal food, can also act as endocrine disruptors [2, 3].

Between 2000 and 2006 the European Commission has contracted diverse studies on the identification and evaluation of this class of substances, and a list of substances potentially endocrine disruptor has been drawn up [4]. Efficient and applicable techniques for removing EDCs in wastewater treatment processes remain a challenge of high environmental and public health significance [5]. One promising approach consists in the use of enzymatic systems able to degrade EDCs into nontoxic or easy to remove products [6]. The promise of phenol oxidases (laccases and tyrosinases) and peroxidases for the elimination of EDCs from aqueous solutions has been established over the last few years and is attracting an increasing attention [7, 8]. Nonetheless, the application of enzymes in continuous systems such as

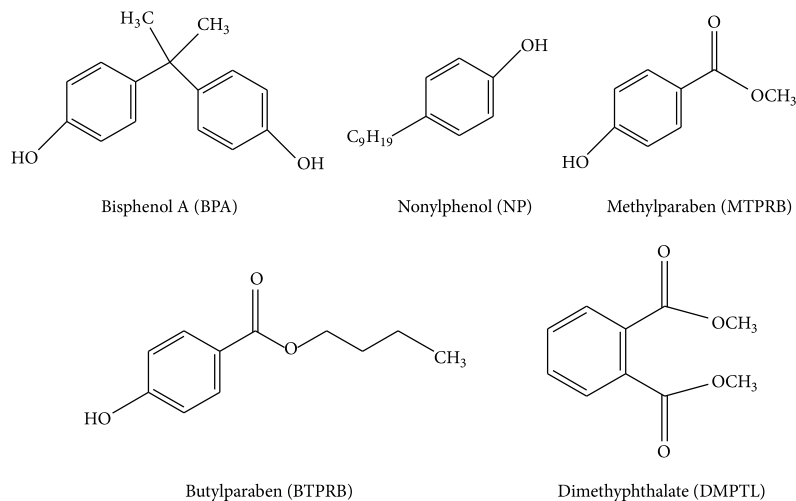


FIGURE 1: Chemical structure of endocrine disrupting substances used in this study.

wastewater treatment plants remains a challenge as it is limited by their non-reusability, the instability of their structures, and their sensitivity to harsh process conditions. Many of these undesirable limitations may be overcome by the use of immobilized enzyme. In the immobilized form, enzymes are more robust and more resistant to environmental changes allowing easy recovery and multiple reuses [8].

As a fact, examples referring to treatment of EDCs molecules [9–11], as well as of contaminated synthetic water and municipal wastewater [12], with different fungal peroxidases, laccases, and tyrosinases are present in the recent literature. In all reported cases, estrogenic activities were completely removed. Recent efforts have been focused on the immobilization of biocatalysts in order to tackle this major limitation and to facilitate their possible reuse [8].

Laccases (p-diphenol-dioxygen oxidoreductases; EC 1.10.3.2) are blue multicopper oxidases, catalysing the oxidation of a broad range of xenobiotics concomitantly with the reduction of molecular oxygen to water. This renders them very attractive compared to other enzymatic systems because no additional/expensive cosubstrate or cofactor is required apart from oxygen. These enzymes usually contain four copper ions distributed in three active sites, which are involved in the electron transfer from the substrate (T1 active site) towards oxygen (T2/T3 active sites) [13].

In this project, among various chemical classes, the EDCs bisphenol A (BPA), nonylphenol (NP), methylparaben (MTPRB), butylparaben (BTPRB), and dimethylphthalate (DMPTL) (Figure 1) have been selected, based on information about their toxicity, the amount discharged per year, and their commercial availability. BPA is a high production volume chemical used as an intermediate in the fabrication of polycarbonate plastic and epoxy resins [14]. Due to its daily use, high concentrations of BPA are observed in wastewater and in wastewater sludge (0.004–1.36 mg kg⁻¹).

NP is a mixture of para-, ortho-, and meta-isomers; the most prevalent of them is para-NP. It is a viscous, colourless liquid and it is subjected to ethoxylation to give alkylphenol ethoxylates [15]. This compound is very toxic and recalcitrant; thus it shows a high potential to bioconcentrate [16]. Parabens are esters of parahydroxybenzoic acid, widely used as preservatives in food, pharmaceutical, and cosmetic industries to prevent bacterial growth [17, 18]. Phthalates are a group of persistent, high production volume chemicals, used for a variety of products, including personal care products (e.g., perfumes, lotions, and cosmetics), varnish, medical devices, pharmaceuticals, solvents, additives, and insect repellents [19].

Four different fungal laccases were used in this study to set up EDCs enzymatic treatment, also in the presence of both synthetic and natural mediators. Three out of four selected enzymes were high redox potential laccases from *Pleurotus ostreatus*: POXC [20, 21], POXA1b [21, 22] heterologously expressed in the filamentous fungus *Aspergillus niger* [23], 1H6C, a POXA1b variant obtained through random mutagenesis [24] and produced in *A. niger* [23]. Finally, a commercial laccase, the Novoprime Base 268 (Novozymes), was also used for enzymatic treatment. Moreover, considering that in the natural environment pollutant mixtures are common, this study also evaluated the effect of the best performing enzyme, both free and immobilized, towards the presence of pollutants mixtures.

2. Materials and Methods

2.1. Organism and Culture Conditions. The *P. ostreatus* (Jacq.: Fr.) Kummer (type: Florida) (ATCC number MYA-2306) fungus was maintained through periodic transfer at 4°C on potato dextrose yeast extract (PDY) 24 g/L potato dextrose; 5 g/L yeast extract. Growth was carried out at 28°C in the

dark by preinoculating 300 mL of PDY in 500 mL shaken flasks with 6 agar plugs of mycelium grown on solid state on Petri dishes (11 mm diameter). 50 mL of a 5-day-old culture was transferred in 1 L flasks containing 450 mL of PDY broth. Cultures were incubated in the dark at 28°C under agitation (150 rpm).

A. niger D15#26 strain [25] was grown in liquid medium (300 mL) containing 70 mM NaNO₃, 7 mM KCl, 200 mM Na₂HPO₄, 2 mM MgSO₄·7H₂O, 5% (w/v) glucose, 2 g/L casamino acids, and 5 g/L yeast extract. pH was daily adjusted to 5.0 by adding 1 M citric acid [23].

2.2. Enzymes. Laccase POXC [20] was purified from *P. ostrea-tus* with slight modifications in the purification protocol. After 10 days of culture, the medium was collected and filtered through gauze. 1 mM of the serine protease inhibitor, phenylmethanesulfonyl fluoride (PMSF), was added to the supernatant. Secreted proteins were precipitated from the filtered medium by addition of (NH₄)₂SO₄ up to 80% saturation and loaded on Phenyl Sepharose High Performance 35/100 (GE Healthcare, Milan, Italy). POXC was eluted with a linear gradient of decreasing (NH₄)₂SO₄ concentration from 1 M to 0 M. Fractions corresponding to POXC were pooled, equilibrated in buffer 50 mM sodium phosphate (NaP) pH 6.5, and loaded onto a DEAE Sepharose Fast Flow column (GE Healthcare, Milan, Italy) with a linear gradient from 0 M to 0.5 M NaCl, and fractions corresponding to POXC were pooled and desalted.

POXA1b and 1H6C were heterologously expressed and purified from *A. niger*, as previously described [23].

Laccase Novoprime Base 268 (Novozymes) was dissolved in 50 mM NaP pH 6.5.

2.3. Assay of Enzymatic Activity. Laccase activity was assayed at 25°C by monitoring the oxidation of 2,2'-azino-bis(3-ethylbenzothiazoline-6-sulphonic acid) (ABTS) at 420 nm ($\epsilon_{420} = 36 \times 10^3 \text{ M}^{-1} \text{ cm}^{-1}$). The assay mixture contained 2 mM ABTS in 100 mM sodium citrate buffer, pH 3.0.

Immobilized enzyme activity was assayed incubating 10 mg of glass beads in 1 mL of 2 mM ABTS in 100 mM sodium citrate buffer (pH 3.0). The activity was determined by measuring the absorbance at 420 nm every 30'' following the reaction for 2 min. Enzymatic units were expressed as U/g.

2.4. Laccase Immobilization on Glass Beads. Glass beads type S (0.4–0.6 mm diameter) were supplied by Silibeads (Sigmund Lindner GmbH, Germany). Beads were pretreated with 1.2 M HNO₃ at 60°C for 4 hours, extensively washed with water, and then dried at 60°C. Carrier derivatization was performed as follows: 5 g of dry pretreated beads was mixed with 10% APTES (γ -aminopropyltriethoxysilane, Sigma-Aldrich) in 50 mL distilled water and incubated at 80°C for 2 h under constant mixing. The suspension was then washed thoroughly with 50 mM NaP buffer pH 6.5 and treated with 2.5% glutaraldehyde for 1 h at room temperature. The activated beads were extensively washed with the overcited buffer and finally incubated for 1 h with a solution

of laccase mixture in 50 mM NaP buffer, pH 6.5 at room temperature. Residual active glutaraldehyde was inactivated by 1 h incubation with 100 mM glycine at room temperature. Immobilization yield (Y) was defined as the ratio between laccase activity assayed on the solid biocatalyst and total activity available in the liquid solution at the beginning of the immobilization processes. A yield of 83% was obtained following this procedure.

2.5. EDCs Enzymatic Degradation. 1 mM stock solution of each EDC (Sigma-Aldrich, Milan, Italy) was prepared in hot water. To improve the solubility of NP and DMPTL in hot water, methanol (0.4% v/v) and Tween 80 (0.1% w/v) were added, respectively. 100 μ M of each EDC was incubated for 1 h at 25°C in a reaction mixture containing 1.5 U/mL of purified laccase in 50 mM sodium citrate buffer, pH 5.0; total reaction volume was set to 4 mL. Amounts of EDC were quantified every 30 minutes (t_0 , $t_{30'}$, $t_{60'}$) by reverse-phase HPLC. Enzymatic reaction was stopped by adding 50 μ L of hydrochloric acid (HCl) to 500 μ L of reaction mixture and centrifuging at 15, 100 g for 15 min at room temperature. 100 μ L of the supernatant was analysed by HPLC. Degradation of EDCs mixture was performed in the same condition, using a final concentration of 25 μ M of each EDC, but for DMPTL. Thus, the final concentration of EDCs mixture was of 100 μ M. Control reactions were always performed in the same conditions without enzyme addition. Mediators used were ABTS, dissolved in sodium citrate buffer 50 mM, pH 5.0, and acetosyringone (AS), dissolved in hot sodium citrate buffer, 50 mM, pH 5.0. Concentrations used for both mediators were 20 μ M and 200 μ M.

Degradation of EDCs mixture by means of immobilized enzyme was performed in the same conditions, using an amount of beads corresponding to 6 U total in the presence of 20 μ M AS.

2.6. High-Performance Liquid Chromatography. All EDCs were quantitatively analysed using a C18 column (Grace Vydac, Hesperia, CA, USA) on an HPLC instrument (Agilent Technologies, Italy). The fractions were eluted by using a linear gradient of water-acetonitrile (A solvent 0.1% trifluoroacetic acid in Milli-Q (MQ) water; B solvent 0.07% trifluoroacetic acid, 5% MQ water in acetonitrile) at a flow rate of 1 mL/min. The gradient program for BPA analysis was 0–3 min (acetonitrile 30%), 3–9 min (acetonitrile 30–90%), 9–12 min (acetonitrile 90%), 12–13 min (acetonitrile 90–30%), and 13–15 min (acetonitrile 30%). The eluted sample was monitored by UV absorbance at 227 nm. The retention time for BPA was 6.9 min under these conditions. As regards NP, the applied gradient was 0–3 min (acetonitrile 20%), 3–9 min (acetonitrile 20–90%), 9–12 min (acetonitrile 90%), 12–13 min (acetonitrile 90–20%), and 13–15 min (acetonitrile 20%). The detection wavelength was 277 nm. The retention time for NP was 14.5 min under these conditions. The gradient program for parabens analyses was 0–7 min (acetonitrile 30–70%), 7–8 min (acetonitrile 70–90%), 8–11 min (acetonitrile 90%), 11–12 min (acetonitrile 90–30%), and 12–14 min (acetonitrile 30%). The detection wavelength was 254 nm. Under these

conditions the retention times for MTPRB and BTPRB were 5.8 min and 8.8 min, respectively. As regards DMPTL, the applied gradient was the same used for parabens, while the detection wavelength was 274 nm. The retention time for DMPTL was 6.8 min under these conditions.

As far as the EDCs mixtures are concerned, each molecule was analysed with its optimised program.

The peak area on the chromatogram was used to calculate the remaining amount of EDC as a percentage of the initial value.

3. Results and Discussion

3.1. Endocrine Disruptors Degradation by Enzymes. Enzymatic degradation of EDC bisphenol A (BPA), nonylphenol (NP), methylparaben (MTPRB), butylparaben (BTPRB), and dimethylphthalate (DMPTL) was tested in solution at pH 5.0 in the presence of the different selected laccases. Among the EDC molecules, only BPA was degraded by enzymes in the absence of any mediator within the time of incubation analysed (Figure 2). After 1 hour of incubation Novoprime Base 268 was able to degrade 60% of BPA, whereas POXC degradation rate was slower than that obtained by Novoprime 268, reaching 30% of BPA degradation after both 30 minutes and 1h incubation. Both POXA1b and 1H6C were less efficient, with the latter being more able to degrade BPA, probably thanks to its higher redox potential [23]. The rate of BPA degradation was comparable with that obtained for other laccases in similar conditions. A careful comparison of results present in the recent scientific literature reveals that different strategies have been used to obtain BPA removal, along with different time of reaction and concentration of both enzyme and substrate. Gassara and coworkers [26] reported a rate of BPA degradation of 13% after 2 hours of incubation in the presence of 0.05 U/mL of a laccase from *Phanerochaete chrysosporium*. A purified laccase from *Grifola frondosa* was able to degrade 15% BPA (0.65 mM) in 1 hour [27], whereas a purified laccase from *Phlebia tremellosa* [28] removed around 65% of BPA estrogenic activity after 3 h incubation with 50 U of enzymatic activity. Interesting results were obtained using a purified laccase by *Trametes villosa*, able to totally degrade 2.2 mM BPA after 3 h incubation [29].

3.2. EDCs Degradation by Enzymes in the Presence of Mediators. With the aim to enhance laccase efficiencies towards selected EDCs, two different mediators, a synthetic and a natural one, were added to the reaction mix. The selected mediators were ABTS, the first acknowledged laccase mediator [30], and the natural mediator AS, an eco-friendly, easily and economically available mediator [31].

As it is shown in Figure 3(a), the presence of both mediators enhances laccase performances towards BPA but for Novoprime 268 and ABTS mediator is more effective than AS with all the tested laccases. As a fact, in the presence of ABTS, POXC was able to almost fully degrade BPA (95%) after 1 hour reaction. It is also possible to note that in the presence of both mediators POXA1b and 1H6C showed the same efficiency. Unexpectedly, the presence of mediators did not

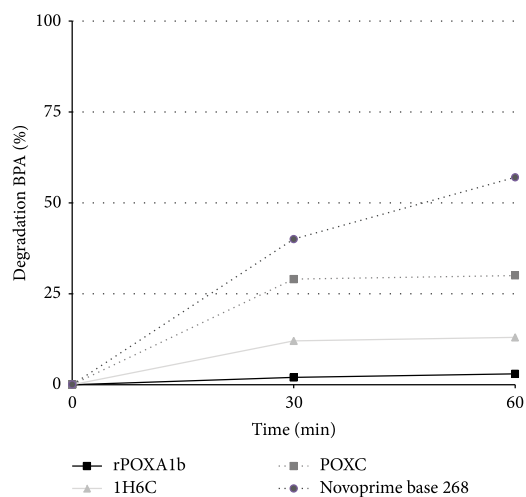


FIGURE 2: Percentage degradation (%) of BPA by fungal laccases. Reaction conditions: 100 μ M BPA, pH 5.0 (50 mM sodium citrate buffer), 25°C, and 1.5 U/mL laccase, with a reaction time of 1h. All results are averages from two replicate experiments and the standard deviation is less than 10%.

influence or even decreased Novoprime base 268 efficiency. A similar effect has also been observed for a *Corioliopsis polyzona* laccase towards NP using 1-hydroxybenzotriazole (HBT) as mediator [10].

Also when considering nonylphenol, the presence of both mediators enhances laccase performances, with ABTS being more effective than AS with all tested laccases (Figure 3(b)). In this case, POXC and Novoprime base 268 showed almost the same degradation rate both in the presence of ABTS and AS. On the other hand, POXA1b and 1H6C showed an opposite behaviour. As a fact, in the presence of ABTS, 1H6C was more effective than POXA1b, whereas in the presence of AS, POXA1b proved to be more efficient than its variant. This result seems to indicate that no simple rule regarding redox potential or affinity can be easily drawn, as the whole reaction mechanism is quite complex. The obtained results seem promising if carefully compared with other systems. Indeed, a laccase from the white rot fungus *C. polyzona* was able to eliminate 50% BPA and 66% NP in the presence of 10 μ M ABTS as mediator [10]. When the synthetic mediator HBT (200 μ M) was used to improve laccase degradation, an enhanced degradation of almost 1.3-fold for both substrates was observed, reaching a degradation of 95% and 80% for BPA and NP, respectively [32].

When the mediator concentration was increased up to 200 μ M, AS was revealed to be the best mediator, since all enzymes were able to also degrade methylparaben and butylparaben after 1 h incubation (Table 1). Also in this case, POXC showed the best performances, being able to degrade in 30 minutes 50% and 60% of methyl and butylparaben, respectively (degradation did not improve after 1 h incubation). Among parabens, butylparaben was more susceptible

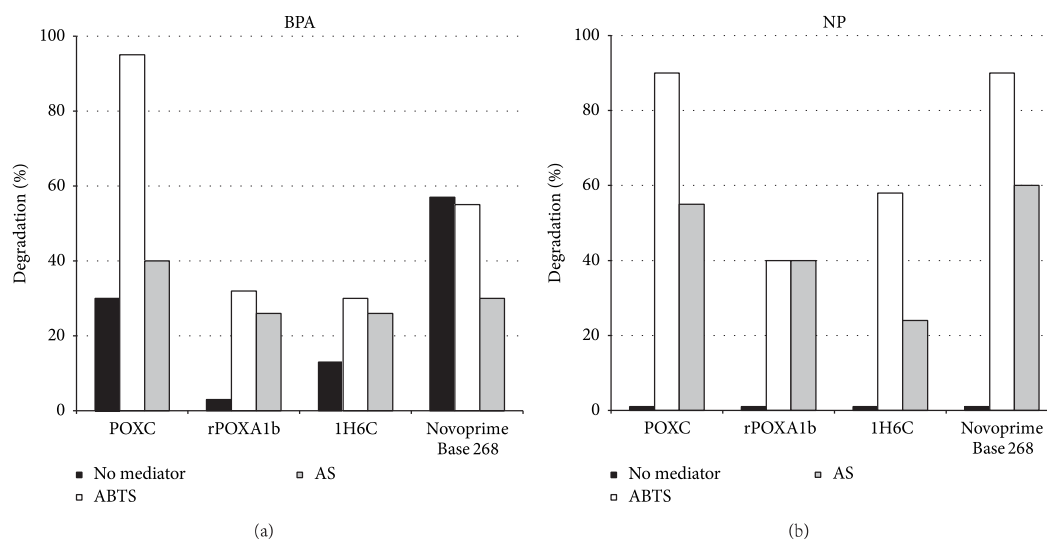


FIGURE 3: Effect of absence of mediator, 20 μ M of ABTS, or AS on the removal of EDCs after a 1 h treatment at pH 5.0 and at a temperature of 25°C with 1.5 U/mL of laccases. (a) BPA; (b) NP. All results are averages from two replicate experiments and the standard deviation is less than 10%.

TABLE 1: Degradation of MTPRB and BTPRB in the presence of 200 μ M of ABTS, or AS after a 1 h treatment at pH 5.0 25°C with 1.5 U/mL of laccases. All results are averages from two replicate experiments and the standard deviation is less than 10%.

Enzymes	MTPRB (% degradation)		BTPRB (% degradation)	
	ABTS	AS	ABTS	AS
POXC	—	50	15	60
rPOXA1b	—	35	—	40
1H6C	5	7	7	8
Novoprime Base 268	—	40	—	50

to laccase degradation in the presence of mediators than methylparaben. In the scientific literature are present only few reports regarding paraben degradation by laccases. Mizuno and coworkers [33] demonstrated that both iso-butylparaben and n-butylparaben were almost completely removed (95%) after 2 h of treatment and completely disappeared after 4 h of treatment with 0.5 U/mL of laccase activity in the presence of 2 mM HBT. The only substrate recalcitrant to laccase oxidation in all the tested conditions was dimethylphthalate.

3.3. Degradation of EDCs Mixture by Free and Immobilized POXC. POXC, the best performing enzyme, was chosen for further degradation analyses against a mixture of the selected EDCs in a total final concentration of 100 μ M. The analyses were conducted in the presence of four out of five substrates. As a fact, DMPTL was not used, considering its recalcitrance to laccase degradation under all the tested conditions. It is worth to note that in the absence of any mediator POXC

is able to degrade almost 40% BPA and 80% NP after 1 h incubation, whereas methyl and butylparaben were not degraded (Figure 4). As far as BPA is concerned, a slower degradation rate was observed when BPA concentration was lowered if compared with the degradation observed with high BPA concentration. When mediator was added to the reaction, the efficiency was greatly enhanced, and full disappearance of BPA was observed in the presence of AS. On the other hand, POXC is able to efficiently degrade NP at low concentration also in the absence of mediators, and no increase is observed when mediators are added to the reaction mix. Thus, it may be hypothesized that the enzyme shows a higher affinity towards NP than towards BPA. Parabens at low concentration were not oxidised in the presence of both mediators.

When immobilized POXC was used towards EDCs mix in the presence of AS, NP degradation improved with respect to the free enzyme, reaching the same extent of degradation (80%) within only 15 min, and no further increase was observed. On the other hand, a slightly lower BPA removal (80%) was observed using the immobilized enzyme with respect to the free one. Parabens were not degraded, following the same trend already observed for the soluble counterpart. Control reactions were carried out using the silanized and derivatized carrier (without enzyme) against the mix of EDCs and no adsorption on the carrier was observed. Laccase immobilized on glass beads maintained significant activity during storage at 4°C in 50 mM phosphate buffer pH 6.5. After one month of storage, the retained laccase activity was 100%.

In order to assess reusability of the immobilized laccase against mixture of EDCs, six successive cycles of batch degradation were performed. After six cycles, there was a 20%

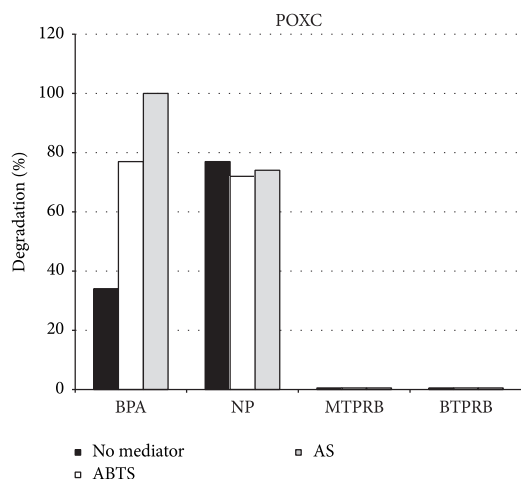


FIGURE 4: Effect of absence of mediator, 20 μM of ABTS, or AS on the removal of EDCs mixtures by POXC. Reaction conditions: 25 μM of each molecule, pH 5.0 (50 mM sodium citrate buffer), 25°C, and 1.5 U/mL laccase, with a reaction time of 1 h. All results are averages from two replicate experiments and the standard deviation is less than 10%.

drop in laccase activity (Figure 5). As far as EDC removal is concerned, a gradual loss of BPA degradation during six cycles was observed. On the other hand, NP degradation was decreased up to 40% after the first cycle, but no further drop was observed during the following 5 cycles.

4. Conclusions

The growing attention accorded to the removal of EDCs from environmental matrices makes oxidative enzymes an attractive candidate in the bioremediation arsenal. Four different laccases were chosen for their interesting characteristics and tested towards EDC molecules. The obtained results have shown that all laccases are able to oxidize different EDCs. In particular, BPA is the only substrate oxidized under all conditions tested. Furthermore, to improve laccase capabilities, mediators were added to reaction mixtures. Among the chosen laccases, POXC was the enzyme with the highest bioremediation capacity under all conditions analysed. Its performance was increased in the presence of both mediators. Interesting results were obtained in the presence of the natural mediator acetosyringone. When used at high concentration, this natural mediator enhanced the bioremediation capacity of POXC determining a rate degradation of 50% of both parabens in 30 minutes. Thus, results herein obtained confirm laccase capabilities [33] to degrade this kind of substrates, very poorly investigated till now. Furthermore, oxidative capabilities of POXC were also studied in the presence of EDCs mixtures. Removal rates were different in micropollutant mixtures if compared with removal rates obtained treating individually the different molecules with alternating results towards BPA and

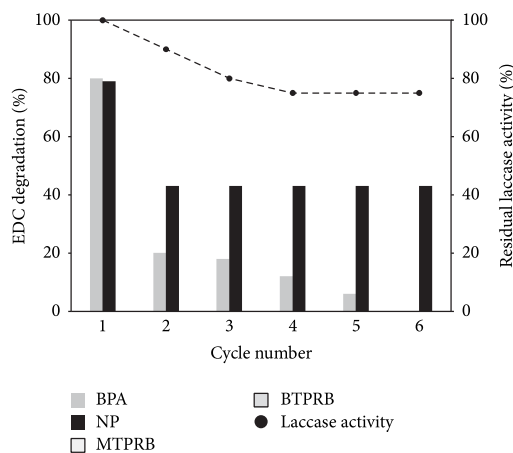


FIGURE 5: Percentage degradation (%) of BPA and NP by immobilized POXC. Reaction conditions: 6 U_{TOT} versus 25 μM each EDC, pH 5.0 (50 mM sodium citrate buffer), 25°C, and in the presence of 20 μM AS with a reaction time of 1 h. Residual laccase activity is reported as filled black circle. All results are averages from two replicate experiments and the standard deviation is less than 10%.

NP, respectively. Improvement of enzyme performances in NP removal was achieved through immobilization on glass beads.

These results highlight the influence on the enzymatic degradation efficiency of the ratio between xenobiotic concentration and enzyme affinity. Thus, a challenge still open to face EDCs degradation is the discovery/tailoring enzymes capable of degrading the target compounds with an affinity constant of the same order of magnitude with respect to the actual concentrations of the EDCs in the environment. As a fact, since EDCs concentration in real wastewater is very low (ng/L), enzymes displaying a very high efficiency (high turnover together with high affinity) towards this molecule are excellent candidates to efficiently achieve their removal.

Conflict of Interests

The authors declare that there is no conflict of interests regarding the publication of this paper.

Acknowledgment

This work was supported by grants from the Italian MIUR (Ministero dell'Università e della Ricerca Scientifica Progetti di Rilevante Interesse Nazionale) PRIN 2009STNWX3.

References

- [1] T. T. Schug, A. Janesick, B. Blumberg, and J. J. Heindel, "Endocrine disrupting chemicals and disease susceptibility," *Journal of Steroid Biochemistry and Molecular Biology*, vol. 127, no. 3–5, pp. 204–215, 2011.

- [2] S. Combalbert and G. Hernandez-Raquet, "Occurrence, fate, and biodegradation of estrogens in sewage and manure," *Applied Microbiology and Biotechnology*, vol. 86, no. 6, pp. 1671–1692, 2010.
- [3] E. Diamanti-Kandarakis, J.-P. Bourguignon, L. C. Giudice et al., "Endocrine-disrupting chemicals: an Endocrine Society scientific statement," *Endocrine Reviews*, vol. 30, no. 4, pp. 293–342, 2009.
- [4] European Union, "Commission staff working document. An implementation of the community strategy for endocrine disruptors—a range of substances suspected of interfering with the hormone systems of humans and wildlife," no. 1372, Belgium, Brussels, 2004.
- [5] Z.-H. Liu, Y. Kanjo, and S. Mizutani, "Removal mechanisms for endocrine disrupting compounds (EDCs) in wastewater treatment—physical means, biodegradation, and chemical advanced oxidation: a review," *Science of the Total Environment*, vol. 407, no. 2, pp. 731–748, 2009.
- [6] P. Galliker, G. Hommes, D. Schlosser, P. F.-X. Corvini, and P. Shahgaldian, "Laccase-modified silica nanoparticles efficiently catalyze the transformation of phenolic compounds," *Journal of Colloid and Interface Science*, vol. 349, no. 1, pp. 98–105, 2010.
- [7] H. Cabana, J. P. Jones, and S. N. Agathos, "Elimination of endocrine disrupting chemicals using white rot fungi and their lignin modifying enzymes: a review," *Engineering in Life Sciences*, vol. 7, no. 5, pp. 429–456, 2007.
- [8] S. Yang, F. I. Hai, L. D. Nghiem et al., "Understanding the factors controlling the removal of trace organic contaminants by white-rot fungi and their lignin modifying enzymes: a critical review," *Bioresource Technology*, vol. 141, pp. 97–108, 2013.
- [9] Y.-J. Kim and J. A. Nicell, "Impact of reaction conditions on the laccase-catalyzed conversion of bisphenol A," *Bioresource Technology*, vol. 97, no. 12, pp. 1431–1442, 2006.
- [10] H. Cabana, J.-L. H. Jiwan, R. Rozenberg et al., "Elimination of endocrine disrupting chemicals nonylphenol and bisphenol A and personal care product ingredient triclosan using enzyme preparation from the white rot fungus *Corioloropsis polyzona*," *Chemosphere*, vol. 67, no. 4, pp. 770–778, 2007.
- [11] C. Nicolucci, S. Rossi, C. Menale et al., "Biodegradation of bisphenols with immobilized laccase or tyrosinase on polyacrylonitrile beads," *Biodegradation*, vol. 22, no. 3, pp. 673–683, 2011.
- [12] M. Auriol, Y. Filali-Meknassi, R. D. Tyagi, and C. D. Adams, "Laccase-catalyzed conversion of natural and synthetic hormones from a municipal wastewater," *Water Research*, vol. 41, no. 15, pp. 3281–3288, 2007.
- [13] P. Giardina, V. Faraco, C. Pezzella, A. Piscitelli, S. Vanhulle, and G. Sannia, "Laccases: a never-ending story," *Cellular and Molecular Life Sciences*, vol. 67, no. 3, pp. 369–385, 2010.
- [14] D. P. Mohapatra, S. K. Brar, R. D. Tyagi, and R. Y. Surampalli, "Parameter optimization of ferro-sonication pre-treatment process for degradation of bisphenol A and biodegradation from wastewater sludge using response surface model," *Journal of Hazardous Materials*, vol. 189, no. 1-2, pp. 100–107, 2011.
- [15] X. Jie, L. Jian Mei, F. Zheng, L. Gong, B. Zhang, and J. Yu, "Neurotoxic effects of nonylphenol: a review," *The Central European Journal of Medicine*, vol. 125, no. 3-4, pp. 61–70, 2013.
- [16] Commission Directive 2002/8/EC of 6 February 2002 amending Directives 72/168/EEC and 72/180/EEC concerning the characteristics and minimum conditions for examining vegetable and agricultural varieties respectively.
- [17] M. G. Soni, G. A. Burdock, S. L. Taylor, and N. A. Greenberg, "Safety assessment of propyl paraben: a review of the published literature," *Food and Chemical Toxicology*, vol. 39, no. 6, pp. 513–532, 2001.
- [18] P. W. Harvey and P. Darbre, "Endocrine disrupters and human health: could oestrogenic chemicals in body care cosmetics adversely affect breast cancer incidence in women? A review of evidence and call for further research," *Journal of Applied Toxicology*, vol. 24, no. 3, pp. 167–176, 2004.
- [19] M. J. Tsai, P. L. Kuo, and Y. C. Ko, "The association between phthalate exposure and asthma," *Kaohsiung Journal of Medical Sciences*, vol. 28, no. 7, pp. 28–36, 2012.
- [20] G. Palmieri, P. Giardina, L. Marzullo et al., "Stability and activity of a phenol oxidase from the ligninolytic fungus *Pleurotus ostreatus*," *Applied Microbiology and Biotechnology*, vol. 39, no. 4-5, pp. 632–636, 1993.
- [21] A. M. Garzillo, M. C. Colao, V. Buonocore et al., "Structural and kinetic characterization of native laccases from *Pleurotus ostreatus*, *Rigidoporus lignosus*, and *Trametes trogii*," *Journal of Protein Chemistry*, vol. 20, no. 3, pp. 191–201, 2001.
- [22] P. Giardina, G. Palmieri, A. Scaloni et al., "Protein and gene structure of a blue laccase from *Pleurotus ostreatus*," *Biochemical Journal*, vol. 341, no. 3, pp. 655–663, 1999.
- [23] G. Macellaro, M. C. Baratto, A. Piscitelli et al., "Effective mutations in a high redox potential laccase from *Pleurotus ostreatus*," *Applied Microbiology and Biotechnology*, 2014.
- [24] A. Miele, P. Giardina, E. Notomista, A. Piscitelli, G. Sannia, and V. Faraco, "A semi-rational approach to engineering laccase enzymes," *Molecular Biotechnology*, vol. 46, no. 2, pp. 149–156, 2010.
- [25] C. L. Gordon, V. Khalaj, A. F. J. Ram et al., "Glucoamylase: green fluorescent protein fusions to monitor protein secretion in *Aspergillus niger*," *Microbiology*, vol. 146, no. 2, pp. 415–426, 2000.
- [26] F. Gassara, S. K. Brar, M. Verma, and R. D. Tyagi, "Bisphenol A degradation in water by ligninolytic enzymes," *Chemosphere*, vol. 92, no. 10, pp. 1356–1360, 2013.
- [27] T. Nitheranont, A. Watanabe, T. Suzuki, T. Katayama, and Y. Asada, "Decolorization of synthetic dyes and biodegradation of bisphenol A by laccase from the edible mushroom, *Grifola frondosa*," *Bioscience, Biotechnology and Biochemistry*, vol. 75, no. 9, pp. 1845–1847, 2011.
- [28] Y. Kim, S. Yeo, M. K. Kim, and H. T. Choi, "Removal of estrogenic activity from endocrine-disrupting chemicals by purified laccase of *Phlebia tremellosa*," *FEMS Microbiology Letters*, vol. 284, no. 2, pp. 172–175, 2008.
- [29] T. Fukuda, H. Uchida, Y. Takashima, T. Uwajima, T. Kawabata, and M. Suzuki, "Degradation of bisphenol A by purified laccase from *Trametes villosa*," *Biochemical and Biophysical Research Communications*, vol. 284, no. 3, pp. 704–706, 2001.
- [30] R. Bourbonnais and M. G. Paice, "Oxidation of non-phenolic substrates. An expanded role for laccase in lignin biodegradation," *FEBS Letters*, vol. 267, no. 1, pp. 99–102, 1990.
- [31] A. I. Cañas and S. Camarero, "Laccases and their natural mediators: biotechnological tools for sustainable eco-friendly processes," *Biotechnology Advances*, vol. 28, no. 6, pp. 694–705, 2010.
- [32] Y. Tsutsumi, T. Haneda, and T. Nishida, "Removal of estrogenic activities of bisphenol A and nonylphenol by oxidative enzymes

- from lignin-degrading basidiomycetes,” *Chemosphere*, vol. 42, no. 3, pp. 271–276, 2001.
- [33] H. Mizuno, H. Hirai, S. Kawai, and T. Nishida, “Removal of estrogenic activity of iso-butylparaben and n-butylparaben by laccase in the presence of 1-hydroxybenzotriazole,” *Biodegradation*, vol. 20, no. 4, pp. 533–539, 2009.



Contents lists available at ScienceDirect

journal homepage: www.elsevier.com/locate/foodchem

Efficient immobilization of a fungal laccase and its exploitation in fruit juice clarification



Vincenzo Lettera^{a,b,*}, Cinzia Pezzella^{a,b}, Paola Cicatiello^a, Alessandra Piscitelli^{a,b}, Valerio Guido Giacobelli^a, Eugenio Galano^a, Angela Amoresano^a, Giovanni Sannia^a

^a Dipartimento di Scienze Chimiche, Università di Napoli Federico II, Via Cinthia 4, 80126 Napoli, Italy

^b Biopox srl, Via Salita Arenella 9, Napoli, Italy

ARTICLE INFO

Article history:

Received 16 June 2015

Received in revised form 15 October 2015

Accepted 18 October 2015

Available online 19 October 2015

Keywords:

Response Surface Methodology

Phenols

Laccase immobilization

Food industry

Mass spectrometry analysis

ABSTRACT

The clarification step represents, in fruit juices industries, a bottleneck process because residual phenols cause severe haze formation affecting juice quality and impairing customers acceptance. An enzymatic step can be efficiently integrated in the process, and use of immobilized enzymes entails an economical advantage. In this work, covalent immobilization of recombinant POXA1b laccase from *Pleurotus ostreatus* on epoxy activated poly(methacrylate) beads was optimized thanks to a Response Surface Methodologies approach. Through regression analysis the process was well fitted by a quadratic polynomial equation ($R^2 = 0.9367$, adjusted $R^2 = 0.8226$) under which laccase activity reached $2000 \pm 100 \text{ U g}^{-1}$ of beads, with an immobilization efficiency of 98%. The immobilized biocatalyst was characterized and then tested in fruit juice clarification reaching up to 45% phenol reduction, without affecting health-effective flavanones content. Furthermore, laccase treated juice displays an improved sensory profile, due to the reduction of vinyl guaiacol, a potent off-flavor possessing a peppery/spicy aroma.

© 2015 Elsevier Ltd. All rights reserved.

1. Introduction

According to the “European fruit juice association” (www.ajjn.org), EU fruit juice and nectars consumption is forecast to stand at 10.3 billion liters by 2017. The ongoing consumer health and wellness trend in many countries offers strong potential for increasing this market, due to the well-established beneficial effects associated to fruit juices consumption (Bharate & Bharate, 2014). Polyphenols in fruit juices are a natural source of antioxidants, and are responsible of the reported health benefits (Agcam, Akyıldız, & Akdemir Evrendilek, 2014). However, the same compounds are also the main factors involved in maderization process causing turbidity, color intensification, aroma and flavor alteration and formation of haze or sediments, affecting final product shelf life and consumer perception (Pezzella, Guarino, & Piscitelli, 2015). In order to reduce the impact of this phenomenon on the beverage products and to stabilize fruit juices, industries commonly use clarification processes through physical–chemical adsorbents and/or filtration technology. One disadvantage of these

techniques is that processed juices are not always stable, but rather tend to produce pronounced haze and enzymatic and non-enzymatic browning, caused by reactive phenolic compounds that cannot be removed (Friedman, 1996). Research has been concentrated, in recent years, to find effective and economical ways to reduce this phenomenon, with enzymes continuously gaining importance. Among enzymes useful within this process, several authors have proposed the use of laccases as stabilizing agents, due to their ability to oxidize most of the phenols present in juices (Neifar et al., 2011 and Gassara-Chatti et al., 2013) causing their polymerization and subsequent ease of removal.

Immobilization provides an excellent base for enzymes exploitation by increasing their reusability, enhancing their structural and catalytic stability in different environmental conditions, and reducing product inhibition (Sheldon, 2007). Apart from being affordable, immobilization generates continuous economic operations, automation, high investment/capacity ratio and recovery of product with greater purity (D'Souza, 1998). Several methods are used for enzyme immobilization and various factors influence the performance of the immobilized enzymes (Pezzella, Russo, Marzocchella, Salatino, & Sannia, 2014). The choice of the most suited method and the chemical nature of support material clearly depends on the application that enzyme is devoted to. Particularly, covalent binding is the most widely applied method in industrial

* Corresponding author at: Department of Chemical Sciences, University of Naples “Federico II” Complesso Universitario Monte S. Angelo, Via Cinthia, 4, 80126 Napoli, Italy.

E-mail address: lettera@biopox.com (V. Lettera).

applications due to several advantages including improved operational stability, robustness and reusability. The stabilization provided by covalent bonding is usually counterbalanced by partial enzyme deactivation. This negative effect can be mitigated by carefully optimizing the immobilization conditions in order to maximize the ratio between immobilized enzyme activity and activity of the primary enzyme solution.

In this work, covalent immobilization of the recombinant fungal laccase POXA1b (rPOXA1b) from the edible fungus *Pleurotus ostreatus* (Giardina et al., 1999) on epoxy activated poly(methacrylate) supports (Mateo et al., 2002 and Mateo et al., 2007) was investigated and the solid bio-catalyst was tested in fruit juices treatment. Laccases are widespread enzymes able to oxidize a wide range of phenolic substrates, using only molecular oxygen as cofactor and generating water as unique by-product. Due to its high redox potential and belonging to an enzymatic system of an edible fungus (Macellaro, Pezzella, Cicatiello, Sannia, & Piscitelli, 2014), rPOXA1b laccase has a great potential exploitability in food and beverage industries. The successful application of laccases in these fields require production of high amounts at reduced costs (Osma, Toca-Herrera, & Rodríguez-Couto, 2010). Concomitantly to strategies for their recombinant overexpression in suitable hosts, several approaches have been adopted along with optimization of immobilization processes to achieve affordable and reusable enzymatic system (Di Cosimo, McAuliffe, Pouloseb, & Bohlmann, 2013; Durán, Rosa, D'Annibale, & Gianfreda, 2002; Jesionowski, Zdzarta, & Krajewska, 2014 and Mateo, Palomo, Fernandez-Lorente, Guisan, & Fernandez-Lafuente, 2007). In this work an empirical modeling technique, named Response Surface Methodology (RSM), was used to optimize laccase immobilization yield. In RSM statistically designed experimental models are carried out to evaluate the relationship between a set of controllable experimental factors and observed results, thus to identify the optimum conditions for a multivariable system. We adopted one of the most common design, the Box Behnken (Box & Behnken, 1960), that reduces the number of experimental trials for its application and resulted in high efficiency of modeling of multiple parameters and their interactions (Costa Ferreira et al., 2007).

Stability and catalytic parameters of immobilized laccase were also assessed in comparison with the soluble counterpart. The solid optimized biocatalyst was exploited in the clarification of raw orange juice investigating the effect of laccase treatment on juice phenolic composition.

2. Materials and methods

2.1. Materials

Recombinant POXA1b laccase from *P. ostreatus* expressed in the eukaryotic host *Pichia pastoris* was provided by Biopox srl (Italy). Epoxy activated poly(methacrylate) beads (Sepabeads EC-HFA) were purchased from Resindion srl (Italy). All reagents were purchased from Sigma–Aldrich Corp. (St. Louis, MO) unless otherwise specified.

2.2. Fruit juice extraction

Mature ripened orange (*Citrus sinensis*), pomegranate (*Punica granatum*), apricot (*Prunus armeniaca*), peach (*Prunus persica*), cherry (*Prunus avium*) and apple (*Malus domestica*) fruits were obtained from a major market in Naples, Italy. The oranges were washed and peeled. The juice was extracted using a domestic juice extractor. The pomegranate fruit was peeled and the skin covering seeds was removed. The remaining part were homogenized by blender (Waring, USA) and centrifuged at 10,200×g for 5 min.

The pellet was discarded. The apricot, peach and cherry were pitted and homogenized by Waring blender. The apple was peeled and homogenized. All the juices were immediately processed after the extraction.

2.3. Enzyme immobilization

Immobilization reaction was performed incubating a variable quantity of poly(methacrylate) beads with 30 mL of 20,000 U L⁻¹ rPOXA1b laccase solution (1000 U g⁻¹ of protein) in 5 × 10⁻² M of different buffers (sodium citrate for pH 3, sodium phosphate for pH 6, Tris–HCl for pH 9) under magnetic stirrer (200 rpm) for 1 h at room temperature. Afterwards the supernatant was decanted and the biocatalyst particles washed with 30 mL of 5 × 10⁻² M phosphate buffer for 5 min for 3 times. Laccase activity was measured in the rinsing solution to calculate the immobilization yield (Y) as ratio between the total enzymatic IU presents in solution before (Ui) and after (Uf) immobilization reaction (%Y = [1 – (Uf/Ui)] × 100). Laccase activity (IU) was assayed by monitoring the oxidation of 2,2'-azino-bis(3-ethylbenzothiazoline-6-sulfonic acid) (ABTS) (see enzyme assay, Section 2.5). The biocatalyst was stored at 4 °C in the phosphate buffer with 5 × 10⁻³ M glycine to saturate possible not reacted sites.

2.4. Experimental design and statistical analysis

The RSM was set up through a Box Behnken design choosing three independent variables (quantity of beads, pH and temperature) selected on the basis of preliminary experiments and the related experimental domain was fixed for each variable (Table 1). The ratio between the amount of enzyme and beads was varied keeping constant the volume and concentration of laccase solution and varying the quantity of beads (expressed in grams). A total of 15 or more experimental sets were carried out for each run.

Data obtained through the experimental matrix were computed for the determinations of regression coefficient of the second order multiple regression model:

$$Y = \beta_0 + \sum_{i=1}^k \beta_i x_i + \sum_{i=1}^k \beta_{ii} x_i^2 + \sum_{j=1}^{j-1} \sum_{i=1}^k \beta_{ij} x_i x_j$$

where Y is the predicted response variable, β_0 , β_i , β_{ii} and β_{ij} are regression coefficient of the model, x_i , x_j represent the independent variables in the form of actual value. The analysis of regression and

Table 1
Experimental Box Behnken design on the selected independent factors. For each factor three values (levels) were selected: high, low and average level.

	g of beads ^a	pH ^b	Temperature ^c (°C)
1	Average	Average	Average
2	High	Average	High
3	Low	Low	Average
4	Average	High	Low
5	Low	Average	Low
6	Average	Low	Low
7	Average	High	High
8	High	Average	Low
9	Average	Average	Average
10	Low	High	Average
11	Low	Average	High
12	Average	Average	Average
13	Average	Low	High
14	High	High	Average
15	High	Low	Average

^a Selected levels for g of beads are 1, 4.5, 8 for low, average, and high, respectively.

^b Selected levels for pH are 3, 6, 9 for low, average, and high, respectively.

^c Selected levels for temperature are 4, 22, 40 °C for low, average, and high, respectively.

variance was performed by Minitab 16 (Minitab Inc., LEAD Technologies).

2.5. Enzyme assay

Laccase activity was assayed at 25 °C by monitoring the oxidation of ABTS at 420 nm ($\epsilon_{420} = 36 \times 10^3 \text{ M}^{-1} \text{ cm}^{-1}$). The assay mixture contained $2 \times 10^{-3} \text{ M}$ ABTS in $1 \times 10^{-1} \text{ M}$ sodium citrate buffer, pH 3.0. Laccase activity towards 2,6-dimethoxyphenol (DMP) was assayed in a mixture containing $1 \times 10^{-3} \text{ M}$ DMP in McIlvaine's citrate phosphate buffer adjusted to pH 5.0. Oxidation of DMP was followed by an absorbance increase at 477 nm ($\epsilon_{477} = 14.8 \times 10^3 \text{ M}^{-1} \text{ cm}^{-1}$).

Immobilized enzyme activity was assayed incubating 1 mg of beads in 1 mL of substrate in the corresponding reaction buffer. The activity was determined by measuring, every 30 s, change in absorbance and following the reaction for 2 min. Enzymatic units were expressed as U g^{-1} of beads.

2.6. Characterization of free and immobilized laccase

2.6.1. Topographical characterization

Scanning electron microscope (SEM) analysis of epoxy activated poly(methacrylate) beads, before and after the laccase grafting step, were achieved using SEM Ultra Plus (Zeiss, Germany) with FEG (field emission gun) source operated at 10 kV. SEM samples were sputtered with gold through Sputter coater HR 208 (Cressington, England), achieving a gold layer thickness of 20 nm.

2.6.2. Determination of kinetic parameters

Michaelis–Menten constants K_M values were estimated for free and immobilized laccases using the software GraphPad Prism (GraphPad Software, USA; <http://www.graphpad.com/>) on a wide range of substrate concentrations ($5 \times 10^{-5} - 3 \times 10^{-3} \text{ M}$) through the following equation:

$$V = \frac{V_{\max}[S]}{K_M + [S]}$$

where V is the velocity of the reaction, V_{\max} is the maximum velocity of the reaction and $[S]$ is the concentration of the substrate.

Enzyme activity was expressed in international units (IU).

2.6.3. Effect of pH and temperature

Laccase activity (free or immobilized) as a function of pH was assayed using ABTS and DMP as substrates in McIlvaine buffers (pH 2.0–8.0) at room temperature. The effect of temperature on laccase activity towards ABTS was evaluated in the temperature range of 25–85 °C in $5 \times 10^{-2} \text{ M}$ sodium phosphate buffer adjusted to pH 6.0. The activity was assayed as previously described.

2.6.4. Stability at pH and temperature

pH stability was evaluated by incubating enzymes in $5 \times 10^{-2} \text{ M}$ citrate buffer pH 3, $5 \times 10^{-2} \text{ M}$ phosphate buffer pH 6 and $5 \times 10^{-2} \text{ M}$ Tris–HCl pH 9 at 25 °C up to 65 days. Thermal stability was determined incubating free and immobilized laccases at the selected temperatures (25 °C, 55 °C, 65 °C) in $5 \times 10^{-2} \text{ M}$ phosphate buffer pH 6 until day 40. Residual laccase activity was assayed at room temperature in standard conditions with ABTS. The half-life ($t_{1/2}$) at different temperatures or pH is referred to the time corresponding to the 50% of residual activity. This value was extrapolated from the tendency curve related of enzyme deactivation in each condition.

2.6.5. Storage stability

For testing the storage stability of enzymes, free and immobilized laccase in $5 \times 10^{-2} \text{ M}$ sodium phosphate buffer pH 6.5 were stored at 4 °C for 6 months. Remaining laccase activity was assayed at room temperature in reference conditions at different times.

2.6.6. Reusability

Several consecutive oxidative cycles were performed in standard condition. At the end of each oxidation cycle, the immobilized laccase was washed three times with $5 \times 10^{-2} \text{ M}$ phosphate buffer pH 6.5 for 5 min under magnetic stirrer (200 rpm) and gravity filtered on a gauze. The procedure was then repeated with a fresh aliquot of substrate.

2.7. Fruit juices treatment

4 ml of fresh fruits juice were incubated with 0.5 g of immobilized enzymes (2000 U g^{-1}) for 1 h at room temperature in continuous stirring. The juices were then decanted and analyzed for phenol content. Controls were performed incubating 0.5 g of epoxy activated poly(methacrylate) beads in 4 ml of fruit juice in the same conditions.

Ultrafiltered samples were obtained treating 4 ml of fruit juice on 10,000 Dalton cut-off membrane on an amicon device (Merck Millipore Corporation, Italy).

2.8. Extraction and determination of total phenolic compounds

The extraction procedure was carried out with 0.5 mL juice/methanol (1:1) for 30 min at -20 °C . The sample was centrifuged for 30 min at $23,900 \times g$ and the supernatant recovered was assayed.

The total phenolic content of fruit was determined by using Folin–Ciocalteu assay (Singleton & Rossi, 1965). Gallic acid stock solution, (1 mg mL^{-1}) and standard concentrations of 0, 10, 25, 50, 100, 250 and $500 \mu\text{g mL}^{-1}$ were prepared in deionized water. The Folin–Ciocalteu procedure consisted of transferring 50 μL standard or sample into a 4–5 mL borosilicate tube, followed by additions of 430 μL H_2O and 20 μL Folin–Ciocalteu reagent. After mixing the samples, 50 μL 20% sodium carbonate and 450 μL H_2O were added. The sample mixtures were allowed to stand for 1 h at room temperature. The absorbance was measured at 725 nm. The phenolic content of samples was measured against the gallic acid (GA) calibration standard (0–500 ppm). Phenol reduction was estimated as percentage respect to untreated samples.

2.9. Mass spectrometry analyses

In order to obtain a molecular investigation of species occurring in the different samples, aliquots of methanolic extracts from fruit juice were submitted to mass spectral analyses by using both GCMS and LCMS/MS techniques.

2.9.1. GC–MS analysis

Aliquots of 1 μL of each methanolic extracts were directly analyzed using a GC–MS equipped with a 5975 MSD quadrupole mass spectrometer (Agilent technologies, USA) and a gas chromatograph 7820A (Agilent technologies, USA) by using a ZB-5MS fused silica capillary column (30 m length, 0.25 mm ID, 0.25 μm Film Thickness) from Phenomenex, (USA). The injection temperature was 250 °C. During analyses, the oven temperature was increased from 60 °C to 300 °C at 10 °C min^{-1} and held at 300 °C for 10 min. Electron ionization mass spectra were recorded by continuous quadrupole scanning at 70 eV ionization energy, in the mass range 50–600 m/z. Each specie was interpreted on the basis of electron impact spectra (NIST 2011 library, Scientific Instrument Services, USA, and Analyst Software, SCIEX, Canada).

2.9.2. LC–MS/MS analysis

Methanolic extracts were dried under vacuum and resuspended in 200 μL of 0.1% formic acid. The resulting samples were filtrated using cellulose acetate spin filters (0.22 μm) from Agilent and 1 μL of each sample was analyzed by nanoLC Chip MS/MS, using a CHIP MS 6520 QTOF equipped with a capillary 1200 HPLC system and a chip cube (Agilent Technologies, USA). After loading, the samples were first concentrated and washed at 4 $\mu\text{L min}^{-1}$ in 40 nL enrichment column (Agilent Technologies chip, USA), with 0.1% formic acid as eluent, and then fractionated on a C18 reverse-phase capillary column (75 $\mu\text{m} \times 43 \text{ mm}$ in the Agilent Technologies chip, USA) at flow rate of 400 nL/min with a linear gradient of eluent B (0.1% formic acid in 95% ACN) in A (0.1% formic acid in 2% ACN) from 7% to 60% in 50 min. Mono charged analytes were selected and analyzed using data-dependent acquisition of one MS scan (mass range from 100 to 1500 m/z) followed by MS/MS scans of the three most abundant ions in each MS scan. Collision energy (CE) applied during fragmentation is calculated by the sequent empirical equations: $\text{CE} = 4V/100 \text{ Da} - 2.4V$. Raw data from nanoLC–MS/MS were analyzed using Qualitative Analysis software (Agilent MassHunter Workstation Software, version B.02.00, USA).

2.10. Statistical analysis

Those analysis not concerning RSM represent the mean of triplicate measurements and are expressed as mean \pm S.D. (standard deviation of the mean). One-way analysis of variance (ANOVA) followed by the unpaired Student's *t* test or Tukey's test was used. $p < 0.05$ was considered statistically significant, unless otherwise specified.

3. Results and discussions

3.1. Immobilization of laccase on Sepabeads EC-HFA

Applicability at industrial scale of an enzyme is dependent on its performances as well as on its manufacturing costs, which have to be conformed to commercial and industrial demands. In this context, design of suitable immobilization process and its optimization in operating conditions are of utter importance. In the present work covalent immobilization of rPOXA1b laccase on epoxy activated poly(methacrylate) beads was chosen as a promising method to provide a useful catalytic system for several applications (Mateo et al., 2007). A RSM approach was applied to define process parameters improving laccase immobilization through the characteristic three major steps: performing statistically designed experiments, estimating the coefficients in a mathematical model, and predicting the response and checking the adequacy of the model. Box Behnken design was performed selecting the range of levels variation for each factor on the basis of empirical and theoretical consideration concerning enzyme stability and volumetric constrain. As a fact, a pH range from 3 to 9 was chosen, avoiding extreme pH values that could negatively affect enzyme stability (Miele et al., 2010). Moreover, the quantity of poly(methacrylate) beads usable for this process is limited by the necessity of incubating them in an enzymatic solution properly covering their surface. Laccase immobilization yield was considered as response variable and it was evaluated as ratio between the total enzymatic IU presents in solution before and after immobilization reaction ($\%Y = [1 - (Uf/Ui)] * 100$). According to this design, 15 runs, replicated three times, were performed and experimental data (Table 2 column named "Yield") were obtained. Results obtained after running the trials of the Box Behnken design were fitted to a factorial equation to explain the dependence of lac-

Table 2

(A) experimental conditions of the experimental design for laccase immobilization and the corresponding experimental responses. (B) Analysis of variance (ANOVA) for the fitted quadratic polynomial model of laccase immobilization.

	g of beads	pH	Temperature	Yield (%)		
(A)						
1	4.5	6	22	70		
2	8	6	40	74		
3	1	3	22	13		
4	4.5	9	4	70		
5	1	6	4	45		
6	4.5	3	4	24		
7	4.5	9	40	50		
8	8	6	4	94		
9	4.5	6	22	70		
10	1	9	22	45		
11	1	6	40	36		
12	4.5	6	22	47		
13	4.5	3	40	23		
14	8	9	22	97		
15	8	3	22	20		
Source	DF	Seq Ss	Adj SS	Adj MS	F value	Prob > F
(B)						
Regression model	9	9177.07	9177.07	1019.67	8.21	0.016
Linear	3	7117.50	7117.50	2372.50	19.11	0.004
g of beads enzyme/beads	1	2664.50	2664.50	2664.50	21.46	0.006
pH	1	4140.50	4140.50	4140.50	33.36	0.002
Temperature	1	312.50	312.50	312.50	2.52	0.173
Square	3	1432.82	1432.82	477.61	3.85	0.091
g of beads enzyme/beads * g of beads enzyme/beads	1	22.02	3.39	3.39	0.03	0.875
pH * pH	1	1406.79	1410.01	1410.01	11.36	0.020
Temperature * Temperature	1	4.01	4.01	4.01	0.03	0.864
Interaction	3	626.75	626.75	208.92	1.68	0.285
g of beads enzyme/beads * pH	1	506.25	506.25	506.25	4.08	0.099
g of beads enzyme/beads * Temperature	1	30.25	30.25	30.25	0.24	0.642
pH * Temperature	1	90.25	90.25	90.25	0.73	0.433
Residual	5	620.67	620.67	124.13		
Lack of fit	3	268.00	268.00	89.33	0.51	0.716
Pure error	2	352.67	352.67	176.33		
Total	14	9797.73				
$R^2 = 93.67\%$						
$R^2 \text{ adj.} = 82.26\%$						

DF – (Total degrees of freedom) are the amount of information data estimates. Sequential SS (Sequential Sum of Squares) are the numerators of the linear *F*-statistic.

Adjusted SS – (Adjusted sums of squares) are measures of variation for different components of the model. The order of the predictors in the model does not affect the calculation of the adjusted sum of squares.

Adjusted MS – (Adjusted mean squares) measure how much variation a term or a model explains, assuming that all other terms are in the model, regardless of the order they were entered.

F value – probability distribution value used in the ANOVA.

case immobilization yield on the designed variables as shown in the equation:

$$Y = -64.1346 - 0.958050 * \text{g of beads} + 30.7526 * \text{pH} - 2.17130 * \text{pH} * \text{pH} + 1.07143 * \text{g of beads} * \text{pH}$$

The second-order regression equation provided the levels of immobilized laccase as a function of parameters which can be presented in terms of coded factors. The factors can affect the results in different ways and are integrated in the equation as "linear" (g of beads * pH), "square" (pH * pH) or "interacting" (g of beads * pH) coefficients. The statistical significance of regression equation was checked by *F*-test, and the analysis of variance (ANOVA) is shown in Table 2B.

The Model *F*-value found of 8.21 corresponding to *p*-value 0.016 implies that the model is significant. The value of the determination coefficient R^2 calculated from the quadratic regression model

was 0.9367, while the value of the adjusted R^2 was 0.8226 indicating high degree of correlation between the observed and predicted values. Thus, the regression model provides a good explanation of the relationship between independent variables and the response (Yield). Other values reported in the ANOVA Table 2B are used by the software to calculate the p -value for a term and the R^2 statistic. Usually, interpretation of results is based on the p -values, the R^2 statistic and the adjusted R^2 statistic instead of the degrees of freedom, the sums of squares and the adjusted mean squares.

The lack-of-fit test measures the failure of the model to represent data in the experimental domain, at points which are not included in the regression. This test is desired to be non-significant to support the model (Montgomery, 2001). In this study, the lack of fit F -value of 0.51 with p -value 0.716 implies that the lack of fit is not significant.

All these results suggest that the quadratic model is statistically significant for the response, and therefore it can be used for further analysis. The 3D response surface plots (Fig. 1) were obtained by plotting the response (yield) on the Z -axis against any two variables while keeping the third variable at its average level. Based on the above analysis, in the range of our research, high pH values and high quantity of enzyme positively affects laccase immobilization, while temperature seems not to affect immobilization yield in the range of the tested conditions.

The maximum laccase immobilization yield of 100% was predicted at the following optimum conditions: 8 g of beads for 30 ml of 20,000 U L⁻¹ rPOXA1b solution, in a buffer at pH 9, incubating at 4 °C. Another three experiment sets were carried out to confirm the prediction. An average of 98 ± 5% yield was achieved, theoretically corresponding to an immobilization of 75 U g⁻¹ of beads, thus indicating an excellent fit with the predicted value. Notably, we reached 2000 ± 100 U g⁻¹ of beads with a remarkable increase of enzyme specific activity respect to that of the free counterpart of more than 25 folds. This effect has been already reported in other works (Rodríguez, Ortiz, Berenguer-Murcia, Torres, & Fernández-Lafuente, 2013), and it is probably due to 3D structure variations after covalent attachment on a solid support. Thus, the process could facilitate a conformational rearrangement of the active site, *i.e.* unveiling the binding pocket, that positively affects the catalytic proprieties.

As expected, when the immobilization process was performed at room temperature, similar yields (96%) were obtained, thus providing the conditions for a less expensive procedure.

3.2. Immobilized enzymatic system characterization

3.2.1. Morphological characterization

Morphologies of beads surface were investigated using Scanning Electron Microscope before and after immobilization procedure. As shown in SEM micrographs (Fig. 2B), surface of the treated beads was looked like a mesh, and showed very compact structures, revealing an increase of surface roughness upon enzyme loading respect to the not-treated ones (Fig. 2A).

3.2.2. Kinetic analysis

Apparent K_M constants were determined for the immobilized enzyme against two different laccase substrates, ABTS and DMP, and compared with the free counterpart (Supplementary material, Fig. S1). An opposite effect was observed for the two tested substrates. K_M value vs ABTS of the immobilized enzyme (0.032 ± 0.006 mmol l⁻¹) is lower (p -value < 0.05) in respect to that observed for the soluble rPOXA1b (0.063 ± 0.004 mmol l⁻¹). Conversely, a slight increase (p -value < 0.05) in the K_M value vs DMP was observed for the solid catalyst (0.227 ± 0.030 mmol l⁻¹) respect to the free enzyme (0.160 ± 0.010 mmol l⁻¹). Expected phenomena occurring during enzyme immobilization –such as elec-

trostatic and partitioning effects in the immobilized enzyme microenvironments, substrate mass transfer effects and/or changes in enzyme conformation– may differently affect properties of immobilized catalyst in a substrate dependent manner (steric hindrance, reaction mechanism *etc.*) (Pezzella et al., 2014).

3.2.3. Temperature and pH activity profiles

The effect of the temperature on the activity of free and immobilized laccases was determined in the range 25–85 °C. Both catalysts display a maximum at 75 °C, although free rPOXA1b retains most of its activity in a wider temperature range when compared with the immobilized enzyme (Supplementary material, Fig. S2). A reduced flexibility, caused for example by the occurrence of multi-point attachments, may explain the observed results.

Enzyme immobilization determines a shift in the optimal pH (from 4 to 5) towards ABTS along with a reduced enzyme activity at more acidic pHs (Supplementary material, Fig. S3). On the other hand, free and immobilized laccase show a similar pH activity profile against DMP.

3.2.4. Thermostability and pH stability

Enzyme thermostability was evaluated incubating free and immobilized rPOXA1b at selected temperatures (Supplementary material, Fig. S4). The immobilized enzyme displays and increased stability at all tested temperatures with a twofold increase in the $t_{1/2}$ values (Table 3). pH stability was investigated at values 3, 6 and 9 (Table 3 and Supplementary material, Fig. S5). The solid catalyst exhibits an enhanced stability at all pH values (p value < 0.05, for each value of immobilized vs free enzyme), further boosting rPOXA1b peculiar stability at alkaline pH (Miele et al., 2010) and improving its performances at acidic pH.

3.2.5. Immobilized biocatalyst stability

Laccase immobilized on Sepabeads was efficiently stored at 4 °C in 5 × 10⁻² M phosphate buffer pH 6.5 preserving almost 95% of its activity after 4 months and about 90% after 6 months. Under the same storage conditions, soluble laccase shows a 50% drop in activity after six months.

As far as enzyme reusability, immobilized enzyme retains 67% of initial activity after ten cycles of ABTS oxidation at room temperature (Supplementary material, Fig. S6). These performances, having a great influence on process economics, are superior than those previously reported, showing 50% residual activity under similar conditions (Liu et al., 2012 and Rekuć, Bryjak, Szymańska, & Jazębski, 2009).

3.3. Fruit juice treatment with immobilized laccase

The effectiveness of immobilized laccase in fruit juices treatment was investigated choosing orange juice as a model. Raw orange juice was incubated for 1 h at room temperature with the solid catalyst and the total phenol content analyzed in comparison with that of an ultra-filtered sample. Ultra-filtered juices are not always stable, but rather tend to produce pronounced subsequent haze, caused by reactive phenolics compounds that cannot be retained by the ultra-filtration membrane (Neifar et al., 2011). Laccase treatment generates up to 45% reduction, whereas after ultra-filtration, only a 15% phenols decrement was measured. No phenol reduction was observed in the control tests (fruit juice incubated with the poly(methacrylate) solid support without enzyme). Thus, it is possible to rule out a possible effect due to endogenous polyphenol oxidase activities.

The solid catalyst can be reused up to three times in juice treatment without losing efficiency.

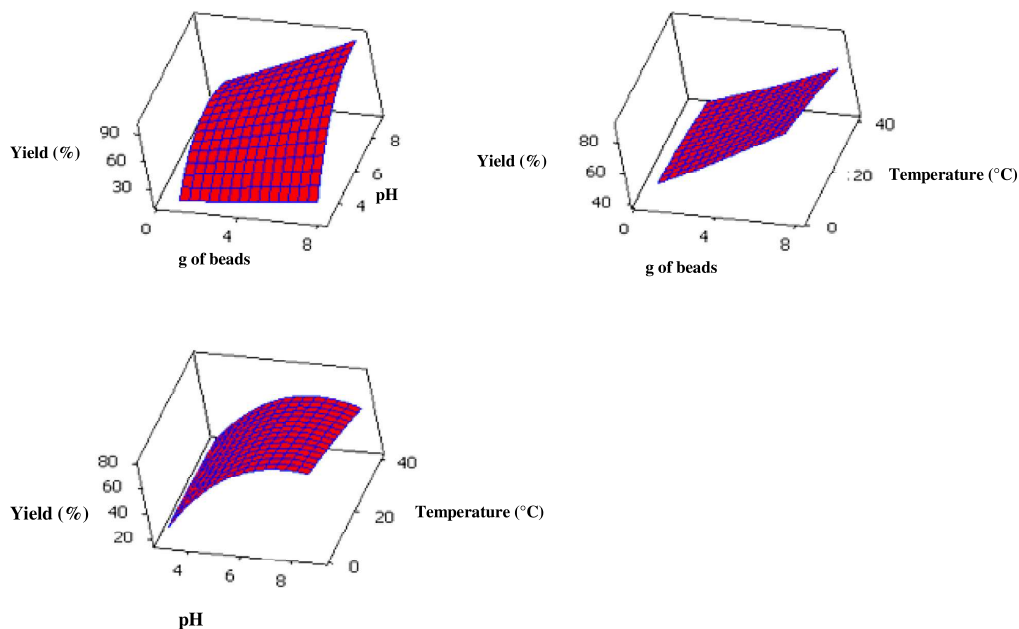


Fig. 1. 3D surface plot for the laccase yield immobilization as a function of temperature, pH and enzyme/beads ratio.

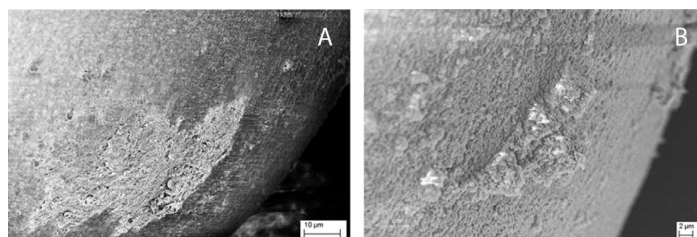


Fig. 2. Sem image analysis of epoxy activated poly(methacrylate) beads before, (A) and after (B) laccase immobilization.

Table 3

Temperature and pH stability profiles of (A) free and (B) immobilized laccase expressed as half-life. ABTS was used as the substrate for the enzyme assay. Each value represents the mean of triplicate measurements and varies from the mean by not more than 10%.

	$t_{1/2}$ temperature (h)			$t_{1/2}$ pH (day)		
	25 °C	55 °C	65 °C	pH 3	pH 6	pH 9
Free rPOXA1b	7.1	3.5	0.8	2.9	6.8	23.1
Immobilized rPOXA1b	16.3	7.8	1.5	5.7	16.0	63.7

3.3.1. Compounds identification

Citrus phenolics have been subject of increased interest in the last few years because their presence contributes to the sensory quality of fruit and juice, affecting color, bitterness, astringency, antioxidant activity and flavor (Sousa, da Rocha, Cardoso, Silva, & Zanoni, 2004). Sample aliquots of treated and not-treated raw orange juice were analyzed by LC–MSMS mass spectrometry to evaluate flavanones content. The total ion current chromatograms (TIC) showed a similar behavior. No decrease in flavanones contents could be appreciated in the LC–MSMS analyses (Supplemen-

tary material, Fig. S7). Thus, laccase treatment does not affect these health-effective molecules (Silva et al., 2014), probably due to a peculiar affinity towards other species present in the orange juice, such as phenols, that could compete for or avoid the oxidation of flavanones. This finding is unexpected if compared to the natural or induced oxidation process occurring in other fruit beverages like grape juice and wine, where the flavanones oxidation plays a prominent role in the formation of brown pigments (Shahidi & Naczki, 2003). Moreover, mass spectrometry analyses were used to evaluate the laccase treatment effect on phenolic content. Phenol standard mixture, containing coumaric acid, caffeic acid, synapinic acid, ferulic acid, vanillic acid and syringic acid (Barberis et al., 2014) was analyzed by GC–MS in order to set up the best chromatographic and mass spectral conditions (Supplementary material, Fig. S8). Mass spectral analyses were carried out on laccase treated orange juices. Commercial orange juice was used as control. The species were identified on the basis of electron impact mass spectra showing a general decrease in phenol content after laccase treatment. In particular, while caffeic acid seems to be unaffected by laccase treatment, the TIC showed the

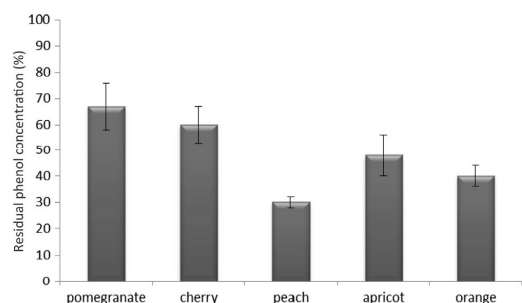


Fig. 3. The reduction effect of phenol content in different fruit juices after immobilized laccase incubation. The values are expressed in percentage of residual phenol concentration. Standard deviations derive from three independent replicates.

decrease of coumaric and ferulic acid. Moreover, in the laccase treated juice, the chromatograms showed an intense reduction of vinylguaiacol, a degradation product of ferulic acid. Vinylguaiacol is described as possessing a peppery/spicy aroma and is considered a potent off-flavor (Naim, Striem, Kanner, & Peleg, 1988). Thus, it can be conveyed that laccase treatment improves orange juice sensory profile and extends its shelf life.

Furthermore, in order to evaluate the versatility of the developed catalytic system, immobilized laccases were tested on different raw fruit juices. As reported in Fig. 3 the immobilized laccase system is able to sensitively reduce the phenol content of several fruit juices at a level comparable with that achieved for the orange juice.

4. Conclusion

Optimal conditions for laccase immobilization were set-up through a RSM approach using the Box Behnken design. Laccase based juice treatment allowed to reach up to 45% phenol reduction. The health-effective flavanones molecules are not affected by the treatment. Furthermore, laccase treated juice displays an improved sensory profile, due to the reduction of vinyl guaiacol, a potent off-flavor possessing a peppery/spicy aroma.

Acknowledgments

This work was supported by grants from the European project “Optimized oxidoreductases for medium and large scale industrial biotransformations, INDOX” (KBBE-2013-7 613549) and from P.O. R. Campania FERS 2007/2013 – Bio Industrial Processes (BIP) project for a Regional Biotechnologies Network in Campania, CUP B25C13000290007.

The authors thank Salvatore Morra, Alberto Colella and Carolina Fontanarosa for technical assistance.

Appendix A. Supplementary data

Supplementary data associated with this article can be found, in the online version, at <http://dx.doi.org/10.1016/j.foodchem.2015.10.074>.

References

Açgac, E., Akylidiz, A., & Akdemir Evrendilek, G. (2014). Comparison of phenolic compounds of orange juice processed by pulsed electric fields (PEF) and conventional thermal pasteurization. *Food Chemistry*, *143*, 354–361.

Barberis, A., Spissu, Y., Bazzu, G., Fadda, A., Azara, E., Sanna, D., ... Serra, P. A. (2014). Development and characterization of an ascorbate oxidase-based sensor-

biosensor system for telemetric detection of AA and antioxidant capacity in fresh orange juice. *Analytical Chemistry*, *86*, 8727–8734.

Bharate, S. S., & Bharate, S. B. (2014). Non-enzymatic browning in citrus juice: Chemical markers, their detection and ways to improve product quality. *Journal of Food Science and Technology*, *51*, 2271–2288.

Box, G., & Behnken, D. (1960). Some new three level designs for the study of quantitative variables. *Technometrics*, *2*, 455–475.

Costa Ferreira, S. L., Bruns, R. E., Paranhos da Silva, E. G., Santos, W. N. L., Quintella, C. M., Mauricio David, J., ... Neto, B. B. (2007). Statistical designs and response surface techniques for the optimization of chromatographic systems. *Journal of Chromatography A*, *1158*, 2–14.

D'Souza, S. F. (1998). Immobilized enzymes in bioprocess. *Current Science*, *77*, 69–79.

Di Cosimo, R., McAuliffe, J., Pouloueb, A. J., & Bohlmann, G. (2013). Industrial use of immobilized enzymes. *Chemical Society Review*, *42*, 6437–6474.

Durán, N., Rosa, M. A., D'Annibale, A., & Gianfreda, L. (2002). Applications of laccases and tyrosinases (phenoloxidases) immobilized on different supports: A review. *Enzyme and Microbial Technology*, *31*, 907–931.

Friedman, M. (1996). Food browning and its prevention: An overview. *Journal of Agricultural and Food Chemistry*, *44*, 631–653.

Gassara-Chatti, F., Brar, S. K., Ajila, C. M., Verma, M., Tyagi, R. D., & Valero, J. R. (2013). Encapsulation of ligninolytic enzymes and its application in clarification of juice. *Food Chemistry*, *137*, 18–24.

Giardina, P., Palmieri, G., Scaloni, A., Fontanella, B., Faraco, V., Cennamo, G., & Sannia, G. (1999). Protein and gene structure of a blue laccase from *Pleurotus ostreatus*. *Biochemical Journal*, *341*, 655–663.

Jesionowski, T., Zdzarta, J., & Krajewska, B. (2014). Enzyme immobilization by adsorption: A review. *Adsorption*, *20*, 801–821.

Liu, Y., Zeng, Z., Zeng, G., Tang, L., Pang, Y., Li, Z., ... Xie, G. (2012). Immobilization of laccase on magnetic bimodal mesoporous carbon and the application in the removal of phenolic compounds. *Bioresour Technol*, *115*, 21–26.

Macellaro, G., Pezzella, C., Cicatiello, P., Sannia, G., & Piscitelli, A. (2014). Fungal laccases degradation of endocrine disrupting compounds. *BioMed Research International*. <http://dx.doi.org/10.1155/2014/614038>.

Mateo, C., Abian, O., Fernandez-Lorente, G., Pedroche, J., Fernandez-Lafuente, R., Guisan, J. M., ... Daminati, M. (2002). Epoxy Sepabeads: A novel epoxy support for stabilization of industrial enzymes via very intense multipoint covalent attachment. *Biotechnology Progress*, *18*, 629–634.

Mateo, C., Grazu, V., Palomo, J. M., Lopez-Gallego, F., Fernandez-Lafuente, R., & Guisan, J. M. (2007). Immobilization of enzymes on heterofunctional epoxy supports. *Nature Protocols*, *2*, 1022–1033.

Mateo, C., Palomo, J. M., Fernandez-Lorente, G., Guisan, J. M., & Fernandez-Lafuente, F. (2007). Improvement of enzyme activity, stability and selectivity via immobilization techniques. *Enzyme Microbial Technology*, *40*, 1451–1463.

Miele, A., Giardina, P., Notomista, E., Piscitelli, A., Sannia, G., & Faraco, V. A. (2010). Semi-rational approach to engineering laccase enzymes. *Molecular Biotechnology*, *46*, 149–156.

Montgomery, D. C. (2001). *Design and analysis of experiments* (5th ed.). New York: Wiley, pp. 455–492.

Naim, M., Striem, B. J., Kanner, J., & Peleg, H. (1988). Potential of ferulic acid as a precursor to off-flavors in stored orange juice. *Journal of Food Science*, *53*, 500–503.

Neifar, M., Ghorbel, R. E., Kamoun, A., Baklouti, S., Mokni, A., Jaouani, A., & Chaabouni, S. E. (2011). Effective clarification of pomegranate juice using laccase treatment optimized by response surface methodology followed by ultrafiltration. *Journal of Food Process Engineering*, *34*, 1199–1219.

Osma, J. F., Toca-Herrera, J. L., & Rodríguez-Couto, S. (2010). Uses of laccases in the food industry. *Enzyme Research*, *2010*, 918761.

Pezzella, C., Guarino, L., & Piscitelli, A. (2015). How to enjoy laccases. *Cellular and Molecular Life Sciences*, *72*, 923–940.

Pezzella, P., Russo, M. E., Marzocchella, A., Salatino, P., & Sannia, G. (2014). Immobilization of a *Pleurotus ostreatus* laccase mixture on perlite and its application to dye decolorisation. *BioMed Research International*. <http://dx.doi.org/10.1155/2014/308613>.

Rekuć, A., Bryjak, J., Szymańska, K., & Jazębski, A. B. (2009). Laccase immobilization on mesostructured cellular foams affords preparations with ultrahigh activity. *Process Biochemistry*, *44*, 191–198.

Rodrigues, R. C., Ortiz, C., Berenguer-Murcia, A., Torres, R., & Fernández-Lafuente, R. (2013). Modifying enzyme activity and selectivity by immobilization. *Chemical Society Reviews*, *42*, 6290–6307.

Shahidi, F., & Naczk, M. (2003). *Phenolics in food and nutraceuticals*. Taylor & Francis Inc. p. 285.

Sheldon, R. A. (2007). Enzyme immobilization: the quest for optimum performance. *Advanced Synthesis & Catalysis*, *349*, 1289–1307.

Silva, L. C., David, J. M., Borges Rdos, S., Ferreira, S. L., David, J. P., Dos Reis, P. S., & Bruns, R. E. (2014). Determination of flavanones in orange juices obtained from different sources by HPLC/DAD. *Journal of Analytical Methods in Chemistry*. <http://dx.doi.org/10.1155/2014/296838>.

Singleton, V. L., & Rossi, J. A. (1965). Colorimetry of total phenolics with phosphomolybdic-phosphotungstic acid reagents. *American Journal of Enology and Viticulture*, *16*, 144–158.

Sousa, W. R., da Rocha, C., Cardoso, C. L., Silva, D. H. S., & Zanoni, M. V. B. (2004). Determination of the relative contribution of phenolic antioxidants in orange juice by voltammetric methods. *Journal of Food Composition and Analysis*, *17*, 619–633.

Supplementary Material

Fig.S1. Effect of ABTS and DMP concentrations on the activity of free laccase and on the enzyme immobilized on poly(methacrylate) beads.

Enzyme activity was determined in the presence of ABTS at concentrations in the range from 10^{-5} to $4 \cdot 10^{-3}$ M, in sodium citrate buffer (50mM) under standard conditions, at pH 3.0.

Each value represents the mean of triplicate measurements. Standard deviation is reported as error bar, when not visible the standard deviation is less than 5%.

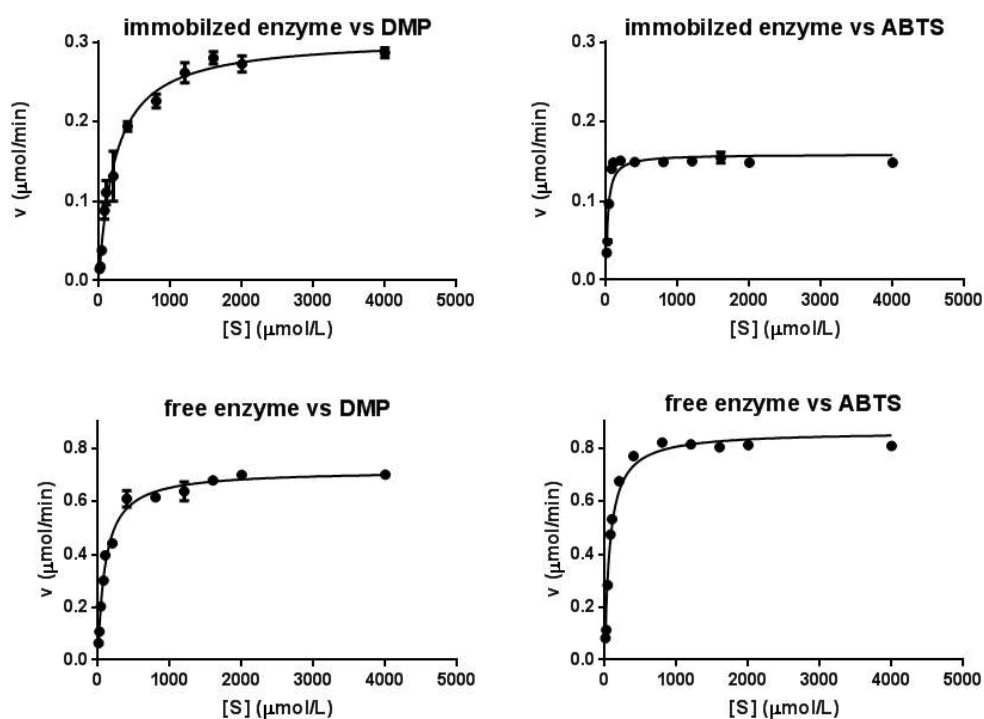


Fig.S2. Effect of temperature on the activity of free laccase and on the enzyme immobilized on poly(methacrylate) beads.

Enzyme activity was measured at various temperatures in citrate buffer (50×10^{-3} M) under standard conditions at pH 3.0 for free and immobilized laccases (dotted and solid lines, respectively). The maximum activities of free and immobilized laccases are shown as 100% residual activity. Data represent the mean of triplicate measurements. Standard deviation is reported as error bar.

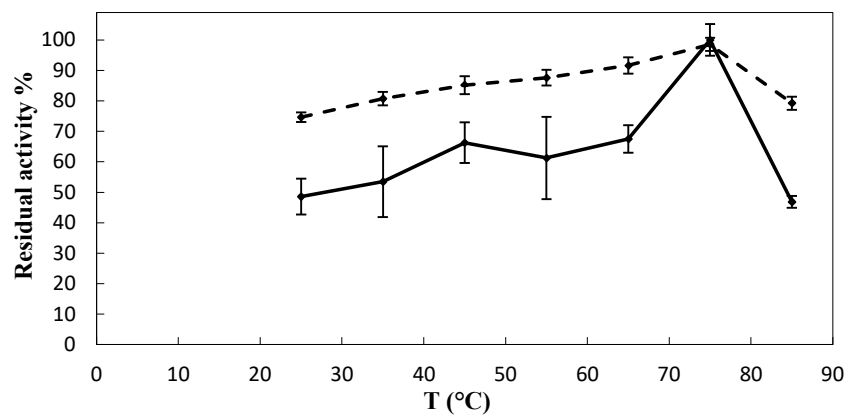


Fig.S3. Effect of pH on the activity of free laccase and on the enzyme immobilized on poly(methacrylate) beads.

The effect of pH was determined using sodium citrate or sodium phosphate buffers (50×10^{-3} M) to obtain the desired pH in the standard assay. Black and gray lines represent the residual laccase activity vs ABTS and DMP, respectively. Dotted and solid lines represent the free and immobilized laccases, respectively. The maximum activities of free and immobilized laccases are shown as 100% residual activity.

Each value represents the mean of triplicate measurements. Standard deviation is reported as error bar, when not visible the standard deviation is less than 5%.

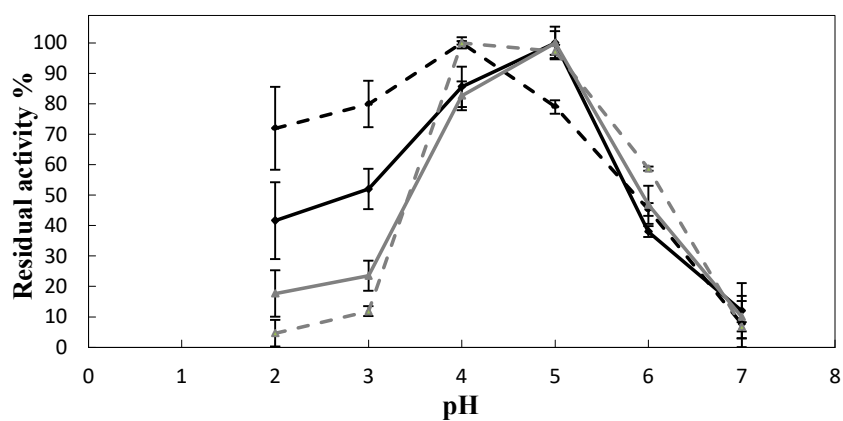


Fig.S4. Effect of temperature on the stability of free laccase and on the enzyme immobilized on poly(methacrylate) beads.

Free and immobilized laccases (dotted and solid lines, respectively) incubations were performed at various temperatures in 50×10^{-3} M sodium phosphate buffer at pH 7.0. Aliquots were withdrawn at the indicated times and residual activity vs ABTS was assayed under standard conditions in 50×10^{-3} M sodium citrate buffer at pH 3.0. The maximum activities of free and immobilized laccases at time 0 are shown as 100% residual activity. Dotted and solid lines represent the free and immobilized laccases, respectively. Gray squares, black circles, black triangles, represent the residual laccase activity at 65°C, 55°C and 25°C, respectively.

Data represent the mean of triplicate measurements. Standard deviation is reported as error bar, when not visible the standard deviation is less than 5%.

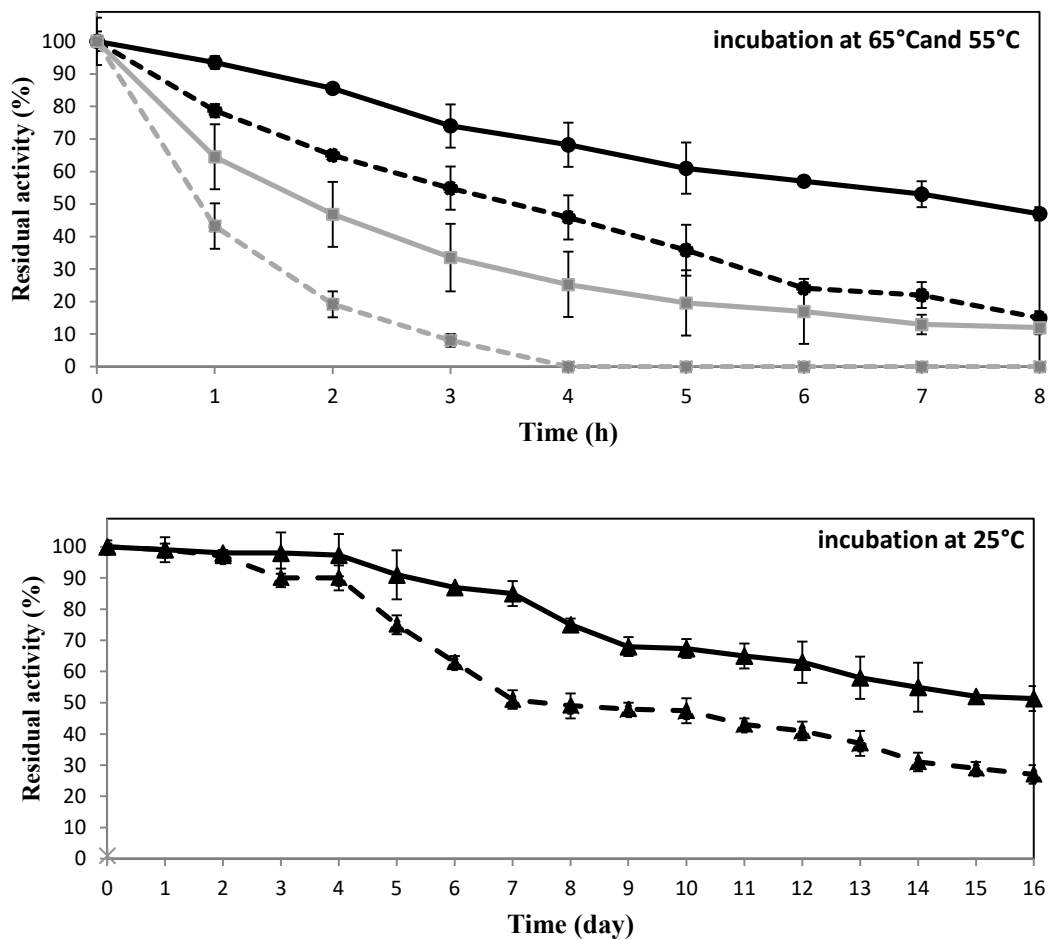


Fig.S5. Effect of pH on the stability of free laccase and on the enzyme immobilized on poly(methacrylate) beads.

The effect of pH was determined using different buffers ($50 \cdot 10^{-3}$ M) to obtain the desired pH in the standard assay. Symbols used for the buffers: circles, sodium citrate (pH 3.0); squares, phosphate (pH 6.0); triangles, Tris-Cl (pH 9.0). Filled and open symbols, as well as dotted and solid lines, represent the free and immobilized laccases, respectively. The maximum activities of free and immobilized laccases are shown as 100% residual activity.

Each value represents the mean of triplicate measurements. Standard deviation is reported as error bar, when not visible the standard deviation is less than 5%.

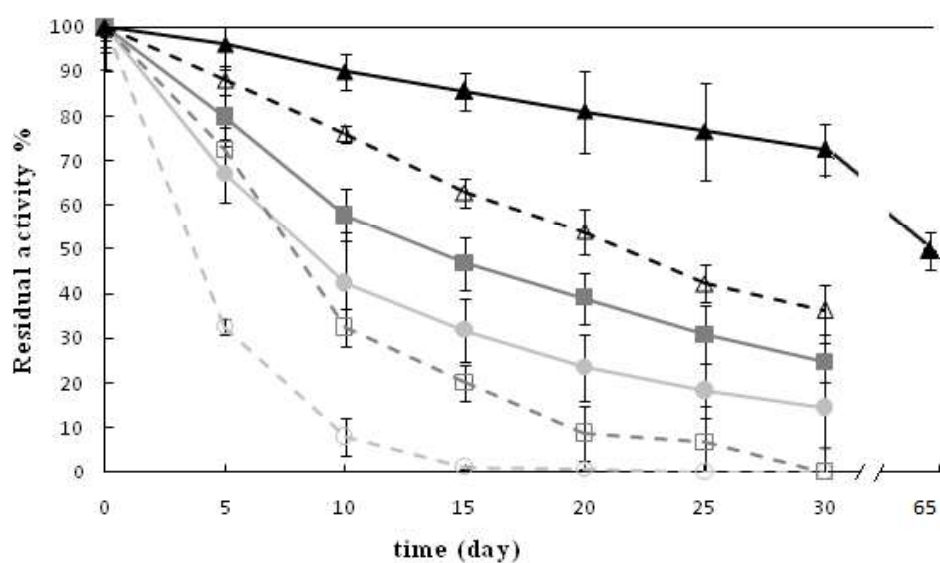


Fig.S6. Reusability of immobilized laccase.

Immobilized laccase activity was assayed at room temperature in 50×10^{-3} M sodium citrate buffer at pH 3.0. Residual activity vs ABTS was assayed under standard conditions for each cycle. One cycle is defined as the time required to oxidize all the ABTS substrate present in the reaction mixture under standard assay conditions. The maximum activity is shown as 100% residual activity (first cycle).

Each value represents the mean of triplicate measurements. Standard deviation is reported as error bar, when not visible the standard deviation is less than 5%.

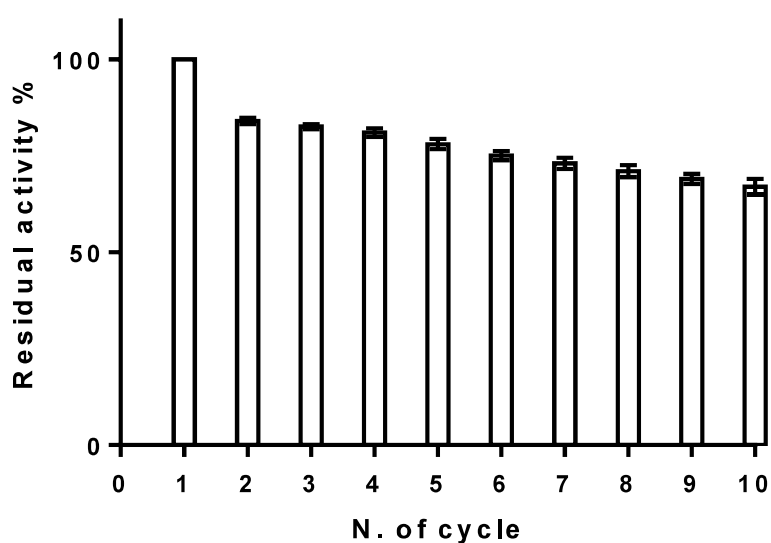
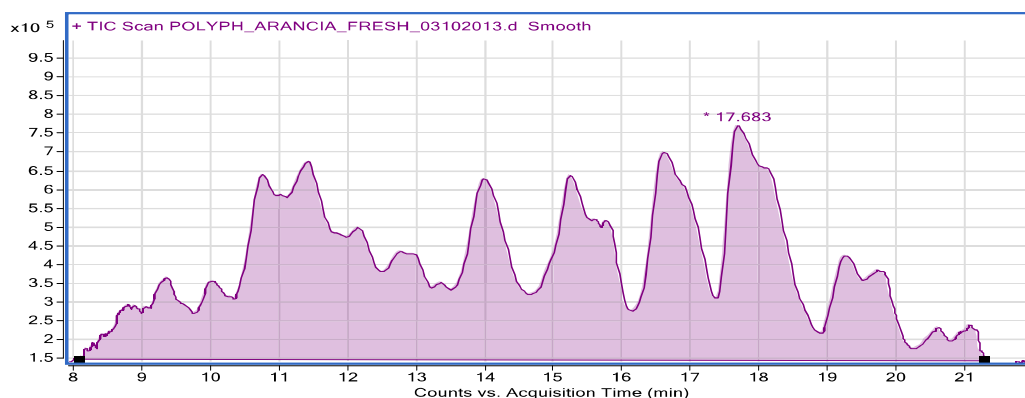


Fig.S7. LC-MS/MS analyses on orange juice extracts.

Total ion current chromatograms obtained from the analysis of untreated (Panel A) and laccase treated (Panel B) orange juice extracts . The Total ion current areas are indicated in the figures. The main flavanols identified in the extracts are summarized in the Table shown in the Panel C together with the MS/MS spectrum of Hesperidin (Panel D).

Panel A - Total area (8-21 min): 1.7×10^8 (169195918)



Panel B - Total area (8-21 min): 1.5×10^8 (152002396)



PANEL C

Compound	RT (min)	MS	MS/MS
Tannin	9,5	595,17	457,11
Eriocitrin	12,3	597,18	289,07
Naringin	13,2	581,19	273,08
Hesperidin	15,9	611,20	303,09
Poncirin	19,2	595,20	287,09

PANEL D

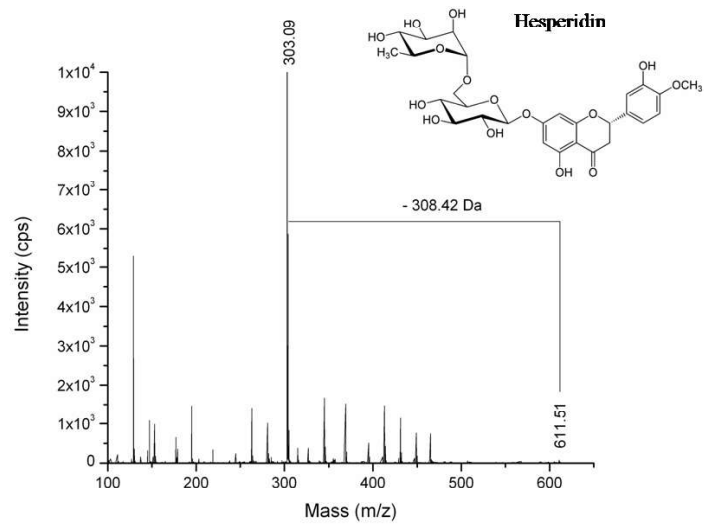


Fig.S8. Detection of phenol content in orange juice by GC-MS.

Full Total Ion Chromatogram (TIC) obtained from untreated (A) and treated (B) orange juices

All species were identified on the basis of the electron ionization mass spectrum. The abundance of each analyte was reported as percentage. Percentage values represent the mean of triplicate measurements and varies from the mean by not more than 15%. Statistical analysis between untreated and treated samples was significant (p value <0.05) for all molecules but for caffeic acid.

